

SYNTHESIS OF FUNCTIONAL NANOMATERIALS WITHIN A GREEN
CHEMISTRY CONTEXT

by

JENNIFER ANN DAHL

A DISSERTATION

Presented to the Department of Chemistry
and the Graduate School of the University of Oregon
in partial fulfillment of the requirements
for the degree of
Doctor of Philosophy

December 2007

“Synthesis of Functional Nanomaterials within a Green Chemistry Context,” a dissertation prepared by Jennifer Ann Dahl in partial fulfillment of the requirements for the Doctor of Philosophy degree in the Department of Chemistry. This dissertation has been approved and accepted by:

Prof. Catherine J. Page, Chair of the Examining Committee

Nov. 26, 2007

Date

Committee in Charge: Prof. Catherine J. Page, Chair
Prof. Mark C. Lonergan
Prof. Darren W. Johnson
Prof. Raghuveer Parthasarathy

Accepted by:

Dean of the Graduate School

© 2007 Jennifer Ann Dahl

An Abstract of the Dissertation of

Jennifer Ann Dahl for the degree of Doctor of Philosophy

in the Department of Chemistry to be taken December 2007

Title: SYNTHESIS OF FUNCTIONAL NANOMATERIALS WITHIN A GREEN
CHEMISTRY CONTEXTApproved: _____
/ Prof. James E. Hutchison, Advisor

In recent years, nanoscience has evolved from a multidisciplinary research concept to a primary scientific frontier. Rapid technological advancements have led to the development of nanoscale device components, advanced sensors, and novel biomimetic materials. However, potential negative impacts of nanomaterials are sometimes overlooked during the discovery phase of research. The implementation of green chemistry principles can enhance nanoscience by maximizing safety and efficiency while minimizing the environmental and societal impacts of nanomaterials.

This dissertation introduces the concept of green nanosynthesis, demonstrating the application of green chemistry to the synthesis of nanomaterials. A comprehensive review of the synthesis of metal nanomaterials is presented, demonstrating how individual green chemistry principles can improve traditional synthetic routes as well as guide the design of new materials. Detailed examples of greener syntheses of

functionalized gold nanoparticles with core diameters of 2-10 nm are described in subsequent chapters, beginning with a method for functionalizing citrate-stabilized gold nanoparticles that are desirable for advanced applications.

Although citrate-stabilized gold nanoparticles can be easily produced from a classic procedure using mild reagents and benign methods, functionalization via ligand exchange is often unsuccessful. It was discovered that an ill-defined layer comprised of citrate and other ligands interferes with functionalization processes. By removing excess citrate in a manner where overall structure and stability is maintained, gold cores produced by this route are readily functionalized by incoming thiols, affording unprecedented control over surface composition and functionality.

A direct route to functional nanomaterials using Bunte salt precursors is discussed next, describing the use of easily synthesized shelf-stable alternatives to thiols in the preparation of water-soluble gold nanoparticles. Control of core size and surface chemistry is demonstrated through simple manipulation of reagent ratios, yielding products similar to those produced by traditional direct syntheses which rely on the use of thiols.

The use of functionalized nanoparticles as “building blocks” for more complex structures was demonstrated in self-assembly processes. Cationic gold particles were deposited upon DNA scaffolds to create linear arrays.

A discussion of the future outlook of green nanosynthesis concludes this work, identifying immediate challenges and long-term goals. This dissertation contains previously published and co-authored materials.

CURRICULUM VITAE

NAME OF AUTHOR: Jennifer A. Dahl

PLACE OF BIRTH: Oshkosh, WI

DATE OF BIRTH: 1976

GRADUATE AND UNDERGRADUATE SCHOOLS ATTENDED:

University of Oregon, Eugene, OR

University of Wisconsin-Oshkosh, Oshkosh, WI

DEGREES AWARDED:

Doctor of Philosophy, Chemistry, December 2007, University of Oregon

Master of Science, Chemistry, March 2004, University of Oregon

Bachelor of Science, Chemistry, June 2002, University of Wisconsin-Oshkosh

AREAS OF SPECIAL INTEREST:

Nanotechnology

Surface Modification and Analysis

Green Chemistry

PROFESSIONAL EXPERIENCE:

National Science Foundation Integrative Graduate Education and Research
Training Fellow, University of Oregon, 2005-2007

Graduate Teaching Fellow, Department of Chemistry, University of Oregon,
2002-2005

Process Engineering Intern, Inspection Analysis, Hynix Semiconductor
Manufacturing America, Eugene, OR, September 2004-February 2005.

Intern, Environmental Technology Division, Kimberly Clark Corporation,
Neenah, WI, 2002.

GRANTS, AWARDS AND HONORS:

National Science Foundation Integrative Graduate Education and Research
Training Fellowship, University of Oregon, 2005-2007

Westbrook Environmental Research Award, University of Wisconsin-Oshkosh,
2002

PUBLICATIONS:

Dahl, J. A.; Maddux, B. L. S.; Hutchison, J. E. Toward greener nanosynthesis. *Chemical Reviews*, **2007**, *107*, 2228-2269.

Harper, S. L.; Dahl, J. A.; Maddux, B. L. S.; Tanguay, R. L.; Hutchison, J. E. Proactively designing nanomaterials to enhance performance and minimize hazard. *International Journal of Nanotechnology*, **2007**, in press.

Dahl, J. A.; Jespersen, M. L.; Hutchison, J. E. Functionalization of citrate stabilized nanoparticles with water soluble thiols. *Journal of the American Chemical Society*, submitted.

Lohse, S. E.; Dahl, J. A. Hutchison, J. E. Direct aqueous synthesis of large functionalized gold nanoparticles (AuNPs) using Bunte salts as ligand precursors. *Langmuir*, submitted.

ACKNOWLEDGMENTS

As this is the one and only dissertation I will ever have, it is also the only time I will express (in writing, anyway) my gratitude for those whom have supported my graduate work. If the reader finds this far too saccharine for their taste, do skip ahead to the more scholarly works; in the meantime, I have a few people to thank.

My advisor, Jim Hutchison, has spent many hours counseling me not only on my work in the laboratory, but also on the more human matters related to the conduct of a scientist. His frank criticism, tempered with sincere compassion, helped me overcome numerous challenges throughout my graduate career. Regarding my hopelessly outspoken character, he offered this (paraphrased) comment: one may always say what they are thinking, but you must be careful about how you say it. Rather poignant advice, I think; someday I will heed it.

The members of my graduate committee were always ready to help whenever I approached them for advice. The roster has changed over the years, but I am indebted to the earlier members of the committee for their guidance of my first research efforts, as I am grateful for the assistance of the current members as my thesis work concludes.

Beyond the official overseers of my work, I would like to thank Kristi Mikkelsen for her continued assistance as I make the final transition from graduate student to scientist. She always made me seem more organized than I really am, and was truly helpful during some of my busiest times in Oregon.

There are many colleagues whom played a key role in my research efforts, and my work was certainly made better with their consult. Christina Inman and Evan Foster

provided a very welcoming environment when I joined the Hutch lab, and patiently trained me on nearly every instrument I used. To this day, they are still amongst my very favorite people. Mike Jespersen and Greg Kearns were great friends of mine in the lab, and great collaborators on some of my recent projects; despite this, they are some of the best people to share a pitcher of swill with. Sam Lohse was capable of taking on work that I had started and making it something truly intelligent.

There are many more friends and coworkers that I haven't mentioned, but my acknowledgments are getting a bit too syrupy, even for this sentimental girl. Please don't cut me from your Christmas card mailing list.

Finally, I would like to thank my husband, Bart, and my daughter Amanda. Bart never doubted (and often overestimated) my abilities, and offered his organic chemistry wisdom when asked. As for Amanda, her fluttery, often kicking presence during my final months in the lab caused me to become exceedingly cautious and precise in my work. Every scientist should be so lucky to gain this level of awareness of her actions.

To Amanda Jane, my most beautiful experiment.

TABLE OF CONTENTS

Chapter	Page
I. TOWARD GREENER NANOSYNTHESIS	1
1. Introduction	1
1.1 Green Nanoscience	4
1.2 Application of Green Chemistry Principles to Nanoscience	5
2. Toward Greener Synthetic Methods for Functionalized Metal Nanoparticles	15
2.1 Citrate Reductions	18
2.2 Direct Synthesis of Ligand Stabilized Nanoparticles	21
2.2.1 Thiol Stabilized Nanoparticles	22
2.2.2 Phosphine Stabilized Nanoparticles	34
2.3 Seeded Growth and Shape Control of Nanoparticles	36
2.3.1 Spherical Particles	39
2.3.2 Anisotropic Particles and Nanorods	42
2.3.3 Control of Nanoparticle Shape	49
2.3.4 Size Evolution and Nanoparticle Etching	53
2.4 Emerging Approaches in Nanoparticle Synthesis	59
2.4.1 Preparations Involving Minimal Reagents	59
2.4.2 Advances in Nanoparticle Purification	61
3. Toward Greener Preparations of Semiconductor and Inorganic Oxide Nanoparticles	66
3.1 Cadmium Selenide and Cadmium Sulfide	66
3.2 Zinc Nanomaterials	72
3.3 Iron Oxides.....	74
4. Alternative Solvents for Nanoparticle Synthesis	77
4.1 Supercritical Fluids	78
4.2 Ionic Liquids	80
5. Functionalization	83
5.1 Post Synthetic Modification of the Ligand Shell	84
5.2 Ligand Exchange	85
5.2.1 Place Exchanges Involving Ligands of the Same Class	87

Chapter	Page
5.2.2 Introduction of a New Surface Binding Functionality.....	90
6. Future Challenges for Greener Nanosynthesis	94
7. Bridge to Chapter II	99
II. FUNCTIONALIZATION OF CITRATE STABILIZED GOLD	
NANOPARTICLES WITH WATER SOLUBLE THIOLS	101
1. Introduction	101
2. Experimental	107
3. Results and Discussion	112
4. Conclusions	122
5. Bridge to Chapter III	123
III. DIRECT AQUEOUS SYNTHESIS OF LARGE GOLD	
NANOPARTICLES USING BUNTE SALTS.....	124
1. Introduction	124
2. Experimental	127
3. Results and Discussion	131
4. Conclusions	138
5. Bridge to Chapter IV	138
IV. NANOPARTICLE ASSEMBLY ON BIOMOLECULAR SCAFFOLDS ...	140
1. Introduction	140
2. Experimental	145
3. Results and Discussion	147
4. Conclusions	150
5. Bridge to Chapter V	151
V. OUTLOOK AND CONCLUSIONS	152

Chapter	Page
BIBLIOGRAPHY	158

LIST OF FIGURES

Figure	Page
1.1. Translating the 12 Green Chemistry Principles	7
1.2. Key Properties of Nanomaterials	16
1.3. The Electric Double Layer of Nanoparticles in Solution	19
1.4. Large Silver Nanoparticles	20
1.5. Tetraethylene Glycol Terminates a C ₁₁ Alkylthiol Ligand	25
1.6. Lysine Capped Gold Nanoparticles	28
1.7. The Versatile Trifluoroethylester-PEG-Thiol Ligand	30
1.8. Nanoparticles Prepared by Refluxing Gold or Silver Precursors	33
1.9. UV-Vis Absorption Spectra of Gold Nanoparticles	38
1.10. Preformed Gold Nanoparticle Seeds	40
1.11. The Aspect Ratio of Gold Nanorods.....	42
1.12. A Possible Mechanism for Gold Nanorod Formation.....	44
1.13. Diagram of a Pentatwinned Gold Nanorod	46
1.14. Surfactant Directed Growth of Gold Nanorods	47
1.15. TEM Images of Gold Nanoplates	51
1.16. Silver Nanoparticles Prepared by the Polyol Route.....	53
1.17. Triphenylphosphine Stabilized Nanoparticles Evolve	55
1.18. Gold Nanorods Can Be Selectively Oxidized	58
1.19. TEM Images of Nanoparticles Formed via Electron-beam Irradiation	60
1.20. ¹ H NMR Comparison of Nanoparticles Purified by Various Methods.....	65
1.21. Oleic Acid Capped CdSe Nanocrystals.....	71
1.22. The Iterative Formation of Gold Nanoshells around Iron Oxide Cores.....	77
1.23. TEM Image of β-D-glucose Capped Gold Nanoparticles.....	79
1.24. Strategies for Nanoparticle Functionalization	84
1.25. The Labile Triphenylphosphine Ligand Shell	86
1.26. The “Catch and Release” Strategy	89
1.27. A Two-Step Approach to Functionalizing Nanoparticles	92
1.28. A New Strategy for Functionalization	93

Figure	Page
2.1. Schematic of the Diafiltration Apparatus	109
2.2. UV-vis Monitoring of Citrate Molecules in Solution	114
2.3. UV-vis Extinction Spectra of Nanoparticle Solutions.	115
2.4. Thermogravimetric Analysis of Trisodium Citrate Reagent.	116
2.5. Thermogravimetric Analysis of Gold Nanoparticles with Excess Citrate ..	116
2.6. Thermogravimetric Analysis of Stripped Gold Cores.....	117
2.7. XPS Survey Scans of Gold Nanoparticles.....	119
2.8. UV-Vis Extinction Spectra of Gold Nanoparticles.....	120
2.9. TEM Images of Particles	121
3.1. Reaction Scheme for the Synthesis of Gold Nanoparticles.....	127
3.2. The Bunte Salts Used in This Study	128
3.3. UV-Vis Spectra of AuNPs.....	133
3.4. TEM Images of MHT-Stabilized AuNPs.....	135
3.5. A Possible Mechanism of Nanoparticle Growth	137
4.1. Surface Plasmon Resonance in a 1-D Array	141
4.2. Top Down vs. Bottom Up Approaches to Materials Assembly	143
4.3. SEM Images of Si/SiO ₂ TEM Grids	144
4.4. Arrays of Nanoparticles Supported on DNA Scaffolds	148

LIST OF TABLES

Table	Page
2.1. Summary of Nanoparticle Functionalization.....	118
3.1. Summary of Nanoparticle Properties	134

LIST OF SCHEMES

Scheme	Page
1.1. Biphasic Synthesis of 1.4 nm Gold Nanoparticles.....	36
2.1. Strategy for Functionalizing Citrate Stabilized Gold Nanoparticles	106
4.1. Mild Esterification Reactions	150

CHAPTER I

TOWARD GREENER NANOSYNTHESIS

Note: The material in Chapter I originally appeared as a portion of a recent publication, reprinted from Dahl, J. A.; Maddux, B. L. S.; Hutchison, J. E. "Toward Greener Nanosynthesis" *Chemical Reviews*, **2007**, *107*, 2228-2269. The majority of the material appearing in chapter I was authored by Dahl, with contributions from Hutchison; Dahl and Hutchison shared editing tasks in preparation for publication. Portions of the original publication attributed to Maddux were not reproduced in this chapter.

1. Introduction

During the last decade, scientists have developed techniques for synthesizing and characterizing many new materials with at least one dimension on the nanoscale, including nanoparticles, nanolayers, and nanotubes.¹ Still, the design and synthesis (or fabrication) of nanoscale materials with controlled properties is a significant and on-going challenge within nanoscience and nanotechnology.

Nanoscience is still largely in the "discovery phase" wherein new materials are being synthesized (using any means available) on small scales (100s of milligrams or less) for testing specific physical properties. Typically, during this phase of development

of a new technology area, researchers focus mainly on identifying new properties and applications. As a result, the examination of any unintended properties of the material (e.g. environmental or health hazards) or concerns about hazards or efficiencies of the production process is often deferred. Given the anticipated wide application and distribution of these materials in commerce, consideration of the materials design, processes, and applications that minimize hazard and waste will be essential as nanoscience discoveries transition to commercialized products of nanotechnology.

The nature of engineered nanomaterials and their proposed uses provides compelling reasons for the implementation of green chemistry in the development of the new materials and applications. The technology is early in development and expected to be widely applied and distributed. These materials are expected to (i) exhibit new size-based properties (both beneficial and detrimental) that are intermediate between molecular and particulate, (ii) incorporate a wide range of elemental and material compositions, including organics, inorganics and hybrid structures, and (iii) possess a high degree of surface functionality. Assessment of the potential toxicological and environmental effects of nanoscale materials before they are accepted as mature technologies presents an opportunity to minimize putative negative consequences² from the outset and ultimately lead to the design of higher performance materials. Understanding the structure-function relationships that relate specifically to nanomaterials could lead to new “design rules” for producing benign, high-performance nanoscale substances.

Given that green chemistry has been employed successfully in the preparation of highly functionalized products (e.g. pharmaceuticals) that have a strong analogy to the functionalized nanomaterials proposed for a range of future applications, one would expect successful application of this approach for these nascent materials. Application of green chemistry to nanoscience should also prove beneficial in developing production-level commercial scale materials. The development of high-precision, low-waste methods of nanomanufacturing will be crucial to commercialization. In addition to providing enhanced research and development strategies, green chemistry offers an opportunity to improve public perception of nanoscience, as this approach is relatively easy to explain and can be used to convey a responsible attitude toward the development of this new technology. For these reasons, green chemistry can play a prominent role in guiding the development of nanotechnology to provide the maximum benefit of these products for society and the environment.

In this review, we explore the application of green chemistry principles to the field of nanoscience. We first define *green nanoscience*³ and offer examples of the ways in which green chemistry has been, or can be, applied to the design of greener products, processes, and applications. Because the vast majority of the research in this area has, thus far, involved developing greener approaches and processes, this review will focus on nanosynthesis. We further focus the review on those methods that involve wet-chemical approaches to the production, functionalization, purification, and assembly of nanoparticle building blocks. The bulk of the materials covered within the review are ligand-functionalized inorganic nanoparticles, due to the fact that these have been the

most prevalent in the literature to date. Throughout the review, we strive to examine how the application of green chemistry principles to nanoscience can guide technological progress within this emerging field. Because this is an emerging area of technology, we identify future research needs and directions throughout the review.

A number of outstanding reviews on the synthesis and assembly of functionalized nanoparticles have already been published.⁴⁻⁷ This review does not intend to provide comprehensive coverage of these topics but will focus instead on the aspects of these processes that are most relevant to green chemistry. However, publications in nanoscience that identify the environmentally benign aspects of the work are just starting to appear, so we have attempted to identify and highlight the examples from the literature that illustrate greener nanosynthesis concepts and techniques and that help inform the reader of research needs within this emerging field.

1.1 Green Nanoscience

Green chemistry is “the utilization of a set of principles that reduces or eliminates the use or generation of hazardous substances in the design, manufacture, and application of chemical products”.⁸ The 12 principles of green chemistry (originally defined by Anastas and Warner⁸ and summarized in Figure 1.1) have now been applied to the design of a wide range of chemical products and processes with the aims of minimizing chemical hazards to health and the environment, reducing waste, and preventing pollution. Application of these principles has reduced the use of hazardous reagents and solvents, improved the material and energy efficiency of chemical processes, and enhanced the design of products for end of life. Employing these principles toward

nanoscience will facilitate the production and processing of inherently safer nanomaterials and nanostructured devices.

Green nanoscience/nanotechnology involves the application of green chemistry principles to the design of nanoscale products, the development of nanomaterial production methods, and the application of nanomaterials.³ The approach aims to develop an understanding of the properties of nanomaterials, including those related to toxicity and ecotoxicity, and to design nanoscale materials that can be incorporated into high performance products that pose little hazard to human health or the environment. It strives to discover synthesis/production methods that eliminate the need for harmful reagents and enhance the efficiency of these methods, while providing the necessary volume of pure material in an economically viable manner. It also provides proactive design schemes to ensure that the nanomaterials produced are inherently safer by assessing the biological and ecological hazards in tandem with design. Finally, it seeks applications of nanoscience that maximize societal benefit while minimizing impact on the ecosystem. In this way, green nanoscience guides materials development, processing, and application design throughout the life cycle, starting with raw material selection through end-of-life.

1.2 Application Green Chemistry Principles to Nanoscience

Nanoparticles and other nanomaterials that exhibit size-dependent properties are already finding application in products ranging from consumer healthcare goods to high-performance composites.⁹ In addition, a growing number of applications of nanoscience/nanotechnology are being developed that promise environmental benefit,

including new catalysts for environmental remediation,¹⁰ cheap and efficient photovoltaics,¹¹ thermoelectric materials for cooling without refrigerants,¹² lightweight (and thus energy-conserving) nanocomposite materials for vehicles,¹³ miniaturized devices that reduce material consumption, and sensors that eliminate the need for (often) wasteful wet chemical analyses. Nanoscale sensors¹⁴ can also offer faster response times and lower detection limits, making on-site, real-time detection possible. New manufacturing strategies that are additive, rather than subtractive, such as functional group directed processes involving self-assembly, can reduce energy requirements and waste generation. The use of self-assembly methods also enables materials disassembly, incorporating a potential design for end-of-life. To realize new nanotechnologies that pose little harm to human health or the environment and to develop technologies that can be used to improve or protect the environment, it is desirable to design and use greener nanomaterials and develop greener nanoproduction methods.

Nearly all of the principles of green chemistry can be readily applied to the design of nanoscale products, the development of nanosynthesis methods, and the application of nanomaterials (see Figure 1.1). In nearly every case, several of the principles can be applied simultaneously to drive the best design or solution. We will first discuss how the principles *guide* the design and application of nanoscale materials. Next, we describe how the principles *apply* to design, application, and production of nanoscale materials. *Principles of Greener Nanomaterial Design.* Three of the 12 principles (as shown in Figure 1.1) relate directly to nanomaterial design and the application of these materials as

Green Chemistry Principles	Designing Greener Nanomaterial and Nanomaterial Production Methods	Practicing Green Nanoscience
P1. Prevent waste	Design of safer nanomaterials (P4,P12)	Determine the biological impacts of nanoparticle size, surface area, surface functionality; utilize this knowledge to design effective safer materials that possess desired physical properties; avoid incorporation of toxic elements in nanoparticle compositions
P2. Atom economy		
P3. Less hazardous chemical synthesis	Design for reduced environmental impact (P7,P10)	Study nanomaterial degradation and fate in the environment; design material to degrade to harmless subunits or products. An important approach involves avoiding the use of hazardous elements in nanoparticle formulation; the use of hazardless, bio-based nanoparticle feedstocks may be a key.
P4. Designing safer chemicals		
P5. Safer solvents/reaction media	Design for waste reduction (P1,P5,P8)	Eliminate solvent-intensive purifications by utilizing selective nanosyntheses - resulting in greater purity and monodispersity; develop new purification methods, e.g. nanofiltration, that minimize solvent use; utilize bottom-up approaches to enhance materials efficiency and eliminate steps
P6. Design for energy efficiency		
P7. Renewable feedstocks	Design for process safety (P3,P5,P7,P12)	Design and develop advanced syntheses that utilize more benign reagents and solvents than used in "discovery" preparations; utilize more benign feedstocks, derived from renewable sources, if possible; identify replacements for highly toxic and pyrophoric reagents
P8. Reduce derivatives		
P9. Catalysis	Design for materials efficiency (P2,P5,P9,P11)	Develop new, compact synthetic strategies; optimize incorporation raw material in products through bottom-up approaches, use alternative reaction media and catalysis to enhance reaction selectivity; develop real-time monitoring to guide process control in complex nanoparticle syntheses
P10. Design for degradation/Design for end of life		
P11. Real-time monitoring and process control	Design for energy efficiency (P6,P9,P11)	Pursue efficient synthetic pathways that can be carried out at ambient temperature rather than elevated temperatures; utilize non-covalent and bottom-up assembly method near ambient temperature, utilize real-time monitoring to optimize reaction chemistry and minimize energy costs
P12. Inherently safer chemistry		

Figure 1.1. Translating the 12 green chemistry principles for application in the practice of green nanoscience. The principles are listed, in abbreviated form, along with the general approaches to designing greener nanomaterials and nanomaterial production methods and specific examples of how these approaches are being implemented in green nanoscience. Within the figure PX, where X = 1-12, indicates the applicable green chemistry principle.

nanodevices. These are Principle 4 (Designing Safer Chemicals), Principle 10 (Design for Degradation/Design for End of Life) and Principle 12 (Inherent Safety). Application of Principle 4 to product design involves considering the structural features of the nanomaterial (i.e. the size, shape, composition and surface chemistry) that dictate its health hazards (e.g. toxicity) as well as its physical properties. In order to routinely implement this design approach, improved understanding of the structure/activity relationships for nanomaterials is needed. The rich structural diversity of nanomaterials provides significant opportunities to tune and optimize the physical and toxicological properties.

Although a significant body of research exists on environmental and health effects of ultrafine particles, there is still a lack of toxicological data regarding the effects of engineered nanomaterials both on human health and the environment. Ultrafine particle

data show that materials such as silicates, asbestos fibers, and to a lesser extent, carbon black and titanium dioxide, can cause oxidative stress, induce pulmonary inflammation, trigger the release of cytokines and induce signal transduction pathways.^{15,16}

“Nanoparticles” represent intentionally engineered products below 100 nm in diameter with carefully controlled sizes, shapes, and surface chemistries. The unusual properties of nanoparticles (e.g. chemical, optical, or electronic) could lead to adverse biological effects that may be unique compared to larger compositions of the same material.

Variations in particle size¹⁷⁻¹⁹ and surface chemistry^{15,18} can affect the degree of toxicity. For example, nanoparticles may generate free radicals that can adversely affect biological molecules. Significant differences may exist between toxicity of nanoparticles and larger particles of the same chemical composition.^{2,20} For instance, smaller nanoparticles are more likely to enter the circulatory system and travel throughout the body, lodging in distal organs.^{2,15}

Methods developed to analyze the toxicity of ultrafine particles may provide a starting point for determining toxicity of engineered nanoparticles and comparisons can be made in terms of methods of injury (e.g. oxidative stress, inflammatory responses, signal transduction pathways, etc). Traditional testing and screening strategies may be employed initially, leading to novel detection methods that account for the unique properties of nanoparticles. These include *in vitro* cellular assays^{17,21,22} and biochemical analyses which probe the generation of reactive oxygen species and effects on enzymatic pathways. Using *in vitro* assays, route of nanoparticle entry can be determined as well as biochemical effects (such as protein interactions, DNA damage, gene expression changes,

or generation of reactive oxygen species). Genomics and proteomics can track oxidative stress, induction of signal transduction pathways, and apoptosis. Since susceptibility factors vary across a given population based on individual genetic makeup, risk assessment evaluation should accompany information provided by various assays and screens. In vivo studies are essential for identifying potential target organs, travel routes of nanoparticles within the body or other phenotypic changes. Such studies could lead to reliable methods for tracking and quantifying nanoparticles in cells and whole animals.²³ Additionally, dose-response relationships, calculated using a variety of metrics including mass, number of nanoparticles, and surface area, provide a means of normalizing information gathered from individual toxicology studies. As an example, one study analyzed the cellular uptake of citrate-stabilized gold nanoparticles and found acute effects on cell proliferation, motility, and morphology. Unfortunately, only high concentrations were examined, so no definitive conclusions could be drawn on the toxicity of these nanoparticles,²¹ exemplifying how dose-response studies are critical to accurate evaluation of nanoparticles.

Care must be taken in experimental design and analysis of engineered nanoparticles, since variations in structure and purity can lead to altered toxicity. Drastically different methods may be used to produce similar products, but variations in methodology and reaction route often lead to differences in yields, purity, and side products. For example, carbon nanotubes are routinely mass-produced by at least four unique methods, leading to compositionally diverse products.^{20,24} Thus, engineered nanoparticles should be well characterized, with known size and/or distribution, surface

area, shape, solubility, purity, surface chemistry, physical (e.g. crystal structure), electronic or optical properties. Well-characterized nanomaterials are essential to accurate assessments of biological and ecological impacts.

Principle 10 focuses on design related to the environmental impacts of nanomaterials. The approach is to design materials that rapidly degrade in the environment, producing innocuous degradation products. In order to implement Principle 10, further understanding of the fate and transport of designed nanomaterials in the environment will be needed. Long-term effects of nanoparticles in the air, soil, and water are also important considerations in relation to human health because persistence in the environment is directly proportional to the amount of nanoparticles in use.^{19,25}

Environmental impacts of nanoparticles are usually considered in terms of toxicity or exposure,¹⁹ but information garnered from the biological studies described above would complement our understanding of the corresponding environmental implications. For example, bioaccumulation in aquatic and terrestrial organisms will aid in developing models for environmental insult, as well as studies from whole animal analyses and in vitro experiments. Taxonomic and genetic susceptibility are also important considerations. Since chronic exposures often impact the environment in assessing ecological risk, long-term studies analyzing a range of sub-lethal doses should be included. Preliminary studies of the toxicological effects of engineered nanoparticles on *Daphnia magna* have been inconclusive,^{20,26,27} highlighting the present need for carefully designed assessments.

Principle 12 addresses the inherent safety of the material being used. For example, the high surface area and increased reactivity of nanoparticles may lead to explosions and fires in large-scale production, yet when incorporated into macroscale structures, the same material is less likely to be released into the workplace or environment. Taken together, Principles 4, 10 and 12 provide a robust framework for designing nanomaterials with reduced health, environmental or safety concerns.

Principles of Greener Nanomaterial Production. Green chemistry provides a number of advantages in process development and manufacturing as well as product design. Many preparations of the building blocks of nanotechnology involve hazardous chemicals, low material conversions, high energy requirements, and difficult, wasteful purifications; thus, there are multiple opportunities to develop greener processes for the manufacture of these materials.

Some progress toward greener nanosynthesis has already been made. For example, a more efficient and less hazardous synthesis of metal nanoparticles has been developed, producing greater amounts of particles, in less time, under milder conditions, while using less hazardous reagents than the traditional preparation.²⁸ Metal nanoparticles have been synthesized using intact organisms, such as living plants and in microorganisms.²⁹ Microreactors have been used to synthesize nanoparticles in a rapid, continuous process, resulting in reduced waste, improved energy efficiency, and increased control of product properties.³⁰ In each of these processes, green chemistry principles have provided strategies for the development of synthetic methods that are more efficient, reduce waste, and have improved health and environmental impacts.

For the foreseeable future, green nanosynthesis will certainly be an iterative process. As greener methods are developed to provide the nanomaterials needed for testing or applications, the demand for enhanced, or more precise, surface chemistry will often lead to new synthetic methods that require use of materials that are less green. Thus, another round of innovation will be required to meet the material needs while reducing hazards and environmental impact. Reducing the biological and ecological hazards can only be met through tandem testing during the 'discovery' synthesis phase. At each stage of iteration, compromises may arise; thus, metrics will have to be developed to assess the relative greenness of the competing alternatives. As green nanoscience becomes more developed, more benign discovery phase syntheses will be constructed in the first iteration.

One subset of these principles, *Prevent Waste* (P1), *Safer Solvents/Alternative Reaction Media* (P5) and *Reduce Derivatives* (P8), aims to reduce waste by designing methods that minimize the number of processing steps and the amount of ancillary material (solvents, processing aids) used to carry out those steps. An illustrative example involves the fabrication of nanoscale features on a substrate such as a silicon wafer. The traditional strategy for producing these structures is a top-down approach that creates features through a lithographic process involving a significant number of deposition, patterning, etching, and cleaning steps that, in effect, remove material to produce nanoscale structures. This method employs many materials processing and cleaning steps that contribute to the waste stream. The vast majority of the materials used do not end up in the product, therefore resulting in low materials utilization. Alternative greener

approaches include additive or bottom-up processes, employing self-assembly reactions or “direct” write deposition to generate and interconnect the structures. Such alternatives eliminate many processing steps, thus minimizing material and solvent use.

Solvent use is of particular concern in the purification and size selection of nanomaterials. Current methods for purification of nanoparticle samples involve washing or extraction to remove impurities. This process typically requires liters of solvent per gram of nanoparticles and is not usually effective in removal of all the impurities. Size selection is essentially a form of purification that consumes solvents in extraction, fractional crystallization, or chromatographic methods used to separate the different sizes. Development of methods to reduce solvent use in purification and size selection remain essential areas of research in nanoscience.

Another subset of the principles (*Atom Economy* (P2), *Catalysis* (P9), and *Real-time Monitoring* (P11)) aims to maximize materials efficiency, i.e. optimizing conversion of raw materials into desired products by enhancing reaction selectivity and yields. The concept of atom economy (P2) readily applies to wet-chemical nanomaterial preparations in the same fashion as for other synthetic transformations. However, the concept also applies to the fabrication of extended nanoscale structures that use bottom-up approaches such as self-assembly of molecules or nanoscale subunits into more complex structures. Because these approaches incorporate more of the raw materials in the product than corresponding top-down methods, they have higher atom economy. At the molecular level, catalysis (P9) can enhance materials conversion by enhancing the selectivity of reactions, thereby preventing the channeling of raw material into by-products. The

development of highly selective transformations that can be carried out in the presence of diverse, sensitive functionality is a continuing challenge in nanoscience as it is in molecular reaction chemistry. Real-time monitoring (P11) of the production and transformation of nanomaterials, though in its infancy, will be one of the keys to enhancing materials conversion in the future.

Four of the principles, *Less Hazardous Reagents* (P3), *Safer Solvents/Alternative Reaction Media* (P5), *Renewable Feedstocks* (P7), and *Inherent Safety* (P12), can be employed to enhance the process safety or reduce the hazards associated with a process. Many of the “discovery phase” preparations of nanomaterials utilize hazardous reagents (P3, P12) or solvents (P5). There are already a few examples that illustrate the application and benefits of applying these principles to enhance process safety by developing alternatives for toxic and/or inherently hazardous reagents and replacing or reducing the use of hazardous solvents. This is a rich area for investigation as the demand for larger volumes of nanomaterials increases and new methods for nanomaterial synthesis are developed. In some cases, the use of benign feedstocks derived from renewable sources (P7) may prove a successful strategy for enhancing safety in nanomaterial production.

The last subset of the principles involves enhancing energy efficiency and includes *Design for energy efficiency* (P6), *Catalysis* (P9), and *Real-time Monitoring* (P11). Assembly reactions occur under mild conditions with a wide range of suitable materials and synthetic methods to choose from. Bottom-up assembly of nanodevices greatly reduces the number of processing steps, the chances of particle contamination,

and reliance on cleanrooms, all contributing to energy savings. In the event that higher reaction temperatures are needed, as is currently the case for a number of nanoparticle preparations, the development of specific catalysts may be a useful strategy. Given the complexity of many nanoparticle preparation reactions (requiring simultaneous control of composition, dispersity, shape, and functionality), in most cases careful in situ monitoring of reaction conditions and progress (P11) will lead to energy savings as well as improved product characteristics.

This discussion thus far provides an overview of the broad applicability of the green chemistry principles to nanoscience. Each of the 12 principles provides guidance in the design of safer nanomaterials and greener production of these materials. The bulk of this review will describe the current status and on-going challenges for greener synthesis and production of nanomaterials within the context of these defining principles.

2. Toward Greener Synthetic Methods for Functionalized Metal Nanoparticles

Many syntheses of nanoparticles have been developed in recent years, in an effort to produce structures that have specific form and function relevant to a given application. The preparation of functionalized nanoparticles within a green context poses interrelated challenges in terms of maintaining product integrity (such as structure, shape and size dispersity, functionality, purity, and stability) while employing greener methods whenever possible. For example, control over particle size and dispersity may reduce purification requirements by eliminating the need for extensive separations, while the

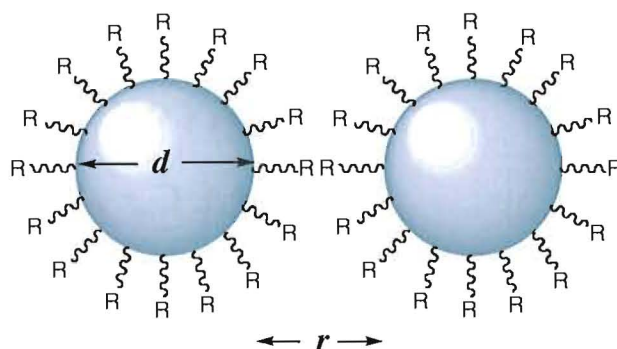


Figure 1.2. Key properties of nanomaterials. The overall size (d) and shape of the particle dictates optical and electronic properties. A stabilizing shell composed of either covalently bound ligands (depicted above) or associated ions provides stability and solubility. Pendant functional groups define reactivity, while the length of the ligand shell determines the minimum interparticle spacing (r).

ability to control surface functionalization, intended to enhance particle stability, dictate surface chemistry, solubility, and the degree of particle interactions (see Figure 1.2) helps to better define the safety and reactivity of nanoparticles.

Nanosynthesis methods are being refined such that they are convenient and scalable, whether it involves the direct synthesis of a functionalized material or the preparation of a versatile precursor particle whose surface properties can be easily modified to meet the demands of a given application.⁵ While a tremendous body of knowledge related to nanosynthesis currently exists, the need for more advanced materials and techniques may bring nanosynthesis back to the discovery phase. Thus, we are presented with a unique opportunity to utilize green chemistry principles while acknowledging existing information, rather than simply retrofitting existing methods to meet greener standards.

To illustrate the status of green nanosynthesis as well as describe the challenges presented by the application of green chemistry to the field of nanoscience, we review the

synthesis of noble metal nanomaterials, beginning first with citrate reductions of metal ions, followed by direct synthesis of ligand stabilized materials. Seeded growth approaches are discussed next, as they relate to both spherical and anisotropic particles. Emerging technologies in green nanosynthesis are discussed, followed by sections describing modifications to nanomaterials that serve not only to impart new functionality, but also allow manipulation of the materials at the nanoscale. Not all of the practices and methods described would be characterized as “green.” Indeed, many classic benchmark methods are described with the intent of providing a historical context for the implementation of green chemistry within nanoscience, while more recent reports offer incremental improvements to traditional practices, addressing process challenges including reducing agent selection, avoiding surfactants, solvent choice, and improving yields, size distribution, and purity. It is by this gradual mechanism that the development of new methods to meet greener standards will occur: without compromise to the overall quality of the nanomaterial products, through continuous effort and revision, rather than as a single revolutionary event.

Direct synthesis of nanoparticles occurs under conditions where the nanoparticles nucleate and grow, usually by the reduction of metal ions. Nanoparticles are often synthesized in the presence of a ligand or a stabilizer that can bind to the surface of the newly formed particle, offering stability and imparting well-defined surface chemistry. Excess ligands may be used to arrest further particle growth, thus offering increased control over nanoparticle size and polydispersity. It is critical that the ligand does not interfere with particle development in an undesirable manner (i.e. by preventing

reduction of the metal ion precursor, or inducing the formation of misshaped particles). Typical ligands include phosphines, thiols, and amines, which may be organic or water soluble, depending on the pendant functionality.

2.1 Citrate Reductions

The reduction of gold salts by citrate anions was pioneered by Turkevich over half a century ago, yielding nearly monodisperse, water soluble gold clusters with diameters ranging from 7-100 nm.^{31,32} Although the synthesis predates green chemistry principles by several decades, it is a rather benign procedure, as the reagents pose little hazard, the preparation does not rely on organic solvents, and few (if any) undesirable side products are generated in the course of the reaction. Revered for its simplicity, requiring only a gold salt (hydrogen tetrachloroaurate, HAuCl_4), trisodium citrate, and water, it remains one of the most reliable methods of creating large gold nanoparticles. Upon addition to a refluxing solution of HAuCl_4 , citrate plays the dual role of reductant and stabilizer, reducing Au(III) to colloidal gold clusters, where virtually all of the gold starting material is converted to product, demonstrating excellent atom economy. Excess citrate stabilizes the particles by forming a complex multilayered assembly of anions having various oxidation states, lending an overall negative charge to the surface, imparting repulsive forces to prevent aggregation. The stability of colloidal and nanoparticle solutions is attributed to the collective effects of van der Waals interactions, electrostatics, and steric forces (figure 1.3).³³ However, these solutions are very sensitive to changes in pH, ionic strength of the medium, and the presence of other organic

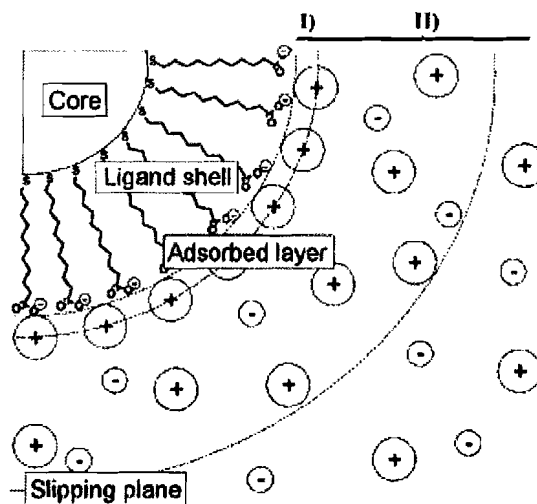


Figure 1.3. The electric double layer of nanoparticles in solution. The tightly bound Stern layer (or adsorbed layer) prevents aggregation by maintaining interparticle repulsion, while a graduated diffuse layer of ions provides compatibility between the dissolved nanomaterials and their solvent environment. (reproduced with permission from Laaksonen, T., Ahonen, P., Johans, C. Kontturi, K. *Chem. Phys. Chem.* **2006**, 7, 2143, Figure 1. Copyright 2006 Wiley Publishing.)

materials, thus complicating efforts to modify the surface chemistry by standard ligand exchange techniques.

Citrate has proven to be a useful reagent in the synthesis of silver nanomaterials, in addition to gold. Pillai and Kamat investigated the role of citrate ions in the synthesis of spherical and anisotropic silver nanoparticles. Citrate reduction of gold ions leads to the formation of spherical particles, but the analogous reaction with silver ions (see Figure 1.4) can yield large silver particles 60-200 nm having a wide range of morphologies, depending upon the reaction conditions, due to citrate's additional role as a complexing agent. The formation of citrate-silver complexes influences crystal growth, and even facilitates photochemical reactions that convert spherical silver nanocrystals to triangular

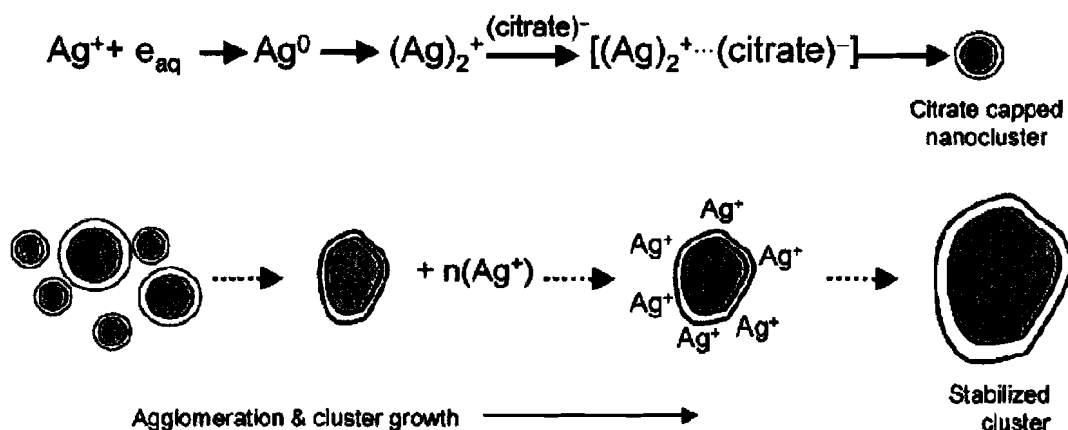


Figure 1.4. Large silver nanoparticles prepared by the citrate reduction route. Excess silver ions permit fusion of smaller particles into a large, stable cluster. Analogous reactions with citrate stabilized gold nanoparticles have been shown to yield higher ordered structures, such as nanowires, from smaller “building block” particles. (reprinted with permission from Pillai, Z. S.; Kamat, P. V *J. Phys. Chem. B* **2004**, *108*, 945, Scheme 1. Copyright 2004 American Chemical Society.)

nanoprisms. Molar ratios of reagents that produce silver crystals in the size range of 50-100 nm produce much smaller nanocrystals (5-20 nm) if a different reducing agent is used, such as sodium borohydride, suggesting that citrate reductions have a unique reaction mechanism. Studies comparing the impact of various concentrations of citrate ions in reactions where the molar amount of silver ion is held constant demonstrate that excess citrate ions dramatically slow the growth of silver nanoparticles. A series of pulse radiolysis experiments demonstrated that citrate ions complex with Ag^{2+} dimers in the early stages of the reaction, hindering seed formation while promoting slow growth of large nanocrystals. These results contrast sharply with the citrate reduction of gold ions, where increased molar ratios of citrate lead to smaller nanoparticles.³⁴

Despite the benign nature of the citrate method, the need for greater stability and precise control over surface chemistry has driven researchers to explore alternative

syntheses which may better suit these goals, but cannot match the green merits of the citrate route. Later sections in the review will highlight methods which preserve or improve upon green aspects of the synthesis of more complex materials, and recent efforts to control the surface chemistry of citrate stabilized gold nanoparticles will be discussed.

2.2 Direct Synthesis of Ligand Stabilized Nanoparticles

A wide range of materials can be generated by reducing metal ions in the presence of a capping agent, providing libraries of diverse materials useful for determining structure/function relationships essential to understanding potential health and environmental impacts, aside from creating materials for targeted applications. The direct preparation of ligand-stabilized nanoparticles provides a simple route to functionalized materials, usually in a single-step, one pot procedure, imparting stability and chemical functionality to the nanoparticle products, often without the need for further modification. Current research challenges are focused on modifying solvents, reaction conditions, and reagents to access a target material, but one should not overlook the opportunity to incorporate greener methods by giving equal consideration to more benign reaction conditions (i.e. choosing safer solvents, avoiding biphasic conditions, and eliminating toxic surfactants), overall yield and atom economy, and environmental fate of new nanoproducts. Additional attention towards controlling average size, dispersity, and purity can further drive processing in a greener direction. The following sections describe the preparation of nanomaterials capped by various classes of ligands, including thiol, amines, and phosphines, highlighting green improvements that have emerged in recent

years. Subsequent discussions will address the synthesis of more complex materials and emerging methods towards greener nanosynthesis.

2.2.1 Thiol Stabilized Nanoparticles

The number of direct syntheses of thiol-stabilized nanoparticles has expanded in recent years since Brust reported the preparation of dodecanethiol-stabilized nanoparticles in 1994. The Brust synthesis provides ready access to functionalized nanomaterials with properties analogous to those of large molecules, as they are stable under ambient conditions and can exist in solvent free forms, in contrast to the less robust citrate based materials. In this reaction a gold salt (hydrogen tetrachloroaurate) is reduced by sodium borohydride in the presence of a capping agent, yielding particles having average core diameters in the range of 2-8 nm. This reaction was first developed within a biphasic context, taking advantage of phase transfer compounds to shuttle ionic reagents to an organic phase where particle nucleation, growth, and passivation occur. Subsequent variations of this procedure demonstrated the full scope of this reaction, substituting a wide range of thiols and varying the ratio of reagents in order to control the average diameter of the products. More recently, reports of water-soluble nanoparticles prepared in this manner have further extended the utility of this procedure, and it remains the simplest direct synthesis of functionalized nanoparticles. The greatest limitation of the Brust prep is that the stabilizing thiol ligands must be compatible with all of the reagents, including NaBH_4 and the phase transfer catalysts (if used for a biphasic preparation of organic soluble particles), thus sidestepping adverse influences on the reaction chemistry. For example, the thiols must not be subject to any unwanted reduction of other functional

groups that may be present on the ligand, and the thiol cannot interact with the phase transfer catalyst in such a way that leads to persistent reagent contamination, or products that are inseparable from the reaction mixture. To this end, Brust-type reactions have been performed in other solvents such as water and THF, permitting a single-phase synthesis of organic soluble gold nanoparticles while eliminating the need for phase transfer reagents.

Here, we will describe modifications to this classic method of synthesizing monolayer-protected clusters, noting refinements offered from Brust and others. Emphasis has been placed on modifications in either design or process that represent improvements within the context of green nanosynthesis, by improving size control and dispersity, utilizing safer solvents, or avoiding surfactants by adapting reactions for a single phase context. Methods that enhance monodispersity are inherently greener, since solvent consumption due to size separation efforts is avoided. Biphasic methods requiring phase transfer reagents are valued for obtaining high quality materials with narrow size distributions, while greener, single phase methods sometimes fail to yield products of equal merit, underscoring the need for continued research efforts within this highly developed class of nanosynthesis.

In 2000, Chen and Murray et al. addressed specific issues of particle growth and monodispersity issues in the preparation of hexanethiol protected gold nanoparticles, monitoring size evolution of the clusters over the course of 125 hrs. Core diameters reached a maximum of 3.0 nm at 60 hrs, and particle growth occurs only if the nanoparticles remain in situ, while toluene solutions of isolated, purified nanoparticles

are stable in solution for extended periods.³⁵ A stable Au₃₈ compound was isolated by a slightly different method, using a reduced temperature adaptation of the Brust synthesis where the biphasic reduction of HAuCl₄ was carried out at 0 °C in the presence of a phenylethanethiol passivating ligand. Reduced reaction temperatures impact nanoparticle growth without significantly slowing nucleation and passivation events, thus leading to a product enriched in smaller particles.³⁶ Jiminez and Murray et al. detailed the synthesis of a Au₃₈ compound having narrow size dispersity. By either reducing the reaction temperature to -78 °C, or by running the reaction at ice temperature with a hyperexcess (300 fold, relative to Au) of thiol, nanoparticle growth is arrested, enriching the products with Au₃₈ clusters.³⁷ The above cases highlight the importance of controlling competing particle nucleation and growth processes in order to limit the size dispersity of nanosynthesis products.

Larger (5-8 nm) gold clusters can be prepared in biphasic water/toluene systems.³⁸ Brust explored a range of biocompatible moieties by using derivatives of thioalkylated polyethylene glycol ligands to impart water soluble ligand shells to 5-8 nm TOAB (tetrabutylammonium bromide) stabilized particles. To access more versatile surface chemistries, a range of target ligands featuring carboxylate, amino, and monohydroxy pendant groups (attached to the terminus of the polyethylene glycol portion of the ligand) were prepared for use in ligand exchange reactions.³⁹ Although the ligands used in these reactions present biocompatible moieties, special care must be taken to ensure that all traces of TOAB are removed from the system prior to use in biological applications.

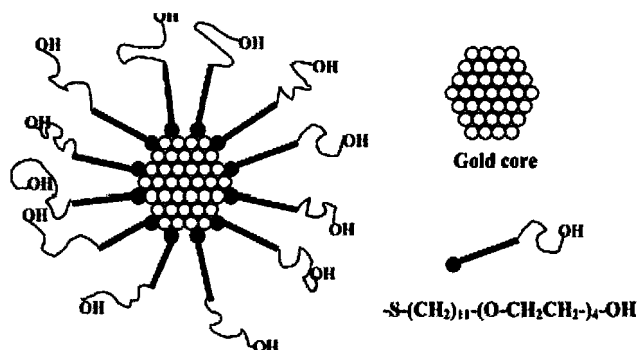


Figure 1.5. Tetraethylene glycol terminates a C_{11} alkylthiol ligand, which offers the combined advantages of water solubility with the high surface coverage characteristic of an alkylthiol capping ligand. (Reprinted with permission from Kanaras, A. G.; Kamounah F. S.; Schaumburg K.; Kiely C. J.; Brust M. *Chem. Commun.*, 2002, 20, 2294, Figure 1. Copyright 2002 Royal Society of Chemistry.)

To generate nanomaterials featuring biocompatible surfaces, Kanaras and Brust used a thioalkylated ligand (monohydroxy (1-mercaptoundec-11-yl) tetraethylene glycol) to introduce a stable, neutral, water soluble functionality to gold nanoparticles by both ligand exchange and direct synthesis routes (see Figure 1.5).³⁸ This work was inspired by Foos' report of water soluble gold nanoparticles capped with short chain thiolated polyethylene glycol ligands that were capable of place exchange reactions, and the work of Murray, whom demonstrated the synthesis of gold clusters in the presence of thiolated PEG. By successfully incorporating water soluble functional groups, these reports inspired researchers to consider new ligands, solvents, and reaction conditions that permit synthesis within a single phase context.

Development of a single phase adaptation of the Brust method of nanoparticle synthesis was motivated by a desire to eliminate issues posed by the use of phase transfer reagents, including cytotoxicity and the potential for persistent contamination. In the course of such developments, many of the single-phase procedures became much greener

as well, sometimes eliminating organic solvents, improving atom economy, and using milder reaction conditions. Quite often the products are benign enough for use in biological applications, especially in the case of certain aqueous procedures. Most single phase adaptations of the Brust method yield products with larger average diameters and size distributions than those produced by the original biphasic procedure, which poses a challenge to researchers targeting smaller functionalized nanoparticles prepared by greener routes. It is believed that variations in product morphology may be attributed to the difference in the ordering of the capping agent in highly polar aqueous environments. Thus, possible solutions may include the use of capping agents that present additional order to aqueous phases (such as those containing hydrogen-bonding moieties) or the substitution of somewhat less polar solvents in lieu of water. The following section highlights some examples of cleaner, more efficient single phase Brust-type syntheses of metal nanoparticles, concluding with some reports of alternative procedures that are likely to open up a new area of innovation in nanosynthesis.

In 1999, Murray et al. reported water-soluble clusters with an average diameter of 1.8 nm, synthesized in single aqueous phase using a method adapted from Brust, where HAuCl_4 was reduced by NaBH_4 in the presence of tiopronin (*N*-2-mercaptopropionyl-glycine). This report focused on the viability of these water soluble nanoparticles as precursors for both ligand exchange and post-synthetic modification via amide coupling reactions.⁴⁰ In the same year, Chen and Kimura reported the synthesis of nanoparticles ranging in size from 1.0 to 3.4 nm by NaBH_4 reduction of HAuCl_4 in the presence of mercaptosuccinic acid, using methanol as a solvent. Although size evolution of the

nanoparticle products in solution became apparent over time, the dried nanoparticle powders were stable and completely redispersible in water. Such nanoparticles could be used to construct various nanostructures by taking advantage of hydrogen bonding or electrostatic interactions controlled by the pendant carboxylate groups.⁴¹

In 2003 a single-phase nanoparticle procedure was developed Pengo, using ligands having common features to those used in the biphasic synthesis of Brust and Twigg. Water-soluble nanoparticles with core sizes ranging from 1.5 to 4.2 nm were synthesized in a single water/methanol phase, using an amphiphilic thiol featuring a hydrophobic mercaptoheptane portion and a hydrophilic triethylene glycol monomethyl ether unit linked together by a central secondary amide. The rate of NaBH_4 addition impacted the average core size and monodispersity, especially if the ratio of gold to thiol was high. The rate of Au reduction corresponds to the initial borohydride concentration: if a reducing agent is added rapidly, small nanoparticles form rapidly and sequester much of the thiols, leaving little capping agent to stabilize (and arrest the growth of) larger nanoparticles.⁴² Such issues are not encountered in the traditional biphasic Brust synthesis, since the rate of NaBH_4 addition is controlled by the phase transfer process at the interface.

A unique approach to water soluble nanoparticles was presented Selvakannan, where aqueous HAuCl_4 is reduced by NaBH_4 in the absence of any potentially toxic stabilizers or phase transfer reagents, yielding 6.5 nm bare gold clusters.⁴³ The amino acid lysine was added to the solution as a capping agent, rather than a thiol. NMR studies suggest that lysine binds to the bare gold clusters via the α -amino group, leading to

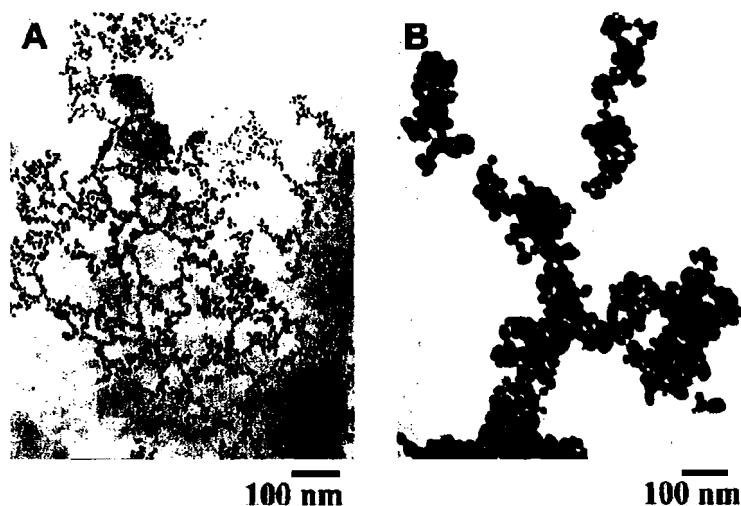


Figure 1.6. Lysine capped gold nanoparticles feature inherently pH-sensitive pendant groups, which may be manipulated to control the degree of interparticle interaction. (Left) Particles at pH = 3. (Right) Particles at pH = 10. (Reprinted with permission from Selvakannan, P. R.; Mandal, S.; Phadtare, S.; Pasricha, R.; Sastry, M., *Langmuir* **2003**, *19*, 3545, Figure 5. Copyright 2003 American Chemical Society.)

reversible pH dependent properties attributed to the pendant carboxyl and amino moieties, agglomerating at pH = 10 and redispersing at lower pH values. TEM images of these structures are shown in Figure 1.6.

Fabris designed thiolated ligands with a various numbers of peptide moieties for use in aqueous Brust procedures, finding that capping agents with greater degrees on conformational constraint (imparted by hydrogen bonding interactions amongst the peptides) yield smaller nanoparticles, reconciling the difference in core sizes provided by biphasic and single phase methods.⁴⁴ Beyond offering more control over the average core size of the products, the presence of hydrogen-bonding peptides increases the overall stability of the particles, evidenced by resistance to cyanide etching.⁴⁵ Conformational constraint appears to be key to the trend reported by Fabris, where Higashi discovered an opposing trend: that increased numbers of helical peptide moieties within a thiol capping

agent lead to larger particles.⁴⁶ However, in Higashi's case, the peptides of neighboring thiols on a nanoparticle probably do not strongly interact with each other (as in Fabris' study) due to their particular conformational arrangement.

In 2004, Rowe and Matzger reported a single-phase synthesis of gold nanoparticles in tetrahydrofuran using metal-to ligand ratios similar to those of the Brust route, yielding products indistinguishable from the biphasic Brust method. While the methods described in this report aren't particularly green, the importance of eliminating phase transfer reagents was highlighted during evaluation of the products. Since small nanoparticles are often synthesized with electrical applications in mind, it is imperative that unnecessary ionic species are removed from the products. The materials obtained by this route were compared to those of the Brust method, and it was found that the charge transport properties of the Brust products were dominated by ionic conduction, overshadowing the tunneling-based behaviors expected of gold nanoparticles.⁴⁷

Besides eliminating issues of contamination associated with biphasic reactions, single phase procedures can provide a facile route to synthesizing water soluble nanoparticles that can act as useful, modifiable precursor materials for use in biologically relevant applications.. For example, Latham and Williams recently developed a unique ligand, trifluoroethylester-polyethylene glycol-thiol, which may be used for direct synthesis, ligand exchange, and post-synthetic modification approaches to functionalized nanomaterials (see Figure 1.7).

has also been used to impart similar chemistries to FePt nanoparticles, which are gaining prominence as MRI imaging agents.⁴⁸

At this point, all discussion has been focused on gold nanoparticles, but further insight can be derived from similar treatments of platinum, lending greater understanding to the preparation of other noble metal materials. For example, Yang and Too et al. described the multiple roles of NaBH_4 in nanosynthesis, demonstrating its additional capability as a stabilizing agent. Platinum nanoparticles were synthesized in the aqueous phase by NaBH_4 reduction of a Pt(IV) precursor. The authors proposed that excess BH_4^- anions hinder transfer to the organic phase by acting as stabilizing agents that hinder the binding of alkanethiols. To confirm this hypothesis, platinum nanoparticles were prepared with a four fold stoichiometric excess of NaBH_4 , and indeed could not be transferred to an alkanethiol/toluene solution unless concentrated HCl was added to the platinum sol in order to accelerate the decomposition of BH_4^- anions. In light of these results, the authors modified their procedure such that the platinum nanoparticles could be transferred to the organic phase immediately upon formation, without the use of a phase transfer reagent, resulting in nanoparticles with an average core size of 2.6 ± 0.4 nm.⁴⁹

Like other methods of preparing gold nanomaterials, weaker reducing agents may be substituted for sodium borohydride. Eklund and Cliffler prepared organic and water-soluble platinum nanoparticles for use as catalytic reagents. Organic soluble particles were synthesized by reducing HAuCl_4 with lithium triethylborohydride (LiTEBH) in the presence of alkanethiols suspended in THF. Aqueous platinum nanoparticles were

prepared in an analogous manner with water soluble thiols, substituting NaBH_4 for LiTEBH and using water as a solvent.⁵⁰ Most recently, the microwave-assisted preparation of platinum nanoparticles catalysts was reported, using only aqueous sugar solutions as a support medium. In this procedure, numerous green challenges were met, including the elimination of organic solvents, surfactants, and strong reducing agents, while demonstrating excellent atom economy.⁵¹

The Brust method of nanoparticle synthesis can be used to generate amine-stabilized nanoparticles by simply substituting an appropriate amine for the thiol. Such particles may provide a route to larger (5-15 nm) materials capable of participating in ligand exchange reactions, since amines are more labile ligands than thiols.

Amine stabilized particles were first prepared by Leff using a method analogous to that of Brust, substituting a primary amine for alkanethiol. Larger nanoparticles having diameters up to 7 nm can be accessed by this method, although dispersity broadens at the upper limit of the size range. If harsh reducing agents (i.e. NaBH_4) are replaced by weaker reagents, or completely omitted from the procedure, even larger noble metal nanoparticles may be obtained, as primary amines are strong enough reducing agents to nucleate and grow particles. Jana and Peng further extended the Brust analogy, synthesizing noble metal nanoparticles in a single organic phase from AuCl_3 (or another organic soluble metal cation), tetrabutylammonium borohydride (TBAB), and either fatty acids or aliphatic amines. Organic soluble articles between 1.5 and 7.0 nm were obtained without the use of surfactants, depending on the amount of capping agent used.⁵²

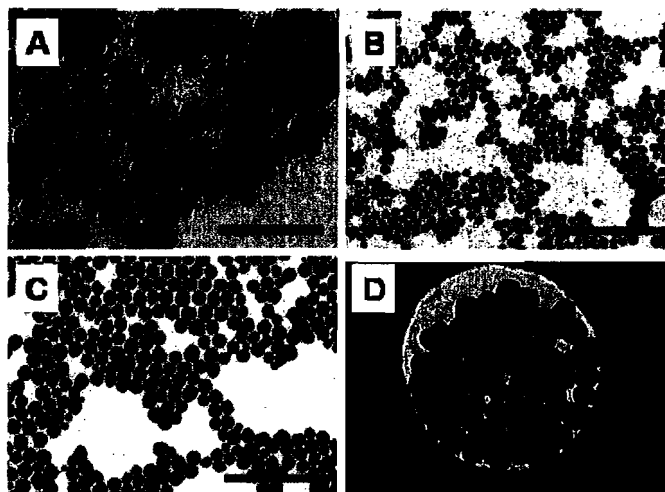


Figure 1.8. Nanoparticles prepared by refluxing gold or silver precursors with oleylamine. (A) 21 nm gold, (B) 9 nm Ag, (C) 12 nm Ag, and (D) 32 nm Ag. Scale bars indicate 100 nm. (Reprinted with permission from Hiramatsu, H.; Osterloh, F. E., *Chem. Mater.* **2004**, *16*, 2509, Figure 1. Copyright 2004 American Chemical Society.)

Hiramatsu and Osterloh found that borohydride reducing agents are unnecessary for the synthesis of nanomaterials in larger size regimes. Gold and silver amine stabilized particles with core diameter ranges of 6-21 nm for gold and 8-32 nm (Figure 1.8) for silver were synthesized in a simple scalable preparation where either HAuCl_4 or silver acetate were refluxed with oleylamine in an organic solvent. Other reducing agents are not necessary, since amines are capable of reducing gold, forming nitriles upon further oxidation. In the case of gold, core size was controlled by regulating the gold to amine ratio, although it is acknowledged that samples with good monodispersity (less than 10%) were achieved only if a minimum of 65 equivalents of amine (relative to gold) were used. Silver nanoparticles were formed by refluxing silver acetate with oleylamine in a variety of organic solvents. The particle size is determined primarily by the reflux temperature associated with each solvent: hexanes (bp: 69°C) yield 8.5 nm particles, while the use of

toluene (bp: 110 °C) and 1,2-dichlorobenzene (bp: 181 °C) results in 12.7 and 32.3 nm particles, respectively.⁵³

Aslam and Dravid et al. reported a similar method of generating water-soluble gold nanoparticles that eliminates harsh reducing agents and organic solvents, while demonstrating greatly improved atom economy. HAuCl_4 is reduced by oleylamine in water, creating nanoparticles that are water soluble despite the apparent mismatch in polarity between the solvent and the stabilizing ligand. Gold is used in excess over the amine, perhaps leading to products with mixed ligand shells whose stability is bolstered by chloride complexes. The products of this reaction have core sizes of 9.5 to 75 nm, and the greatest monodispersity is achieved for particles at the lower end of the size range, where a 10:1 ratio of gold:amine is used. Lesser amounts of amines lead to particles with very wide polydispersities.⁵⁴

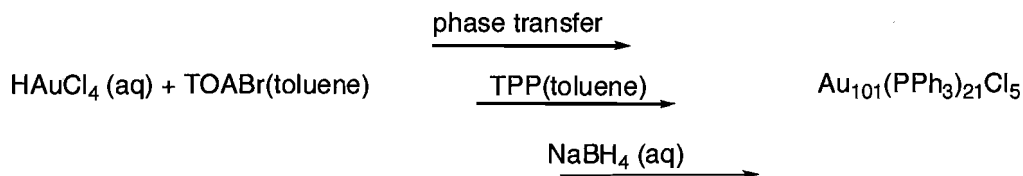
2.2.2 Phosphine Stabilized Nanoparticles

The Brust method of nanoparticle synthesis is a valuable technique for preparing thiol-stabilized nanoparticles, where functional groups are limited only by the compatibility of thiols. However, the identification of a unique set of reaction conditions is often required for the preparation of each functionalized target, and it is often difficult to access smaller nanomaterials by this route. An approach pioneered in our laboratories involves producing a nanoparticle precursor having a temporary stabilizing ligand shell, amenable to ligand exchange reactions with an incoming molecule that has the desired chemical functionality. By optimizing the preparation of a common precursor (synthon) one can generate libraries of diverse nanoparticles that bear pendant functional groups,

thus introducing the desired chemical functionality to the surface of the particle.

Although this procedure requires two steps and employs triphenylphosphine as temporary stabilizing group, this synthon approach has permitted greater control of nanoparticle size, dispersity, and functionality. The tradeoff made is the use of an additional step to avoid the inefficiencies and waste generating purification steps inherent in developing a specific preparation for each direct synthesis. While somewhat unstable, as-synthesized triphenylphosphine stabilized nanoparticles are valued for their ready participation in ligand exchange reactions (which will be discussed in later sections of this review covering nanoparticle functionalization and exchange reactions). The earliest reported syntheses of such particles by Schmid provided the benchmark method for preparing high quality small gold nanoparticles.⁵⁵⁻⁵⁷ $\text{AuCl}(\text{PPh}_3)$ is prepared from HAuCl_4 , suspended in warm benzene, and reduced by a stream of diborane gas, presenting significant health and explosion hazards. Despite the hazards involved, this method remained the most reliable large-scale preparation of phosphine stabilized gold nanoparticles for nearly two decades.

In 1997, Hutchison et al. presented a convenient, safer, and scalable synthesis (Scheme 1.1) that yields high-quality 1.4 nm triphenylphosphine stabilized gold nanoparticles through a much greener route that eliminates the use of diborane gas (>40 L diborane/g nanoparticle) and benzene (>1000g benzene/g nanoparticle). This biphasic synthesis involves the use of a phase transfer reagent (TOAB) to facilitate the transfer of chloroaurate ions from an aqueous solution to an organic phase (toluene) containing triphenylphosphine. Reduction is carried out using aqueous NaBH_4 delivered to the organic phase via complexation with TOAB. There is still opportunity to further



Scheme 1.1. Biphasic synthesis of 1.4 nm gold nanoparticles stabilized by triphenylphosphine.

green this preparation. Substitutions of NaBH_4 for diborane and toluene for benzene are clearly beneficial, however, it would be preferable to avoid using TOAB and find a yet greener solvent. In addition the purification of these particles still requires solvent washes. If membrane filtration methods suitable for use with organic solvents could be developed to replace solvent washes as the purification step, the preparation could be made even less wasteful.

The triphenylphosphine stabilized nanoparticles may be stored as a powder under cold, dry conditions until they are needed for ligand exchange reactions.⁵⁸ Besides being greener and safer, this synthesis also features a great improvement in yield, providing 500 mg of purified nanoparticles from one gram of HAuCl_4 , compared to 150 mg of product from Schmid's method. The products of both preparations yield nanoparticles of equal core diameter, monodispersity, and reactivity. The nanoparticles from Hutchison's prep have been functionalized by a wide range of ligands through ligand exchange reactions, yielding a diverse library of functional nano "building blocks" ideal for use in the bottom up assembly of new nanostructures, all from a versatile gold nanoparticle precursor.

2.3 Seeded Growth and Shape Control of Nanoparticles

In the pursuit of nanoscale materials featuring optical properties, nanoparticles having core diameters exceeding 5 nm can be grown from smaller seed particles through

the epitaxial addition of metal atoms. Delivered to the surface of the seed particle in a partially reduced form, supplemental amounts of a metal salt can be reduced in a surface catalyzed reaction with a mild reducing agent, transforming a solution of small particles to larger colloids. Whether the goal is to grow large spherical particles or nanorods, the use of well-defined seeds is critical to obtaining products with narrow size dispersity. Other reagents such as surfactants may be present as a component of the nanoparticle growth solution, acting in the capacity of a directing agent that promotes the formation of anisotropic materials, or simply as surface passivants and stabilizing agents. Growth of such materials from monodisperse seeds allows the researcher to employ milder reaction conditions for the synthesis of materials, and the wide range of weaker reducing agents capable of reducing metal ions in a growth solution offers increased possibilities for designing greener syntheses. Larger nanomaterials are especially valued for their optical properties, useful for surface enhanced Raman scattering, imaging, sensing, and waveguiding applications, where the optical absorption arising from the surface plasmons (see Figure 1.9) of noble metal materials is key.

The synthesis of larger spherical nanoparticles from smaller seed materials is reviewed, as is the formation of anisotropic nanorod materials. (A complete analysis of seeded growth methods is beyond the scope of this review, but an excellent review of gold nanorods was recently offered by Perez-Juste and coworkers.⁴) A special focus has been placed on studies intended to elucidate the individual roles of nanoparticle seeds, reducing agents, and additives, with respect to their impact on the morphology of the final products. The information garnered from these studies has ultimately contributed to

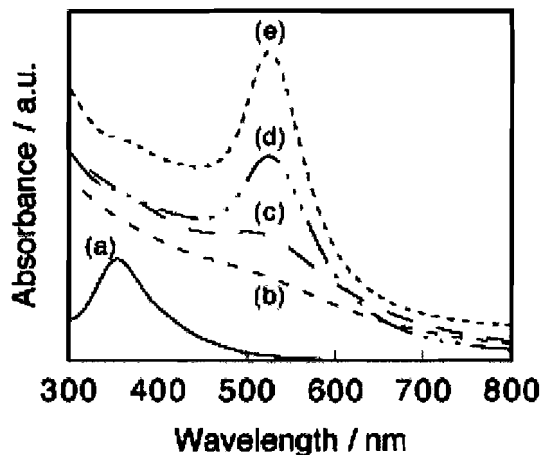


Figure 1.9. UV-Vis absorption spectra of gold nanoparticles corresponding to (a) 1.5 nm (b) 3.4 nm (c) 5.4 nm (d) 6.8 nm and (e) 8.7 nm. Absorptions due to interactions with surface plasmons feature extinction coefficients that increase with particle size, making particles with average diameters > 8 nm appropriate for optical applications. (Reprinted with permission from Shimizu, T.; Teranishi, T.; Hasegawa, S.; Miyake, M. *J. Phys. Chem B.* **2003**, *107*, 2719, Figure 1. Copyright 2003 American Chemical Society.)

a better understanding of the surface chemistry of these materials, which should in turn lead to targeted functionalization methods that will enable their utility in solution-based sensing applications and beyond. Next, shape controlled methods that provide access to more exotic materials are discussed, followed by selective etching techniques (see section 2.3.4) which can be used to give new life to nanomaterials by transforming their shape. Gaining access to larger particles through growth techniques provides a secondary use for small gold clusters (which serve as seeds), while etching techniques can be especially helpful for transforming larger spherical and rodlike structures back to smaller particles. Ultimately, the application of these recycling measures prolongs the useful lifetime of a nanomaterial, reducing the amount of products entering the wastestream.

2.3.1 Spherical Particles

Seeded growth of nanoparticles utilizes a growth solution composed of a weak reducing agent, gold salt, and possibly a surfactant. Small nanoparticle “seeds” are known to exhibit surface selective catalytic properties, and the use of high quality materials allows the researcher to gain additional control over subsequent reactions, whether it involves growth to a larger material or other catalytic applications. The choice of reducing agent was once thought to be the most critical factor in preventing secondary nucleation within a growth solution. Reducing agents such as citrate, some organic acids, and hydroxylamine catalyze the reduction of metal ions at metal surfaces, yet do not contribute to additional nucleation events, since the seed particles themselves act as nucleation centers. Central to seeded growth is the selection of monodisperse, well defined seed particles. Sodium citrate has been used most extensively in this manner to yield particles having average diameters of 20 –100 nm,³¹ although a significant population of gold rods forms with iterative growth. Hydroxylamine is thermodynamically capable of reducing Au³⁺ to the bulk metal, but the rate of this reaction is negligible. Brown and Natan reported the growth of gold nanoparticles with core diameters ranging from 30-100 nm from existing smaller particles prepared by the single-step citrate route, utilizing the surface catalyzed reduction of Au³⁺ by hydroxylamine⁵⁹. The growth of the particles was monitored by visible spectroscopy (see Figure 1.10). The average diameters of the products were governed by the diameter of the seed nanoparticles and the amount of Au³⁺ present in the growth solution. The further utility of this method was demonstrated by exposing a monolayer of nanoparticles

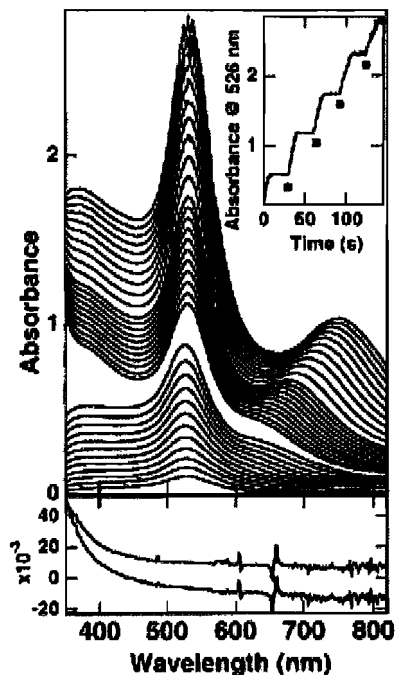


Figure 1.10. Preformed gold nanoparticle seeds are capable of catalyzing further reduction of gold salts at their surfaces in the presence of a mild reducing agent such as hydroxylamine. The reaction between 12 nm gold seeds and a growth solution of HAuCl_4 was followed *in situ* by UV-Vis, showing increased intensity of the surface plasmon band (530 nm) as well as the appearance of higher-order multipole plasmon activity (700-750 nm) indicative of larger gold nanoparticles. (Reprinted with permission from Brown, K. R.; Natan, M. J., *Langmuir* **1998**, *14*, 726, Figure 1. Copyright 1998 American Chemical Society.)

assembled on a solid substrate to hydroxylamine/ HAuCl_4 growth solutions, resulting in the growth of the fixed particles, thereby affording a simple method for decreasing interparticle spacing within a nanoparticle array.

In a follow-up study by Brown, Walter, and Natan,⁶⁰ it was noted that the reduction of Au^{3+} is greatly catalyzed on any surface, and thus other (stronger) reducing agents could be used in seeded growth methods. Growth conditions consisting of the addition of a boiling mixture of citrate to a boiling solution of either 2.4 or 12 nm nanoparticle seeds and Au^{3+} was used to develop the seed particles into larger structures,

even though it is well known that such solutions promote particle nucleation. However, since the rate of reduction at the surface of the seeds greatly exceeds the reduction rate of metal ions in the growth solution, the seed nanoparticles grow at the expense of nucleating new particles.

Jana and Murphy et al. were able to grow nanoparticles having diameters ranging from 5-40 nanometers with narrow polydispersity from 3.5 nm seeds, using stock solutions of HAuCl_4 and a surfactant, cetyltrimethylammonium bromide (CTAB), as a growth medium. The reduction of Au^{3+} was carried out by ascorbic acid. The authors found that an iterative approach to nanoparticle growth, where seed particles are repeatedly exposed to fresh aliquots of growth solutions, yields products of greater monodispersity in terms of both size and shape. The presence of CTAB added stability to the nanoparticle solutions and aided subsequent functionalization by alkanethiols.

The preparation of seeds intended for use in nanoparticle growth procedures need not be by the citrate reduction route. Sau et al. reported the photochemical preparation of seed particles with core diameters ranging from 5-20 nm. Various aqueous solutions of HAuCl_4 were reduced to gold colloids by a photochemically activated reaction with a polymeric stabilizing agent, Triton X-100 (poly(oxyethylene)iso-octylphenyl ether). Nanoparticle growth was initiated by the ascorbic acid catalyzed reduction of surface-adsorbed Au(III) ions, reaching final core sizes ranging from 20-110 nm, depending upon the size of the seed particles and the amount of gold ions present in the growth medium.⁶¹

2.3.2 Anisotropic Particles and Nanorods

Anisotropic metal nanoparticles feature unique optical properties which have generated interest in applications related to surface enhanced Raman scattering, single molecule detection, surface enhanced fluorescence, biological imaging, and scanning optical microscopy techniques, amongst many others.^{4,7,62} Anisotropic materials possess multiple surface plasmon bands with tunable positions (see, for example, Figure 1.11) based on the overall size of the particle and the aspect ratio (length divided by width, in the case of nanorods). Additionally, anisotropic materials feature enhanced electric fields at the tips of the structure,⁷ making them especially well-suited for many of the applications listed here.

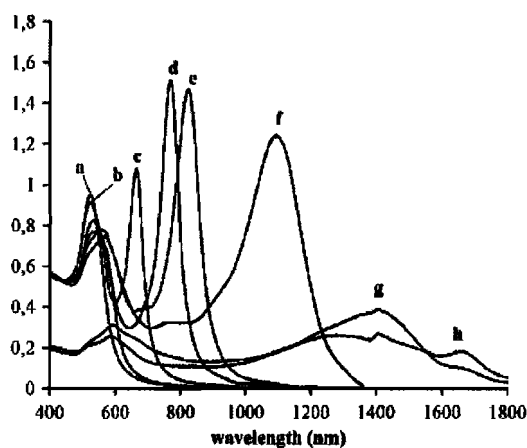


Figure 1.11. The aspect ratio of gold nanorods may be tuned by controlling the ratio of gold seeds:growth solution. The extinction spectra a-h result from increasingly reduced amounts of seed particles, which effectively increases the amount of growth solution available for addition to individual particles. (Reprinted with permission from Jana, N. R.; Gearheart, L.; Murphy, C. J. *Adv. Mat.* **2001**, *13*, 1389. Figure 1. Copyright 2001 Wiley Publishers Ltd.)

While an understanding of growth mechanisms has been accumulated, several challenges remain towards shifting the synthesis and application of these materials toward a greener context. It has been acknowledged that mild conditions may be used for seeded growth approaches, yet efforts to maximize yields of anisotropic materials relative to spherical by-products remains a significant challenge, despite increased mechanistic understanding. The replacement of surfactants with other shape-directing agents would greatly improve the green merits of seeded growth while broadening the range of utility for these materials, enabling their use in applications where low toxicity is a priority. The following contributions offer insight into both the growth mechanisms and unique surface chemistry of anisotropic particles, setting the stage for future refinements in the functionalization and application of these materials.

Formation of nanorods relies on coordination chemistry between the surface of the seed particle and additives such as surfactants, passivants, chelating agents, or polymers which hinder the growth of certain crystal faces, promoting an overall lengthening of the seed particle as the metal ions of a growth solution are reduced at the exposed faces.⁴ Besides presenting a useful synthetic route towards the preparation of reduced-symmetry materials, such approaches may offer a simple means of creating ordered arrays of nanorods if placement of the gold seeds is controlled.^{63,64}

The mechanism by which growing particles break symmetry and favor growth in a particular direction has been the topic of much speculation, as the formation of reduced symmetry materials occurs under a wide range of circumstances. Although nanorods can form spontaneously under conditions intended to favor growth of symmetric colloids, it is

understood that surfactants may act in a capacity beyond that of mere passivants, directing epitaxial growth of a particular crystal face by hindering the growth of others. However, a number of preparations of shape-controlled materials have been reported where symmetry breaking of a growing seed particle is not considered the key step in the growth mechanism (see section 2.3.3).

To favor the formation reduced symmetry particles, the use of a directing agent is required. A surfactant such as CTAB, known to bind preferentially to the pentatwinned crystallographic faces of a seed, leaves other regions of the particle available as growth sites. This method suggests that the surfactant simply acts as a directing agent, rather than a soft micellar template, although the surfactant does form stabilizing bilayers along the length of the nanorod. Surfactants with longer hydrophobic tails naturally form more robust bilayers, and thus higher aspect ratio materials are achieved.

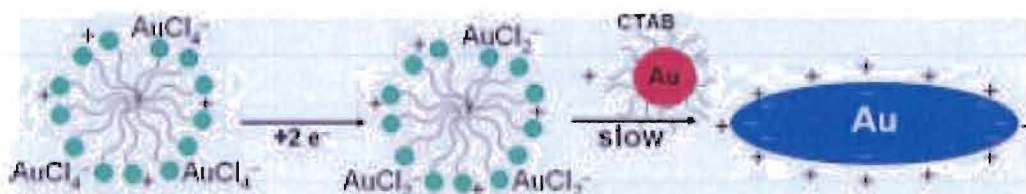


Figure 1.12. A possible mechanism for gold nanorod formation. AuCl_4^- anions displace bromide at the surface of CTAB micelles, where they are reduced from Au(III) to Au(I) by ascorbic acid. Transport from the micelle to the micelle-coated gold seeds is favored by double layer interactions, leading to deposition at the tips of the seeds. (Reprinted with permission from Perez-Juste, J.; Liz-Marzan, L. M.; Carnie, S.; Chan, D. Y. C.; Mulvaney, P., *Adv. Functional Mat.* **2004**, *14*, 571, Scheme 1. Copyright 2004 Wiley Publishers Ltd.)

Mulvaney has suggested an alternative mechanism (see Figure 1.12), where gold ions are encapsulated within micelles and preferentially delivered to the ends of a growing nanorod, since the ends of the rod have the highest electric field gradient compared to the

rest of the structure.⁶⁵ The authors note that while this mechanism may explain anisotropic growth, it does not provide a clear description of the symmetry breaking events that initiate anisotropy.

Murphy, Mann and coworkers explored the crystal structure of nanorods at various stages of growth from smaller seed particles prepared by the NaBH_4 enhanced reduction of HAuCl_4 in the presence of citrate anions, which serve primarily as a capping agent.⁶⁶ Spherical particles were iteratively exposed to fresh growth solutions containing AuCl_4^- , ascorbic acid, and CTAB. After a single exposure to the growth medium, the average particle size had evolved to from 4.3 ± 1.2 nm to 9.6 ± 2.1 nm. Using HRTEM selective area electron diffraction, it was found that shape anisotropy arises from the emergence of a penta-tetrahedral twin crystal at the surface of a growing spherical nanoparticle. It is believed that once symmetry breaking occurs within a spherical particle, subsequent growth will occur preferentially along the $\{110\}$ axis (see diagram in Figure 1.13). Nanorod structures evolve from such a configuration by elongation of the five fold $\{100\}$ axis central to the five (111) faces which will become the capping ends of the nanorod. Subsequent exposures to the growth medium resulted in the formation of larger spherical colloids, in addition to an emerging population of reduced symmetry materials. It is proposed that Au-surfactant complexes are incorporated into the (100) side faces, while non-complexed clusters and ionic species favor the end faces, leading to an overall elongation of the nanorod.

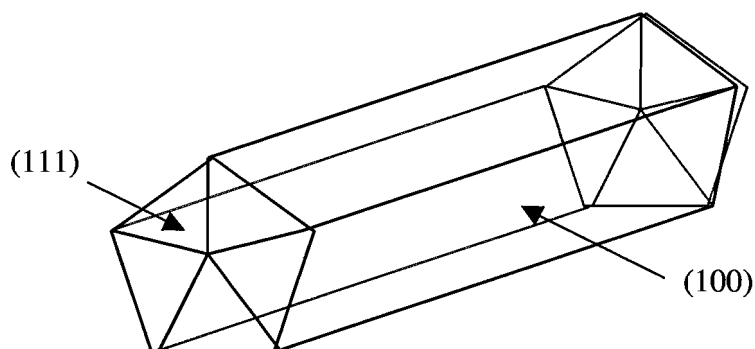


Figure 1.13. Diagram of a pentatwinned gold nanorod, highlighting the major crystal faces of the structure. Preferential binding of stabilizers to a particular face is believed to play a role in nanorod formation. (Adapted from Johnson, C. J.; Dujardin, E.; Davis, S. A.; Murphy, C. J.; Mann, S. *J. Mater. Chem.* **2002**, *12*, 1765, Figure 3a. Copyright 2002 Royal Society of Chemistry.)

As the role of surfactants in seeded growth approaches to nanorod synthesis was better understood, delineating the impact of the nature of the seed particles used in such techniques became the focus of later mechanistic studies. Murphy has suggested that the sterics of the ammonium head group of CTAB are most compatible with the lattice arrangement found along crystal faces making up the length of the nanorod (see Figure 1.14).⁷ Prior to more focused studies of this topic, Nikoobakht and El-Sayed published a follow-up study to Jana's silver ion enhanced studies of seeded growth methods, replacing citrate capped seed materials with CTAB stabilized gold nanoparticles, and assessed the use of a cosurfactant (benzyltrimethylammonium bromide, BDAB) in addition to small amounts of silver ion.⁶⁷ Both modifications of the iterative seeded growth process strongly favored the growth of nanorods over larger spherical colloids to the extent that spherical particles composed only 0-1% of the nanomaterial products.^{68,69}

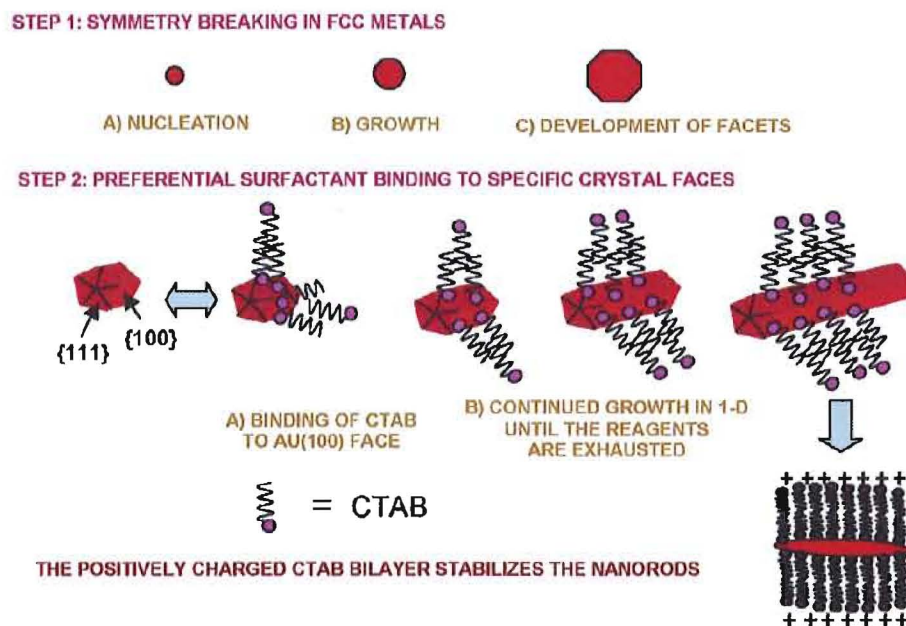


Figure 1.14. Surfactant directed growth of gold nanorods. Once seed particles grow large enough to develop facets, surfactants bind preferentially to (100) faces, permitting growth at the exposed ends of the nanorod. (Reprinted with permission from Murphy, C. J.; Sau, T. K.; Gole, A. M.; Orendorff, C. J.; Gao, J.; Gou, L.; Hunyadi, S. E.; Li, T. *J Phys. Chem. B* **2005**, *109*,13857, Figure 8. Copyright 2005 American Chemical Society.)

A more comprehensive study describing the impact various types of gold seed particles have on nanorod synthesis was undertaken by Gole and Murphy, comparing particles differing in both their average diameter and surface chemistry.⁷⁰ In this work, negatively charged seeds were compared to positively charged seeds (where citrate, mercaptobutylamine, and glucose stabilizers impose a negative charge, and CTAB stabilized particles bear an overall positive charge, due to partial bilayer formation). Negatively charged seeds produced materials with a wider range of aspect ratios, where positively charged seeds produced nanorods with relatively consistent dimensions. The average core size of the particles within these categories was varied, ranging from 3.5 to 18 nm. It was found that the gold nanorod aspect ratio has an inverse relation to the size

of the seed particle, and larger seeds produce bimodal populations of shorter and longer nanorods. Since nanorod synthesis is believed to take place largely through unencumbered epitaxial growth at the ends of the rod coupled with hindered growth along the surfactant-protected longitudinal faces, it is quite likely that facile rearrangement or displacement of the original capping agent is essential to the formation of high aspect ratio materials. Thus, particles having covalently bound thiol capping agents are ill-suited to surfactant directed growth processes, whereas those stabilized by materials similar to those present in the growth medium readily interact in a manner consistent with the proposed nanorod formation mechanism.

Less obvious factors in the synthesis of anisotropic materials have been explored, focusing on the presence of various ions in solution. Gold seeds were added to growth solutions containing CTAB, HAuCl_4 , ascorbic acid, and sometimes AgNO_3 . The morphology of the particles was related to the interdependent factors imposed by the concentrations of the growth solution components, suggesting that the surfactant-induced faceting processes compete with growth kinetics to determine the final shape of product.⁷¹

The role of silver ions is still not completely understood. It is proposed that Ag^+ binds to the surface of the particles as AgBr , restricting growth of the particle in a manner similar to CTAB. Silver ions are not reduced in the presence of ascorbic acid or trisodium citrate at room temperature. Bromide ions were also found to be essential: substitution with iodo- or chloro- analogues of both the silver salt and the ammonium surfactant does not lead to growth of anisotropic materials.⁷ Cyanide dissolution studies of nanorods prepared with either CTAB or Ag^+ as a directing agent have differing degrees of

resistance towards decomposition, suggesting that CTAB may be more densely packed on the rods if Ag^+ is present, leaving the tips of the rods vulnerable to cyanide digestion.⁴

Recently, it was determined that pH has a significant role in directing the formation of gold nanoprisms.⁷² A simple solution phase seeded growth method was used, employing standard procedures similar to those described above, with the exception of NaOH as an additive in the growth medium. Increasing the pH of the growth solution deprotonates ascorbic acid, giving the monoanion form in solution. The monoanion is believed to bind more effectively to the ends of the nanorod, facilitating gold reduction at this site. Paradoxically, at pH values exceeding 5.6, a mixture of large spherical particles and crystalline flat triangular nanoprisms is obtained by this method, rather than the nanorod structures typically afforded by seeded growth in the presence of CTAB.

Clearly, tremendous effort has been put forth toward understanding the mechanisms of anisotropic nanocrystal growth, which will hopefully set the stage for redesigning synthetic methods to meet greener standards. Elimination of surfactants is clearly the greatest challenge, followed by the need to improve yields of nanorods grown from spherical seeds. Aside from these shortcomings, seeded growth approaches allow the researcher to perform nanosynthesis of sophisticated materials under mild conditions, using relatively benign reagents.

2.3.3 Control of Nanoparticle Shape

Modifications of the citrate reduction method for silver and gold ions have led to numerous reports of anisotropic materials synthesis. The following section discusses methods that provide access to nanomaterials with unusual shapes, some of which avoid

the use of harsh reducing agents, surfactants, and organic solvents. Many of these reports expand upon established knowledge of common nanosynthesis techniques (such as seeded growth) while exploring the use of new additives as shape modifying agents.

Pei reported a simple method for synthesizing gold nanowires from spherical citrate stabilized gold particles simply by introducing excess HAuCl_4 to a solution of gold nanoparticles.^{73,74} Excess chloroaurate ions adsorb to the surface of the nanoparticles, introducing an attractive force that draws the particles together, while additional gold ions fill in the gaps between particles. Schatz and coworkers reported a citrate reduction that was bolstered by the addition of hydrogen peroxide and a capping agent, bis-(*p*-sulfonatophenyl)phenylphosphine (BSPP), resulting in the formation of unique, single-crystal branched gold nanoparticles exhibiting one, two, or three distinct tips.⁷⁵ The particles begin as small triangular nuclei, and subsequent selective binding of the BSPP directing agent results in anisotropic crystal growth in a direction parallel to the nuclei edges. Chu recently reported the citrate reduction of a surfactant-gold complex formed between HAuCl_4 and cetyltrimethylammonium bromide (CTAB) yielding flat gold structures. Hexagonal, triangular, and truncated triangular materials (Figure 1.15) can be obtained by varying the ratio of reagents and the reaction time.⁷⁶

Occasionally, removal of the directing agent can be difficult, hindering the use of these materials in applications such as surface-enhanced Raman spectroscopy and self assembly processes, where good control over the particles surface chemistry is essential. Murphy reported the synthesis of crystalline silver nanowires in the absence of surfactants. Silver salt was reduced by citrate anion at 100 °C, in the presence of a small

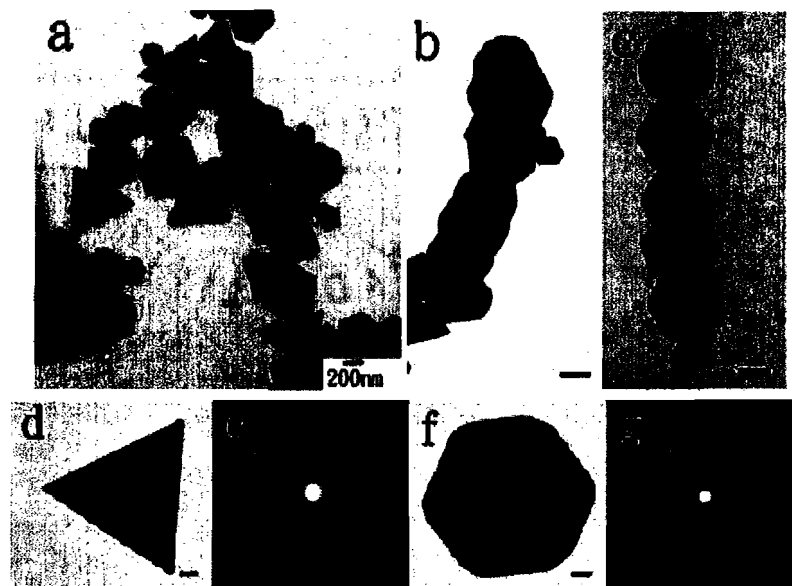


Figure 1.15. TEM images of gold nanoplates and chainlike arrangements of gold nanoplates (a-c). Triangular and hexagonal plates with their corresponding electron diffraction patterns (d-g). (Reprinted with permission from Chu, H.-C.; Kuo, C.-H.; Huang, M. H. *Inorg. Chem.* **2006**, *45*, 808, Figure 4. Copyright 2006 American Chemical Society.)

amount of hydroxide ion. A moderate amount of hydroxide (6-8 μL of 1M NaOH, 40 μL of 0.1 M AgNO_3 dissolved in 100 mL deionized water) yields predominantly nanowires (35 ± 6 nm) when reduced by citrate. If the hydroxide source is omitted, this preparation results in spherical nanoparticles. Citrate performs in multiple capacities in this reaction, as it complexes with silver ions, reduces the ions to metallic silver, and caps the resulting structure, imparting water solubility. The relatively small amounts of NaOH ensure that citrate is completely deprotonated, making it a stronger complexing agent, yet hydroxide competes with citrate for binding sites on the growing nanostructure, thus directing crystal growth.⁷⁷ In an alternative shape-controlling procedure, Swami reported the synthesis of nanoribbons at the air-water interface.⁷⁸ Alkylated tyrosine is capable of acting as a phase transfer material, reducing agent, and a capping stabilizer. Due to the

limited water miscibility of this organic reagent, gold reduction is restricted to the air water interface, reducing the possible degrees of freedom for crystal growth.

More unusual nanocrystal shapes have been produced by the polyol reduction method. In 2003, Xia reported the synthesis of nanoprisms having tunable optical properties.⁶² Silver nitrate was reduced by citrate and sodium borohydride in the presence of poly(vinyl pyrrolidone) (PVP), initially yielding spherical nanoparticles. Irradiation of the solution with a halogen lamp initiated a photochemical reaction leading to the formation of triangular nanoprisms. Further UV irradiation led to an additional morphological change, transforming the nanoprisms to circular disks. In a later report, the synthesis of nanocubes and truncated cubic structures (shown in the TEM in Figure 1.16) by a modified polyol procedure was described, where silver nitrate was thermally reduced in a PVP/ethylene glycol solution.⁷⁹ Initially, only twinned crystals were observed by TEM. After stirring under ambient conditions for two days, single crystal cubes and tetrahedral structures were obtained in high yield. The addition of sodium chloride to the reaction mixture was a critical factor in the evolving crystal morphology. It was proposed that exposure to oxygen selectively etched the twinned materials, and chloride stabilized the liberated silver ions, allowing only the remaining single crystal materials to grow. In a somewhat analogous procedure reported by Kan, gold ions were reduced by a polyol route, yielding large gold nanoplates with morphologies that were dependent upon the reaction times.⁸⁰ Physisorption of polar groups likely restricted crystal growth on the (111) face, leading to flat structures.



Figure 1.16. Silver nanoparticles prepared by the polyol route, featuring cubic and truncated cubic structures. (Reprinted with permission from Wiley, B.; Herricks, T.; Sun, Y.; Xia, Y. *Nano Lett.* **2004**, *4*,1733, Figure 2D. Copyright 2004 American Chemical Society.)

2.3.4 Size Evolution and Nanoparticle Etching

Modification of existing nanostructures such that their size or shape changes with the use of minimal reagents further increases the multitude of uses for materials produced by a single synthetic procedure, opening up the possibility of recycling nanomaterials for secondary uses. For example, smaller nanoparticles having diameters below 2 nm are most often studied for their electronic properties, but if these same particles are transformed (perhaps by a ripening process) to larger single crystal nanoparticles, one could envision launching studies of the optical properties associated with these materials without developing an entirely different synthetic protocol. Such procedures are especially useful if the size evolution process leads to nanomaterials with excellent size monodispersity, as one common drawback of some convenient nanomaterial preparations is the tendency to form polydisperse products, which is often the case for many variations of the Brust nanoparticle synthesis.

Several of the nanoparticle-enlarging techniques described below require the use of (quite toxic) TOAB as a stabilizing agent. The green value of these methods could be greatly improved by identifying an alternative stabilizer. In some cases, commendable efforts toward the removal of TOAB from the final product were made. Purity of nanoproducts will continue to be a universal issue for the application of nanoscience, especially since the elimination of surfactants remains one of the greatest challenges in greener nanosynthesis. With this in mind, we have included a section highlighting various purification methods (see section 2.4.2).

The transformation of larger nanomaterials to smaller structures is also attractive from the standpoint of generating high quality materials, as well as the prospect of studying size dependent physical properties. To this end, the controlled etching of a crystalline nanorod affords the opportunity to study fundamental properties associated with changing aspect ratios, without the complications that arise from multiple product morphologies produced by growing nanorods from spherical seed particles (including highly faceted materials, nanocubes, prisms, and other truncated structures). In this manner, well-defined nanomaterials may serve as synthons, appropriate for reuse in subsequent reactions to yield products with altered morphologies. This section highlights various procedures that can be used to modify the size of nanomaterials, yielding high quality products that can be utilized in applications beyond their initial purpose.

In 1999, Hutchison and coworkers found that they were able to transform 1.5 nm triphenylphosphine stabilized particles to 5 nm amine stabilized materials in a highly reproducible manner, simply by stirring the smaller particles in a solution containing a

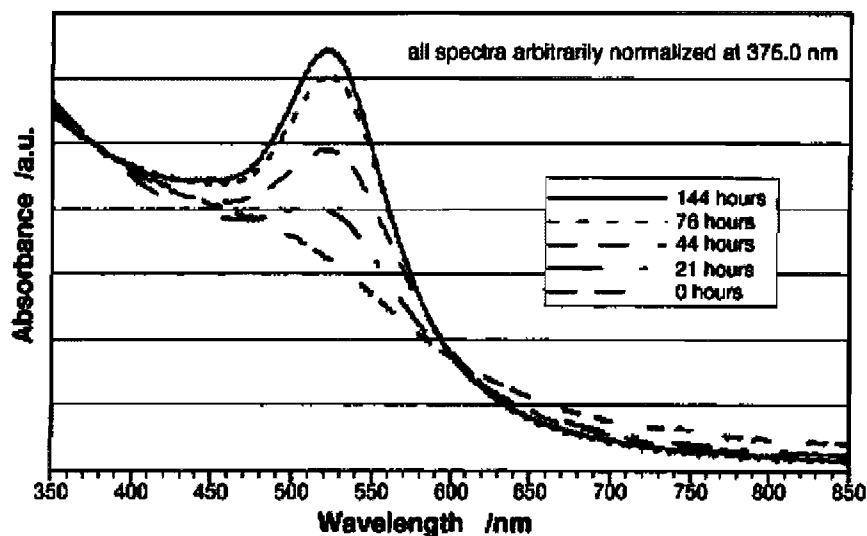


Figure 1.17. Triphenylphosphine stabilized nanoparticles evolve to larger amine stabilized gold nanoparticles with strong optical absorption upon reflux with a solution of alkylamines. (Reprinted with permission from Brown, L. O.; Hutchison, J. E. *J. Am. Chem. Soc.* **1999**, *121*, 882, Figure 3. Copyright 1999 American Chemical Society.)

primary amine.⁸¹ Visible spectroscopy, Figure 1.17, shows the development of a narrow plasmon resonance at ~ 525 nm as the growth process proceeds. Similar conditions are often applied with thiols for the purpose of ligand exchange reactions, but no core size evolution was ever noted in those cases. A bimodal size distribution is maintained throughout the course of the reaction, indicating that smaller particles are consumed as larger particles grow. Analysis of the nanoparticles composition by XPS indicates that displacement of the triphenylphosphine stabilizer is complete, and no small particles remain, yielding products with excellent reproducibility in terms of their size and composition. Besides providing a secondary use for smaller particles, this method also features the green merits of room temperature operation, nearly quantitative yields, and additive processing.

While Hutchison's report is an excellent example of creating larger monodisperse nanoparticles from smaller precursor materials, an even greater challenge lies within the transformation of relatively polydisperse materials to those having a more uniform size distribution. Miyake and coworkers reported size evolution processes in the solid state.⁸²⁻⁸⁴ Having identified the boiling point of a nanoparticle mixture as a key limitation in thermal size evolution processes, dodecanethiol-stabilized particles prepared by the Brust route were used as a starting material for the thermal reaction. When the crude nanoparticles were stripped of their solvent and heated to temperatures of 150, 190, and 230 °C, the 1.5 nm particles grew to sizes of 3.4 ± 0.3 , 5.4 ± 0.7 , and 6.8 ± 0.5 nm, respectively,⁸² suggesting that the nanoparticles grow until they become thermodynamically stable at the heat treatment temperature. Unfortunately, molten TOAB is essential in this reaction, as particles heated treated in its absence did not experience a similar growth.⁸³ Additionally, a mechanism for the thermal reaction was elucidated, whereby the small thiol stabilized particles are believed to melt and coalesce to a thermodynamically stable product, which is once again capped by thiols as the ligands rearrange around the product.

More recently, Miyake and coworkers explored the thermal size evolution of gold nanoparticles stabilized by 11-mercaptopundecanoic acid (MUA).⁸⁴ The pH dependent solubility of the MUA-stabilized particles played a critical role in the thermal reaction. Since it has been established that TOAB is critical to uniform size evolution processes, treatment of the particles with HCl leads to reduced solubility in non-polar solvents, as TOAB readily complexes with the particles in their ionized state. Such pH treatments

were essential for comparison of the thermal treatments in the presence and absence of TOAB, since treatment with HCl is required for the complete removal of TOAB. Once again, the particles formed monodisperse products in the presence of TOAB. Upon heating to temperatures of 150, 160, and 170 °C, the 1.8 nm particles grew to average diameters of 2.4 ± 0.4 , 4.6 ± 0.8 , and 9.8 ± 1.2 nm, respectively. While it is reassuring that excess surfactants may be removed from the products, surfactants must be eliminated from thermal size evolution processes so that the merits of this method (improving monodispersity, materials recycling, and preserved atom economy) overshadow the drawbacks.

In contrast to transforming nanomaterials to larger structures, simple etching processes are helpful for controlling reaction conditions by removing unwanted material from a mixture, as well as the straightforward modification of larger materials to smaller, simpler structures. Etching not only provides a clear route to secondary applications of nanomaterials, but it may also serve as a means of narrowing size dispersity.

Control over nucleation events is critical in the synthesis of many larger and more complex nanostructures. Xia and collaborators reported the use of a selective oxidative etchant capable of reducing the number of seed nuclei in solution, thus allowing larger nanostructures to develop without competitive reactions with emerging nucleation centers.⁸⁵ FeCl_3 was used in conjunction with the polyol reduction of PdCl_4^{2-} , leading to an unprecedented synthesis of larger Pd nanocubes ranging from 25-50 nm. When the same reduction was carried out in the absence of Fe(III), the resulting Pd structures had a maximum dimension of only 8 nm. This reaction was performed under ambient

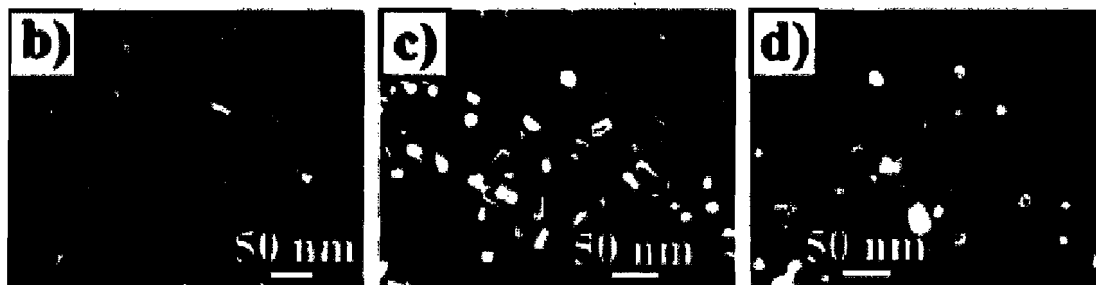


Figure 1.18. Gold nanorods can be selectively oxidized (b) to yield structures with reduced aspect ratios (c). Continued oxidation results in spherical particles (d). (Reproduced from Tsung, C.-K.; Kou, X.; Shi, Q.; Zhang, J.; Yeung, M. H.; Wang, J.; Stucky, G. D. *J. Am. Chem. Soc.* **2006**, *128*, 5352, Figure 1 b,c,d. Copyright 2006 American Chemical Society.)

conditions, which were later determined critical to the suppression of excess nucleation, since oxygen is required to sustain the continuous etching activities by converting Fe(II) back to Fe(III). FeCl₃ is a known noble metal etchant whose use in nanosynthesis could certainly be applied to other materials where control over nucleation and growth processes is key towards reaching a synthetic target structure.

Etching techniques are most commonly used to completely decompose noble metal structures, usually for the purpose of analyzing their organic components. Recently, Stucky et al. reported the use of mild oxidation methods to reduce the aspect ratio of gold nanorods by selectively etching the ends of the structures, eventually arriving at spherical nanoparticles as shown in Figure 1.18. Gold nanorod solutions were acidified with HCl and oxygen gas was bubbled through the stirring solution. The oxidation rate was proportional to the concentration of hydrochloric acid and temperature. This reaction requires the use of additional CTAB to stabilize the nanomaterials as they are etched, but this controlled method of size evolution allows researchers to decompose nanomaterials

in a manner that avoids the use of harsh oxidizers such as nitric acid or concentrated hydrogen peroxide, and entirely toxic reagents, including cyanide.⁸⁶

2.4 Emerging Approaches in Nanoparticle Synthesis

2.4.1 Preparations Involving Minimal Reagents

While continuous efforts have been made to improve overall reaction yields, atom economy is often overlooked as a potential refinement to nanosynthesis techniques. Atom economy can be improved by choosing solvents and reagents capable of serving multiple roles. For example, one could employ reducing agents which also function as a stabilizing material (such as carboxylates and amines), solvents which can act as a reducing agent or stabilizer (such as diglyme), or change solvent systems such that auxiliary materials such as phase transfer reagents may be omitted. From a completely different angle, the use of solid-state techniques provides an opportunity to completely bypass the need for solvents. Another benefit of reducing the number of components of a reaction is that subsequent purification needs are often simplified, or even eliminated. The following section highlights reports of syntheses that have taken advantage of minimal reagent use, while yielding high quality materials.

The Brust synthesis of gold nanoparticles involves the reduction of a gold(I)- thiol polymeric complex, yielding thiol-protected gold nanoparticles. As part of an investigation intended to better characterize these polymeric precursors, Kim et al. found that irradiation under the electron beam of TEM led to the formation of gold nanoparticles. As shown in Figure 1.19, by changing the accelerating voltage of the electron beam, particles ranging from 2 to 5 nm in diameter could be obtained. Higher

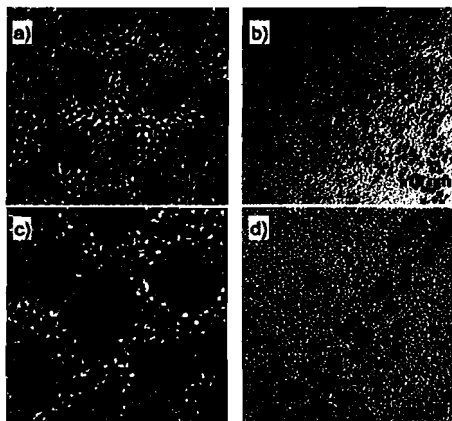


Figure 1.19. TEM images of nanoparticles formed via electron-beam irradiation of gold(I) salts with various hydrocarbon chain lengths and accelerating voltages. (a) Au(I)-SC₁₈ at 300 keV, (b) Au(I)-SC₁₈ at 80 keV, (c) Au(I)-SC₆ at 300 keV, and (d) Au(I)-SC₂ at 300 keV. (Reprinted with permission from Kim, J.-U.; Cha, S.-H.; Shin, K.; Jho, J. Y.; Lee, J.-C. *J. Am. Chem. Soc.* **2005**; *127*, 9962, Figure 2. Copyright 2005 American Chemical Society.)

accelerating voltages promote particle nucleation, where lower voltages favor growth of larger particles. Additionally, like many other nanoparticle preparations, it was found that the length of the hydrocarbon chain of the thiol is inversely proportional to the size of the resulting nanoparticles.⁸⁷ While this example doesn't provide an especially practical means of preparing larger particles, it highlights the importance of product purity, as excess unreacted starting materials can induce changes in product morphology.

Recently it was discovered by Yamamoto and Nakamoto that gold(I) thiolate complexes can form nanostructures via simple pyrolysis reactions. The controlled thermolysis of a gold(I) thiolate complex, Au(C₁₃H₂₇COO)(PPh₃), at 180 °C under inert atmosphere for 1-10 hours leads to particles capped primarily by myristate and a small amount of phosphine, ranging in size from 12-28 nm. This reaction does not require the use of solvents, stabilizers, or reducing agents, although higher reaction temperatures are required, and purity may be an issue. Thermolysis temperatures can be elevated to access

particles with larger diameters. The particles are soluble in acetone and remain in solution for weeks. The reaction occurs by the elimination of the myristate ligand, which reduces the gold and caps the particles. Eliminated PPh_3 reacts with the precursor complex, producing $\text{Au}(\text{PPh}_3)_2\text{C}_{13}\text{H}_{27}\text{COO}$, which does not participate in thermolysis reactions. Triphenylphosphine is believed to act as a stabilizing agent for the intermediate gold(0) species formed during the thermolysis reaction.⁸⁸

Lastly, silver nanoparticles (3-14 nm) were prepared at the air-water interface below Langmuir monolayers of Vitamin E. Using an alkaline solution of Ag_2SO_4 is key to promoting reduction by the phenolic groups of vitamin E, since the resulting phenolate ions are capable of transferring electrons to the silver ions during nanoparticle formation.⁸⁹ This method bears some analogy to the biphasic Brust procedure, in that Vitamin E monolayers behave as a solventless organic phase. The green merits of this procedure are quite pronounced, since it uses no organic solvents, harsh reducing agents, or phase transfer materials, and doesn't require extensive washes or precipitation-based purification techniques. Although the procedure is difficult to scale up in its current form, the use of continuous-flow microchannel reactors may enable greater production.

2.4.2 Advances in Nanoparticle Purification

Although they are not readily detected in the most commonly employed analytical techniques (e.g. TEM and SEM), impurities including unreacted starting materials, excess reagents and by-products resulting from side reactions or degradation pathways are present in nanoparticle samples and have been shown to have significant impact on properties such as reactivity,⁹⁰ stability,⁹¹ and toxicity. Nearly all end applications of

nanomaterials will necessitate the use of highly pure materials, particularly those intended for electronic or medical purposes. The development of structure-activity relationships (SARs) critically depends upon the availability of pure samples. For example, in developing the SARs related to the health impacts of nanomaterials, these studies become more complicated, or impossible, when one must delineate whether or not a nanomaterial is inherently toxic, or if the deleterious effects are due to contaminants and byproducts. Thus, a key to furthering our understanding of SARs for nanoparticles and to designing greener nanoparticles for a wide range of applications is the development of effective purification strategies that can provide samples with fully characterized and reproducible purity profiles. The greenness of the purification methods themselves should be a central focus, since many techniques currently used rely on the use of large amounts of solvents (often liters/gram) for extraction or washing purposes. A brief comparison of purification methods currently in use is offered below, with the intention of illustrating the state of nanoparticle purification methods, guiding the researcher to the most appropriate, efficient techniques and motivating the development of new purification strategies.

Centrifugation and precipitation techniques are amongst the most established means of isolating nanomaterials from the bulk reaction mixture. Centrifugation isolates materials based on mass and relative solubility, while precipitation is effected by a loss of solubility in the reaction media due to the introduction of an antisolvent. Both methods have been used for the separation of noble metal nanoparticles and carbon-based nanomaterials. Each can be time-consuming and solvent intensive. Although the

volumes of solvent consumed in these purifications are hard to quantify based upon the reported procedures, one analysis of a typical purification method has recently been reported. In a traditional purification strategy, purification of a thiol-stabilized gold nanoparticle requires a combination of precipitation, extraction and ultracentrifugation. This sequence of steps generates considerable organic solvent waste (> 15L solvent/gram nanoparticle) and is not effective in removing all the small molecule impurities.⁹² A more rigorous purification required a combination of extraction, ultracentrifugation, and chromatography steps. Recently, extractive methods have been developed to include more sophisticated means of separation, using surface-selective reagents to promote cross-linking or phase separation exclusively amongst the products, ensuring that other contaminants remain in the bulk of the reaction mixture.⁹³⁻⁹⁷

Chromatography provides a means of purification and size fractionation, provided the products are sufficiently stable and not excessively retained by the column support. In the authors' experience working with dozens of ligand-stabilized gold nanoparticles, chromatography (particularly size exclusion chromatography)⁹⁸ has proven effective for removal of small molecule impurities from the nanoparticle products. However, in nearly all cases recoveries are quite low (a few percent) due to sample degradation and/or irreversible binding to the support. Despite these limitations, size-exclusion chromatography is still a viable method for producing milligram quantities of relatively pure material. Others have reported recent advances in this technique that include the separation of carbon nanorods⁹⁹ and recycling of size exclusion materials.¹⁰⁰

Electrophoresis has also been used to separate metal nanoparticles based on the relative

core size, and recently, has been proven to be a useful method of separating particles based on the relative number of functional groups.¹⁰¹ Most chromatographic methods reported to date are also solvent-intensive methods (with the exception of those carried out in water) and have proven difficult to scale to produce larger amounts of pure nanoparticles.

In an attempt to find new methods of purification that reduce solvent consumption while enhancing separation performance, a number of researchers have turned their attention to nanofiltration methods and have made significant strides toward purifying noble metal and magnetic nanomaterials in a greener, more efficient process.^{92,102,103} Such methods typically employ solvents such as water and simple alcohols, as other organic solvents are often incompatible with filter membrane materials. In particular, diafiltration affords a simple, rapid method of isolating nanomaterials with superior purity and yield compared to the more traditional techniques described above. Sweeney et al. demonstrated the efficiency of diafiltration for the purification of ligand-stabilized gold nanoparticles by comparing the proton NMR spectra of products from different purification methods. The spectra in Figure 1.20 show that the sharp signals due to free ligand, top trace, are absent in the diafiltered sample, but exist to varying degrees in the samples purified by the other methods. In this case, diafiltration produces higher purity material while eliminating the use of organic solvent in the purification process. As noted above, the traditional purification of these materials requires liters of solvent per gram of nanoparticle and does not effectively remove the contaminants. Diafiltration, on the other hand, is more effective and eliminates the use of organic solvent in this

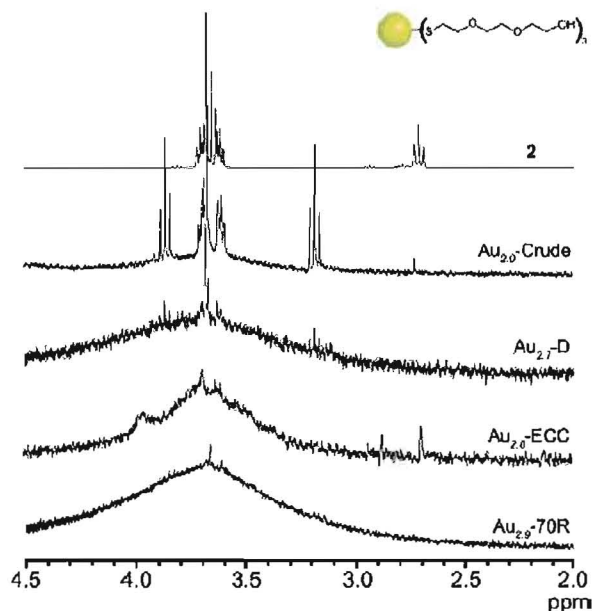


Figure 1.20. ^1H NMR comparison of nanoparticles purified by various methods. From the top, NMR signals arising from the ligand alone, crude nanoparticles, nanoparticles purified via dialysis ($\text{Au}_{2.7}\text{-D}$), extraction, chromatography, and centrifugation ($\text{Au}_{2.8}\text{-ECC}$), and diafiltration ($\text{Au}_{2.9}\text{-R}$). The sample purified via dialysis has an undetectable amount of free ligand, whereas the presence of free ligand is readily detected by NMR for the other samples. (Reprinted with permission from Sweeney, S. F.; Woehle, G. H.; Hutchison, J. E. *J. Am. Chem. Soc.* **2006**, *128*, 3190, Figure 2. Copyright 2006 American Chemical Society.)

purification. Membrane based methods such as diafiltration are scalable to large volumes.

Given the importance of purity for fundamental studies and practical applications of nanoparticles and the convenience and effectiveness of nanofiltration for purification, further research is warranted to develop membranes with finer control over pore size and size dispersity and to develop membranes that are compatible with organic solvents (for use with nanoparticles requiring such conditions).

3. Toward Greener Preparations of Semiconductor and Inorganic Oxide

Nanoparticles

Studies related to greener methods of synthesizing semiconductor nanomaterials are still relatively scarce, and thus presents one largely unexplored frontier in nanoscience. Synthetic challenges are numerous, providing significant opportunities to incorporate green nanoscience principles in the design of new methods. One specific challenge involves the synthesis of true nanoalloys, free of significant phase separation between individual components. Another area of exploration includes controlling the unique surface chemistry of such materials at the nanoscale. Despite the fact that many of these materials are inherently toxic, green nanoscience principles developed through metal synthesis could be applied to semiconductor and oxide materials to enable greener process development to minimize overall impacts on human safety and the environment.

Several particular materials have been the focus of intense research, and a great deal of progress has been made toward greener processing. The discussion below highlights advances in the synthesis of cadmium, zinc, and iron compounds, with special emphasis on processes that reduce hazard in preparation and enable materials applications.

3.1 Cadmium Selenide and Cadmium Sulfide

Although these materials contain toxic elements, they remain the focus of intense study. Fortunately, numerous modifications have been made to standard procedures, leading to safer and greener methods. Ultimately, the inherent safety of these materials is

contingent upon identifying an appropriate substitute for Cd^{2+} , without compromising the optical properties that make these materials so useful.

Typically, CdSe nanocrystal synthesis involves the use of dimethyl cadmium with trioctylphosphine oxide (TOPO). The raw materials (organometallics, usually) are especially toxic, pyrophoric, unstable, and expensive, and the reactions often lack control and reproducibility.¹⁰⁴ The reaction solvent TOPO is prohibitively expensive and hinders the possibility of industrial scale up procedures,¹⁰⁵ and the surface chemistry of such materials is limited, reducing the options for further manipulation of the particles. However, although the established synthetic procedures suffer these apparent shortcomings, this approach has been useful for the formation of high-quality CdSe nanoparticles. Nevertheless, it is clear that greener, more efficient synthetic procedures are needed, although the development of a completely green technique has remained a daunting task. If we accept that the nanoscale products of CdSe/CdS syntheses are likely to retain their inherent toxicity regardless of the synthetic methods used, multiple opportunities to develop greener methods remain. The modification of a single step in these procedures may eventually build the foundation for the use of safer techniques in nano-semiconductor syntheses, leading to a benign methodology resulting from a composite of incremental improvements.

To this end, early progress was made by O'Brien and coworkers, replacing a pyrophoric cadmium source, dimethyl cadmium, with air-stable precursor complexes, specifically, bis(methyl(*n*-hexyl)di-thio or -seleno) carbamate complexes of zinc or cadmium. Nearly monodisperse ($d = 5.0 \pm 0.3$ nm) quantum dots of CdSe, CdS, ZnSe, or

ZnS can be prepared by this route. The use of these air-stable complexes has greatly simplified the preparation of such QDs, requiring only the preparation of a solution with trioctylphosphine, followed by stirring with TOPO at 200 °C, yielding air-stable TOPO capped materials.¹⁰⁶

Peng reported a significant reduction of the hazard associated with the use of highly reactive dimethyl cadmium, achieved by conversion to a stable, isolable cadmium complex via the reaction of cadmium oxide with hexylphosphonic acid (HPA).

Alternatively, this complex can be formed in situ by the reaction of CdO with HPA at elevated temperatures. The use of this precursor in TOPO-mediated reactions with selenium yields CdSe nanocrystals having a diameter > 2 nm, which is difficult to obtain by the traditional route. The full scope of this breakthrough is being explored as other precursors have been formed by reaction of CdO with fatty acids, amines, phosphonates, and phosphine oxides. Thus, hundreds of greener combinations are possible. Larger, monodisperse particles ($d = 1.5 - 25$ nm) have been accessed via syntheses utilizing these precursors, which have a range of reactivity based on the complexing ligand, resulting in a variety of average core diameters.¹⁰⁴

The use of dimethyl cadmium alternatives was further simplified in a one pot synthesis of core-shell CdSe/CdS quantum dots.¹⁰⁷ Beginning with air-stable, readily available cadmium acetate, quantum dots with excellent photoluminescent quantum efficiencies were prepared in a mixture of TOPO, hexadecylamine, and tetradecylphosphonic acid, which serves as a capping agent. Selenium was introduced in a typical manner as a trioctylphosphine complex. Besides acting as a capping agent, the

phosphonic acid slows the growth of the dots, offering more control over the core size. Additionally, the relatively lower reactivity of cadmium acetate (vs. dimethyl cadmium) hinders the formation of excess nuclei and consumption of cadmium monomers, permitting the growth of somewhat larger materials. To develop a CdS passivation shell, H₂S was introduced in the gas phase to the crude reaction mixture via injection through a rubber septum into the headspace of the reaction vessel, permitting slow delivery of the reagent to the quantum dot mixture, thus allowing the slow epitaxial growth at the surface of the CdSe particles.

Cadmium chloride has also proven to be a useful alternative to pyrophoric cadmium sources. Another step was made towards realizing a useful synthetic procedure by eliminating the need for TOPO as a reaction medium.¹⁰⁸ Bao reported the synthesis of CdS nanorods in toluene, utilizing a new class of ligands, alkylisothionium salts, to stabilize the growing nanorods in analogy to the use of alkylammonium salts in the synthesis of reduced symmetry gold and silver materials. A variety of alkyl chain lengths were considered (C12, C14, and C18) and it was found that S-dodecylisothionium (C12) salts yield nanorods with the highest aspect ratios. Thiourea and ethylenediamine play key roles in the mechanism of nanorod formation. The authors propose that ethylenediamine forms a complex with Cd²⁺, which then reacts with thiourea to form CdS nuclei. The surfactants bind preferentially to certain crystal faces, thus directing subsequent growth into a nanorod. More recently, Querner et al. reported the use of another class of bidentate ligand, carbodithioic acids, as an alternative shell material for the passivation of CdSe cores.¹⁰⁹ Besides offering passivation comparable to CdS, ZnS,

and ZnSe, such ligands permit control over the surface chemistry of the nanomaterials. Specifically, the ligands feature a pendant aldehyde that can participate in subsequent coupling reactions, allowing the introduction of various functional groups without disturbing the photoluminescent properties of the core materials.

Commercially available heat transfer solvents have proven to be useful as a direct substitute for TOPO, if one wishes to preserve all other aspects of the traditional preparation of CdSe quantum dots. Wong and coworkers explored the use of two commercially available solvents, Dowtherm A (a mixture of biphenyl and diphenyl ether) and Therminol 66 (a terphenyl-based blend), which are able to sustain the high temperatures which warrant the use of TOPO.¹¹⁰ Cadmium oxide was reacted with a trioctylphosphine selenium complex in the presence of oleic acid, yielding 2.7 nm particles, somewhat smaller than those obtained by analogous reaction conditions in TOPO. Other alternative solvents having high boiling points, such as octadecene and octadecene/tetracosane blends, have also been used to achieve the temperature control required for the greener synthesis of ZnSe and ZnS nanomaterials from the alkylamine-catalyzed reaction of Zn-fatty acid complexes with selenium-phosphine compounds.¹¹¹

As suggested earlier in this section, incremental improvements to the traditional preparation of cadmium-based nanomaterials have the potential to add up to an all-around greener synthesis. An excellent example was offered by Deng and coworkers, using paraffin as the reaction medium for the synthesis of high quality (demonstrated by the characterization methods shown in Figure 1.21) cubic CdSe quantum dots.¹¹² In this greener procedure, CdO and oleic acid were dissolved heated paraffin. Selenium was

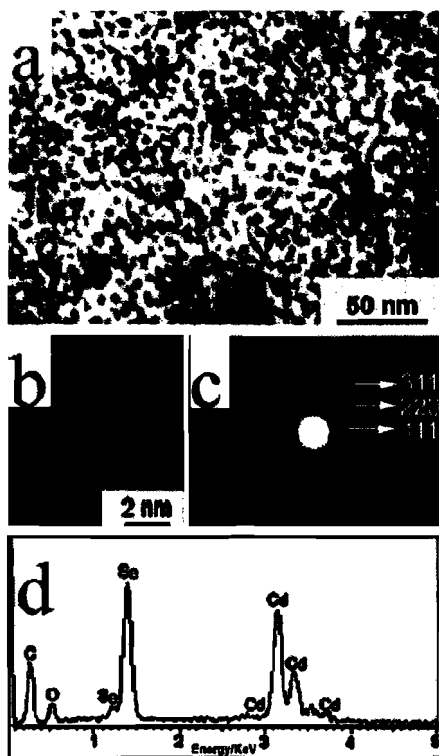


Figure 1.21. Oleic acid capped CdSe nanocrystals. (a) TEM image, (b) HRTEM, (c) electron diffraction pattern, and (d) EDX of corresponding particles. (Reprinted with permission from Deng, Z.; Cao, L.; Tang, F.; Zou, B. *J. Phys. Chem. B* **2005**, *109*,16671, Figure 5. Copyright 2005 American Chemical Society.)

dissolved in a separate aliquot of paraffin, and the two mixtures were combined, yielding particles with diameters of 2-5 nm, depending upon the reagent concentration. This low-cost procedure not only eliminates the use of TOPO, but also dispels the need to prepare a selenium-trioctylphosphine complex, greatly reducing the majority of hazardous reagents and reaction conditions associated with the preparation of these materials.

Although CdSe and CdS quantum dots are inherently toxic regardless of the method of preparation, careful manipulation of the surface chemistry of such materials can facilitate more “hands-off” approaches to the handling of these materials. We have already described the clever use of a chelating ligand that promotes modification of the

pendant functionality of quantum dots, and such approaches are likely to gain further prominence if self-assembly techniques are used in the fabrication of quantum dot arrays. Templating approaches offer an alternative means of dictating the relative positioning of quantum dots. Broadly speaking, templates can serve multiple roles, acting as nucleation centers during synthesis,¹¹³ stabilizing agents for synthesized materials, and assembly directing matrices. While there is a trend towards minimizing risks by reducing the direct handling of quantum dots, it should be noted that this solution is only as robust as the stability of the particles within a given application; that is, accidental release of tethered particles remains a possibility, so long-term greener solutions rely on the identification of alternative materials, rather than the containment of toxic nanoparticles.

3.2 Zinc Nanomaterials

The formation of spherical zinc oxide nanoparticles is a very straightforward process, commonly achieved through a simple base catalyzed reaction of zinc acetate with hydroxide ions, hydrothermal reactions of various Zn(II) sources in the presence of base, and gas phase reactions of organozinc compounds, involving either thermolysis or controlled oxidation. Although the reports are too numerous completely review, they have provided a foundation of knowledge over the years, contributing to the discovery of a number of methods for the synthesis of anisotropic ZnO nanostructures, several of which are especially noteworthy for their greener merits.

The use of ionic precursor compounds is common in the synthesis of anisotropic materials, since their general preparation closely matches the classic techniques of spherical particle synthesis. Chang created 2-D arrays of nanorods through a solution

process using aqueous preparations of zinc nitrate and hexamethylenetetramine (HMTA).¹¹⁴ The amine generates ammonium hydroxide in the presence of water, which reacts with Zn^{2+} to form ZnO. The arrays were formed on various substrates featuring a ZnO overlay formed by atomic layer deposition. It is proposed that such substrates are critical to nucleation events, since their lattice-matched surface templates seed layer formation that leads to the growth of single crystal materials. Electron energy loss spectroscopy revealed the presence of nitrogen at the core of the nanorods, confirming that larger nanorods are the product of smaller, thinner individual rods that fuse together as the reaction proceeds. A somewhat similar process was reported by Sun and Yan et al., whereby ZnO nanowires form via the stacking and fusion of rectangular nanoplates.¹¹⁵ Briefly, $\text{Zn}(\text{OH})_4^{2-}$ is prepared from zinc acetate and sodium hydroxide and reacted in SDS reverse micelles, resulting in the formation of small uniform nanoparticles. The particles fuse together in a hexagonal crystal arrangement (wurzite structure), creating plates that stack together to form nanorods, retaining their rectangular cross section.

Elemental zinc has also proven useful in greener nanosynthesis. Zhao and Kwon synthesized aligned single crystal ZnO nanorods by a hydrothermal reaction between zinc powder and hydrogen peroxide.¹¹⁶ This preparation has the added advantage of being completely templateless, avoiding issues of persistent organic contamination. As a solid state alternative, Chaudhuri's oxygen assisted thermal evaporation of elemental zinc on quartz substrates yields nanorods of various morphologies, depending upon the vapor pressure of zinc.¹¹⁷ This reaction demonstrates excellent atom economy, since no reagents are used save zinc and oxygen. A self-catalyzed vapor-liquid-solid equilibrium between

zinc vapor, liquid zinc, and the substrate is responsible for the formation of nuclei, followed by a simple vapor-solid equilibrium that facilitates longitudinal growth. Again, the products are free of contaminants that may compromise their utility in a given application.

3.3 Iron Oxides

The synthesis of magnetic nanoparticles has received increased attention as the possibility of creating functional materials became more apparent, generating interest as isolable sequestering agents for removal of solution phase contaminants (magnetically assisted chemical separation), heat transfer reagents, and medical imaging enhancers. Typically, colloidal magnetite is synthesized through the reaction of a solution of combined Fe(II) and Fe(III) salts with an alkali.¹¹⁸ Magnetite (Fe_3O_4) precipitates from this solution as particles ranging in size from 5-100 nm, depending upon the solution concentrations, the identity of the alkali, and the general reaction conditions. In the synthesis of such materials, care must be taken to prevent agglomeration driven by the inherent magnetic properties of the particles. The inclusion of excess salts or surfactants provides a general means of passivation. More recently, a simple solid state “ball-milling” technique was reported.¹¹⁹ Anhydrous Fe(II)/Fe(III) salts are mixed with NaOH and excess NaCl and milled in the solid state, yielding particles ranging from 12.5 to 46 nm, depending upon the final annealing temperature. Excess NaCl (rather than excess surfactants and dispersion agents) prevents agglomeration of the magnetic particles, which can be purified through simple washes. While ball-milling is energy intensive, it remains a valuable industrial-scale production method whose green merits can be

improved by avoiding the use of dispersion agents, which in turn require extensive washing to ensure complete removal.

Micellar surfactants have been used as microreactors in the synthesis of maghemite (Fe_2O_3).¹²⁰ Ions (as FeCl_2) have been sequestered within mixed anionic/cationic micellar vesicles composed of CTAB and dodecylbenzenesulfonic acid. Excess extraventricular ions are removed through ion exchange chromatography. Isotonic sodium hydroxide is capable of diffusing to the interior of the micelle, reacting with iron ions to form maghemite nanoparticles. The superparamagnetic particles range from 2.1 to 2.7 nm in diameter, depending upon the size of the micelles and the concentration of NaOH. The magnetic diameter of the particles is somewhat smaller, indicating that the particles possess a deactivated surface layer. Micellar synthesis of such materials presents the advantage of preventing further growth and possible aggregation of the particles.

Ordered arrays of magnetic nanoparticles can be accessed through templating methods. Li et al. reported the synthesis of ordered two-dimensional nanoparticle arrays formed within a porous film. Maghemite structures were obtained by depositing $\text{Fe}(\text{NO}_3)_3$ in between the pores formed by a network of polystyrene beads.¹²¹ Subsequent drying and annealing steps lead to the formation of Fe_2O_3 , and the polystyrene template can be removed via solvent washes. Further control over the size of the nanostructures is made possible by partially dissolving the polystyrene template prior to depositing the iron-based reagents.

As with other nanomaterials, functionalization chemistry provides an opportunity to alter solubility and impart stability to as-synthesized materials. Surfactants have been

used to impart temporary stability to magnetic particles, allowing for subsequent functionalization.¹²² Aqueous maghemite (Fe_2O_3) particles with average diameters of 8 ± 2 nm were synthesized by reacting a mixture of Fe(II)/Fe(III) ions with NaOH in the presence of sodium dodecylsulfate (SDS). Methylmethacrylate was introduced to the solution, displacing SDS. The addition of a polymer initiator led to the growth of poly(methylmethacrylate) around the particles, with no apparent cross-linking. The functionalized particles are stable against oxidation, and present pendant carboxylate groups which allow for further functionalization through grafting techniques, taking advantage of many possible coupling reactions. Core-shell nanoparticles having an iron oxide core and a gold shell have been obtained through seeded growth techniques.¹²³ Magnetic nanoparticles ($d = 9$ nm) were synthesized using standard precipitation methods. Citrate ions were exchanged for hydroxyls on the surface of the particles, in preparation for gold deposition. Gold shells were deposited through a series of treatments (monitored by visible spectroscopy shown in Figure 1.22) with a growth solution of HAuCl_4 and hydroxylamine, leading to particles having a final average diameter of 60 nm. The magnetic properties of the core were unaffected by the presence of the gold shell.

Since some of the most promising applications of magnetic nanomaterials lie within the medical imaging field, functionalization designed with biological environments in mind has been an area of increasing focus. Rotello reported the use of a cubic silsesquioxane ligand to functionalize magnetic materials, resulting in excellent stability in a variety of aqueous solutions, resisting aggregation upon encountering

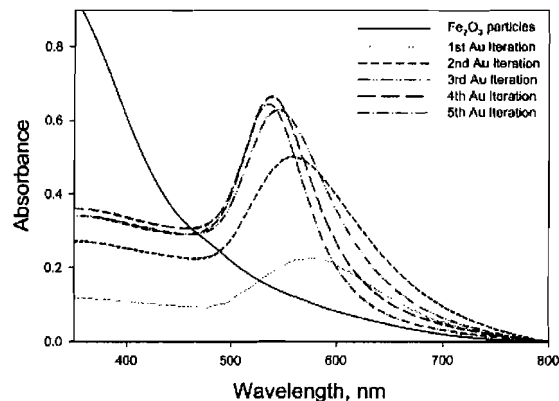


Figure 1.22. The iterative formation of gold nanoshells around iron oxide cores, as followed by changes in the UV-Vis spectrum. (Reprinted with permission from Lyon, J. L.; Fleming, D. A.; Stone, M. B.; Schiffer, P.; Williams, M. E. *Nano Lett.* **2004**, *4*, 719, Figure 3. Copyright 2004 American Chemical Society.)

environmental variations such as changes in pH and salt concentration.¹²⁴ Wang and coworkers reported the functionalization of magnetite nanoparticles by ligands featuring a surface-binding catechol moiety and a bisphosphonate pendant group, designed to remove uranyl ions from blood.¹²⁵ Neither group reports complete functionalization of the particles' surface, but the coverage is adequate to impart new surface properties, thus broadening the range of applications for these materials.

4. Alternative Solvents for Nanoparticle Synthesis

In the pursuit of particular nanosynthetic targets, the choice of starting materials may be somewhat non-negotiable, especially if a particular surface functionality is essential to a given application. Reaction conditions, on the other hand, can often be tuned such that one arrives at the same product in a more efficient, benign manner. Variations in reaction media can involve fairly simple modifications such as substitution of the solvent, reduced temperature and pressure, or more advanced techniques that

provide a supporting environment for the reaction while continuing to produce high-quality products. In this section we highlight recent progress in the use of alternative solvents, including supercritical fluids and ionic liquids, and energy sources, namely photochemical and microwave assisted reactions.

4.1 Supercritical Fluids

At temperatures and pressures beyond the critical point of liquid-vapor equilibrium, supercritical fluids (SCFs), having density, viscosity, and solvation properties that are intermediate between the vapor and liquid phase, have gained attention as benign solvents for the synthesis of inorganic nanoparticles. SCFs such as H₂O and CO₂ are nonflammable, nontoxic, easily accessed materials. The relative strength of the solvent may be continuously tuned by adjusting temperature and/or pressure in the supercritical state, while maintaining unique wetting properties arising from the lack of surface tension, as there is no liquid-vapor interface. Supercritical CO₂ is readily accessed at relatively low temperatures and pressures, although it should be noted that as a solvent, SC-CO₂ acts as a rather nonpolar material; thus, the use of fluorinated metal precursors and capping ligands is often required to impart solubility to inorganic materials. Esumi reported the preparation of particles from a fluorinated organometallic precursor, triphenylphosphine gold(I) perfluorooctanoate, reduced by dimethylamine borane in SC-CO₂.¹²⁶ The products had an average diameter of 1.0 ± 0.3 nm, and could be redispersed in ethanol, although aggregation tends to occur upon standing. On the other hand, SC-H₂O allows the researcher to employ highly elevated temperatures that cannot be sustained by most conventional solvents, which can be a useful property for the synthesis

of many metal and semiconductor materials.¹²⁶⁻¹³⁰ Korgel used supercritical water to create hexanethiol capped copper nanoparticles.¹²⁹

The use of CO₂ emulsions can sometimes mitigate these extreme cases, generating solvent environments with intermediate properties. Silver and copper crystals were prepared in a surfactant-containing water-in-CO₂ microemulsion, where the structure of the emulsion acted as a shape-directing template.¹³¹ Supercritical-CO₂ has been used for both the synthesis and deposition of gold nanoparticles into low-defect films. The use of CO₂-expanded liquids (i.e. organic solvent/SC-CO₂ mixtures) as an alternative to pure SC-CO₂ systems holds the advantage of eliminating the need for perfluorinated compounds by increasing the range of solvent properties, allowing inorganic-hydrocarbon composites to remain stable under SC conditions. This concept

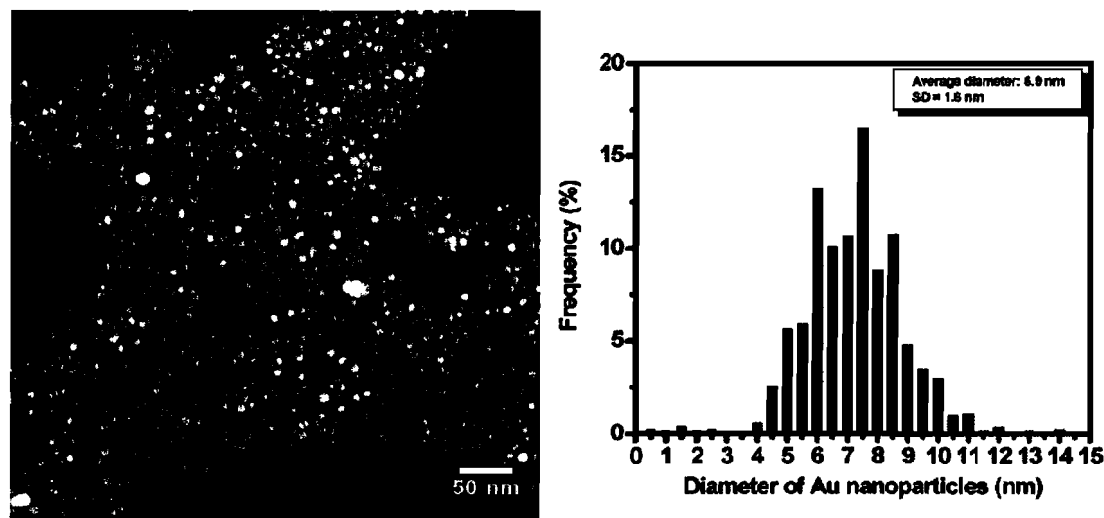


Figure 1.23. TEM image of β -D-glucose capped gold nanoparticles, and a histogram showing the corresponding size distribution. (Reprinted with permission from Liu, J.; Anand, M.; Roberts, C. B. *Langmuir* **2006**, *22*, 3964, Figure 2. Copyright 2006 American Chemical Society.)

was demonstrated recently by Roberts, creating wide area, low defect films of alkanethiol-capped gold nanoparticles (see Figure 1.23) from CO₂-expanded hexane solutions.¹³²

Previously, supercritical CO₂/ethanol mixtures have proven useful for the preparation of copper nanocrystals prepared by thermal decomposition of a perfluorinated organometallics precursor.¹³³ A unique method described as “precipitation by compressed antisolvents” was used to drive the preparation of nickel and cobalt nanoparticles, where SC-CO₂ is fed into a solution of the metal compound. Taking advantage of the limited solubility of inorganic materials in SC-CO₂, supersaturation conditions are reached, leading the precipitation of nanoparticulate materials.¹³⁴ If these reports are taken together, one may conclude that supercritical fluids hold great promise in the development of more benign synthetic routes, with demonstrated utility in nanosynthesis, assembly, and purification. The development of new (benign) surfactants and supercritical solvent systems is likely to increase the range of materials that are soluble under such conditions, potentially eliminating the need for perfluorinated materials in this area of research.

4.2 Ionic Liquids

Ionic liquids (IL) have received attention as alternative solvents and stabilizers for nanomaterials synthesis, due to their general ease of synthesis, stability (nonflammable, thermally stable), and low vapor pressures. Ionic liquids feature low interfacial tension that allows them to adapt to the surrounding reaction media, and their relative solubility may be tuned by varying their anionic and cationic components. Careful choice of anion

is critical to their use within a green chemistry context, since BF_4^- and SF_6^- are believed to evolve hydrofluoric acid over time,¹³⁵ and variations in vapor pressure arise from individual cation/anion combinations. Their limited miscibility with water and organic solvents often simplifies product purification and promotes recovery and recycling, although drying ionic liquids prior to use can be difficult. Nanomaterials composed of noble metals, oxides, and semiconductors have been prepared in such solutions.

The vast majority of IL syntheses are carried out using imidazolium derivatives having various counterions. Kim reported the synthesis of gold and platinum nanoparticles by NaBH_4 reduction of HAuCl_4 in the presence of a thiolated IL, yielding nanoparticles with diameters of 2.0 – 3.5 nm. The monodispersity was dictated by the number of thiol groups present in the reaction mixture.¹³⁶ Tatumi used a zwitterionic material as an IL, based on the imidazolium functionality derivatized with a thiol headgroup and a pendant sulfonate, to synthesize 2.5 nm gold particles.¹³⁷ Others have used ionic liquids as capping agents despite the absence of thiol functionality. Itoh and coworkers described such a use of ILs in the synthesis of gold nanoparticles, finding that the product solubility could be tuned by exchanging the anion.¹³⁸ Large gold nanosheets were prepared by Kim et al. in a neat, microwave assisted reaction between HAuCl_4 and an imidazolium-based IL.¹³⁹ More recently, the synthesis of an alcohol-derivatized IL was reported, where the IL may act as both a reducing agent and a capping material to create nearly monodisperse 4.3 nm gold particles.¹⁴⁰ To further ease isolation and purification of nanomaterials synthesized in ionic liquids, Wang described how the addition of oleic acid

as a primary capping agent facilitates the precipitation of gold nanoparticles from an IL-based reaction mixture.¹⁴¹

Platinum nanoparticles may be synthesized by similar routes. Scheeren et al. reported the reaction of $\text{Pt}_2(\text{dba})_3$ with an imidazolium-type IL to yield nanoparticles with average diameters ranging from 2.0 - 2.5 nm. Larger particles could be accessed by varying the counteranion.^{142,143} Zhao and colleagues recently described the ionic-liquid mediated synthesis of platinum nanoparticle-studded carbon nanotubes.¹⁴⁴

Ionic liquids may also be used for the general synthesis of inorganic nanostructures.¹⁴⁵ Kimizuka reported the synthesis of hollow titania microspheres in a toluene/ionic liquid medium. The nanospheres form at the interface of a microdroplet of toluene and the surrounding ionic liquid.¹⁴⁶ A modified sol-gel technique employing ionic liquids and an immiscible titanium tetraisopropoxide/alcohol solution was used to create 5 nm titania crystals.¹⁴⁷ Ionic liquids have been used to drive the synthesis of ZnO nanostructures with unusual morphologies, as in the case of ZnO pyramids where all exposed surfaces are the very polar (0001) and {1011} planes.¹⁴⁸ The strongly polar environment imposed by ionic liquids helped to form PbO nanocrystals featuring the PbS crystal structure.¹⁴⁹ Manganese oxide molecular sieves were synthesized from ionic liquids, where the ionic liquid acts as a reducing agent, cosolvent, and shape-directing material.¹⁵⁰ The thermal stability of ILs assisted the synthesis of CoPt nanorods from a mixture of $\text{Co}(\text{acac})_3$, $\text{Pt}(\text{acac})_2$, and CTAB (present as a shape-directing agent).¹⁵¹ Unusual Bi_2S_3 “flowers” were synthesized in ILs, and it was discovered that prolonged aging of these materials ultimately led to the structural breakdown, followed by nanowire

growth.¹⁵² Finally, rounding out the range of synthetic applications afforded by this class of reagents, nanoscale metal fluorides were synthesized in ionic liquids, demonstrating predictable rodlike morphologies, regardless of the metal precursor employed.¹⁵³

5. Functionalization

While our primary focus has been on the topic of nanomaterials synthesis, efforts to control the surface chemistry of products are key to defining how the material interacts with its surroundings, whether in a solution or in the solid phase. Nanoparticle syntheses of the Brust-type can provide a direct route towards a product that features the desired surface chemistry as synthesized, assuming reagent compatibility (i.e. the thiol-based capping agent must not react with sodium borohydride). However, there are a few caveats to this approach if multiple products are desired. The preparation of similar nanomaterials differing only in their surface chemistry often requires individualized tailoring of a general synthetic route, since the choice of capping ligand can greatly impact the average size and morphology of the products. Because unique products must be generated in a single batch, larger amounts of solvent are required to support numerous parallel reactions. To circumvent these issues, the preparation of versatile core materials amenable to surface modifications may be a more strategic approach if one wishes to create a diverse library of materials with uniform core sizes. Surface modification methods can be categorized into two major classes (see Figure 1.24): post-synthetic modification of the existing ligand shell, involving simple transformations of pendant functionalities or grafting, and ligand exchange, where an existing ligand shell is displaced by a different incoming ligand.

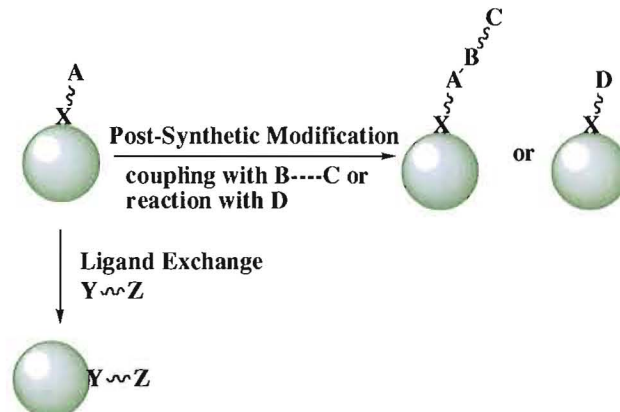


Figure 1.24. Strategies for nanoparticle functionalization. Post synthetic modifications take advantage of the existing stabilizing shell, using either coupling reactions or simple organic transformations to impart the desired functionality. Ligand exchange reactions displace the existing stabilizing shell with a ligand featuring either the same headgroup, or one that demonstrates greater binding affinity than the original.

5.1 Post Synthetic Modification of the Ligand Shell

Post-synthetic modification methods involve the direct synthesis of a stable nanoparticle that can sustain secondary reactions intended to introduce a new chemical functionality to the surface of the particle in a subsequent reaction sequence. Candidates for post-synthetic modifications are generally produced by direct synthesis (ω -functionalized particles created by Brust preps) or sometimes ligand exchange methods (usually involving the introduction of a ligand bearing a reactive pendant functional group). Modification reactions include polymerizations,¹⁵⁴⁻¹⁵⁷ coupling reactions,^{40,48,158-162} or transformation of existing chemical moiety.^{48,163-165} In all cases, the success of such modifications relies not only on the nanoparticles tolerance for various reaction conditions, but also the overall reactivity and steric environment presented by functional groups that are constrained through binding to a nanoparticle. Factors that impact the efficacy of post-synthetic modifications may include: the length of the ligand composing

the stabilizing shell, since this impacts the steric mobility of ω -functional groups, the spatial density of such groups, and the bulk of the incoming nucleophile (for S_N2 type reactions). Nanoparticles featuring amino, carboxylate, and bromo- or iodo- terminal groups are commonly used to generate libraries of functional materials through post-synthetic modifications. Although this method affords greater versatility to a single precursor material, it should be noted that characterization of the modified materials might be exceedingly difficult, due to difficulties encountered when assessing the extent of modification.

5.2 Ligand Exchange

Ligand exchange methods are somewhat of a hybrid technique, as they require the direct synthesis of a versatile precursor nanoparticle stabilized by a labile ligand shell, followed by a ligand exchange step where the original ligand shell is partially or fully displaced by another ligand that bears pendant functional groups, thus introducing the desired chemical functionality to the surface of the particle. This strategy offers multiple green advantages, since a single batch of nanoparticles can be divided and exchanged with multiple ligands, yielding numerous products while consuming minimal resources. Solvent use is reduced, compared to one-off direct synthesis routes, and no coupling reagents are necessary, as is often the case for post-synthetic modifications. The products are easily characterized via NMR and XPS, particularly if a different headgroup is introduced (e.g. thiol vs. phosphine). Triphenylphosphine stabilized nanoparticles, having a relatively labile ligand shell, readily undergo ligand exchange reactions with other phosphines, amines, and thiols. The nanoparticles obtained by Hutchison's procedure

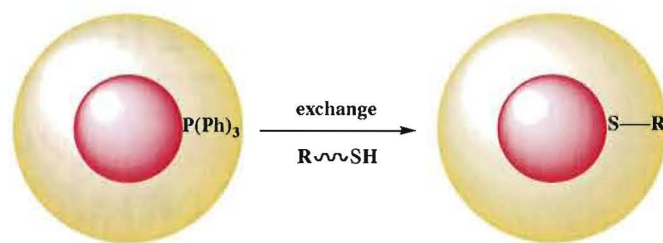


Figure 1.25. The labile triphenylphosphine ligand shell is easily displaced by an incoming thiol without significantly altering core size, allowing for complete ligand exchange and rapid generation of a library of functionalized nanoparticles.

have been functionalized by a wide range of ligands through exchange reactions, yielding a diverse library of functional nano “building blocks” ideal for use in the bottom up assembly of new nanostructures.^{166,167} Ligand exchange reactions that displace phosphines in favor of incoming thiols (Figure 1.25) are amongst the most versatile and well studied examples of ligand exchange reactions;¹⁶⁸⁻¹⁷¹ however, in the past decade, ligand exchanges have been performed on a wide variety of materials having other stabilizing ligands.

Several different classes of ligand exchange reactions have emerged, with one commonality: the incoming ligand used in the exchange reaction has equal or greater affinity for gold than the ligands composing the original stabilization shell for the nanoparticle. Thus one may start from a product that is stabilized by weakly coordinating materials such as organic acids (citrate, ascorbate, tannic acid) and surfactants, or more robust materials (such as phosphines, amines, or thiols), bearing in mind that the options for incoming ligands become more limited as the strength of the initial stabilizing ligand is increased, i.e. a phosphine is unlikely to displace a thiol. Ligand exchange reactions can be carried out under a range of solution conditions that can be tailored to achieve the

desired product, including aqueous, organic, and biphasic conditions, if a change in solubility is likely to occur as the ligand exchange proceeds. The following discussion will illustrate the versatility of ligand exchange by providing examples of ligand exchanges performed on precursor particles with a variety of stabilizing ligand shells.

5.2.1 Place Exchanges Involving Ligands of the Same Class

Phosphine-to-phosphine. This place exchange technique may be used to introduce functionality to phosphine stabilized precursor particles, although complete exchange of the original ligand shell is difficult to achieve.¹⁷² Early examples include the functionalization of triphenylphosphine stabilized undecagold clusters by introduction of ω -functionalized aminophosphine ligands, and the production of water-soluble clusters via exchange with $\text{Ph}_2\text{PC}_6\text{H}_4\text{SO}_3$.^{56,173} Although the exchange kinetics are quite rapid,¹⁷⁴ the use of such exchanges is limited by the general instability of phosphine stabilized clusters and inability to perform complete ligand exchanges.

Thiol-to-thiol exchange The earliest reports of thiol-for-thiol place exchange reactions were performed on alkanethiol stabilized nanoparticles prepared by the Brust route. Alkanethiols featuring a range of ω -functionalities were introduced to stirring nanoparticles, with attention to the molar ratio of incoming ligands, offering control over the extent of the ligand exchange reaction to yield products with mixed ligand shells.^{175,176} These polyfunctional nanoparticles featured pendant groups capable of participating in secondary chemical and redox reactions, providing proof-of-principal for a range of new applications as nanoreactors. Later reports by Foos and Twigg demonstrated phase

transfer during ligand exchange, transferring hexanethiol capped particles to the aqueous phase upon exchange with water soluble ligands.^{177,178}

A great deal of attention has gone toward elucidating the mechanism of thiol-for-thiol exchanges. It is generally accepted that the chain length and steric bulk of an incoming ligand impact exchange rates, with smaller, simpler ligands exchanging most rapidly. The overall mechanism is associative, occurring in two distinct steps, where exchange is initiated at the gold atoms that form the vertices and edges of a nanoparticle surface. The exchanged species then diffuse toward the terraced regions of the surface, eventually leading to an equilibrium state.^{175,179,180} Murray explored several other factors affecting exchange rate, including the charge on the particle and the acid/base environment, finding that ligand exchange reaction proceed faster on particles whose gold cores bear positive charges, as do exchanges that take place in moderately basic environments.¹⁸¹ In a follow-up study, the impact of core size with respect to ligand exchange rates revealed that two distinct rates corresponding to individual steps of the exchange persist for particles regardless of size regime. However, the rate of the second step (involving diffusion and rearrangement of thiolate species on gold terraces) varies, with the rate being slower for larger particles.¹⁸² Recently, Rotello reported a new method of studying exchange kinetics using dye functionalized nanoparticles as substrates for exchange.¹⁷⁹ Since gold nanoparticles effectively quench the fluorescence of bound probes, the progress of the ligand exchange could be monitored by the relative fluorescence of the particle solution, since incoming ligands will displace the dyes as the reaction proceeds. While these studies have provided great insight toward a better

understanding of ligand exchange, the fact remains that precise control over the extent of exchange is a challenge. Worden has offered a solution that allows for exchange of a single ligand, using a “catch and release” strategy (see Figure 1.26).¹⁸³ Polymeric supports served as an anchor for 6-mercaptohexanoic acid (6-MHA), leaving the thiol group free to bind to a gold particle. The 6-MHA dosing was sufficiently low in order to maintain distance between the tethered molecules. A single butanethiol capped nanoparticle could then bind to the free thiol, and liberation of the newly monosubstituted particle was achieved using trifluoroacetic acid. To demonstrate that the particles contained only a single 6-MHA molecule, peptide-coupling reactions were performed using the particles and a diamine, resulting in the formation of nanoparticle dimers.

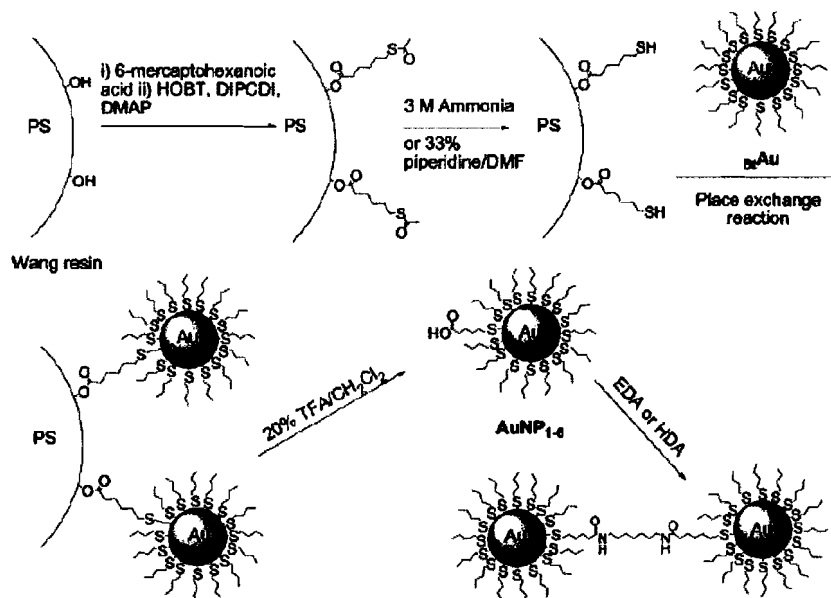


Figure 1.26. The “catch and release” strategy for controlling the extent of ligand exchange, in this case, adding a single incoming ligand to each particle. (Reprinted with permission from Worden, J. G.; Dai, Q.; Shaffer, A. W.; Huo, Q. *Chem. Mater.* **2004**, *16*, 3746, Scheme 1. Copyright 2004 American Chemical Society.)

5.2.2 Introduction of a New Surface Binding Functionality

Phosphine-to-thiol. Already discussed above, this is the most versatile type of exchange reaction, since it is capable of producing monosubstituted clusters bearing a wide variety of terminal functional groups. The pioneering work of Hutchison et al. demonstrated the utility of this exchange with triphenylphosphine stabilized 1.4 nm gold particles by carrying out exchanges in a single organic phase to introduce organic soluble thiols,^{168,184-187} or in a biphasic manner, using water soluble thiols to convert the organic soluble precursor particles to water soluble materials without disrupting the original size of the gold core.^{167,168,171,187} The extent of exchange in the biphasic case is governed by the degree of mutual thiol solubility in both phases: that is, a water soluble thiol that has a partial organic solubility is capable of more extensive ligand exchange than a thiol that is completely insoluble in organic solvents. Phosphine-to-thiol ligand exchange reactions have also been used to functionalize smaller (0.8 nm) nanoparticles having undecagold cores.^{98,188} Murray has reported that the core size of phosphine stabilized nanoparticles increases during ligand exchange processes,¹⁶⁹ but it should be noted that Murray employed much longer reaction times than Hutchison,¹⁸⁷ making Ostwald ripening processes more likely.

Phosphine-to-amine. Amines can displace phosphine ligands in a single-phase reaction. One unique aspect of this reaction is that the size of the gold cores may evolve as the reaction progresses, transforming 1.4 nm triphenylphosphine stabilized particles to larger monodisperse amine stabilized particles, ranging in size from the original 1.4 nm up to 8 nm, depending on the exchange conditions.^{81,184} As mentioned, the amine

stabilized products are nearly monodisperse, and while the exact mechanism of the exchange remains unknown, it is worth noting that a bimodal size distribution is maintained throughout the course of the reaction. These particles are not as robust as those stabilized by thiols, but the relatively labile amine ligands can be exchanged with thiols, potentially providing access to larger functionalized gold nanoparticles by first growing the particles to the desired size through reactions with amines, followed by introduction of surface functionality by an exchange with thiols.

Citrate to thiol. Citrate to thiol exchanges are amongst the most commonly employed yet least understood methods of creating larger functionalized gold nanoparticles. The reduction of HAuCl_4 by citrate anions was pioneered by Turkevich half a century ago, yielding monodisperse, water soluble gold clusters with diameters ranging from 7-100 nm. The clusters are stabilized by a complex multilayered assembly of citrate anions in various oxidation states, lending an overall negative charge to the particles.^{189,190} This highly charged ligand shell makes solutions of the particles very sensitive to changes in pH, ionic strength of the medium,¹⁹¹ and the presence of other organic materials. Incomplete functionalizations involving a few thiolated biomolecular ligands are easily achieved,^{192,193} but full functionalization of these particles by a complete thiol ligand shell remains elusive. Levy and coworkers recognized the functionalization challenge presented by citrate stabilized gold nanoparticles, and designed a ligand featuring not only a gold binding thiol moiety, but also several amino acids capable of stabilizing the citrate surface.¹⁹⁴ For many years, the most successful ligand exchange methods employed a thiol bearing anionic ω -functionality.¹⁹⁵⁻¹⁹⁷ One example of this type

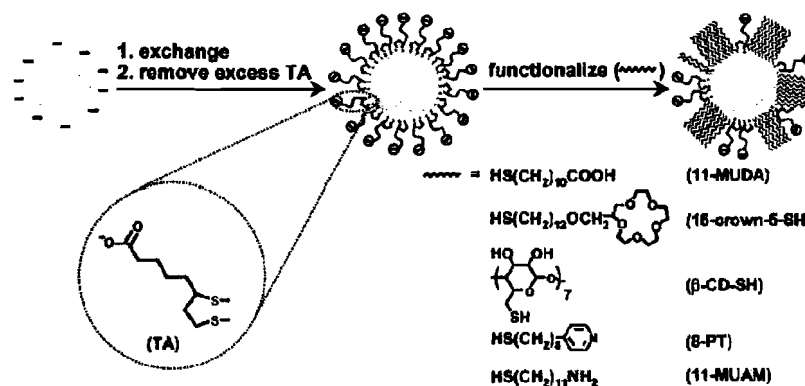


Figure 1.27. A two-step approach to functionalizing nanoparticles. Thioctic acid bind to citrate stabilized gold nanoparticles with minimal disruption of the electrostatic environment, stabilizing the particles for a subsequent exchange with another thiol. (Reprinted with permission from Lin, S.-Y.; Tsai, Y.-T.; Chen, C.-C.; Lin, C.-M.; Chen, C.-h. *J. Phys. Chem. B*, **2004**, *108*, 2134. Scheme 1. Copyright 2004 American Chemical Society.)

of exchange, involving thioctic acid as a ligand, is shown in Figure 1.27.

Recently, investigations of this type of exchange by Hutchison et al. have opened up the possibility of extensive thiol functionalization of citrate stabilized particles by other water soluble thiols, including those having anionic, neutral, and positively charged pendant functional groups. Hutchison found that complete removal of the citrate stabilizing shell by extensive diafiltration is required for maximum surface coverage by thiols (Figure 1.28). The stripped gold cores remain soluble in water, permitting the introduction of thiol ligands without the usual problems of low surface coverage, aggregation, or cross-linking. The use of a thiol bearing pendant trimethylammonium functionality is unprecedented in the case of citrate-stabilized gold nanoparticles, as excess citrate anions promote cross-linking and aggregation as functionalization proceeds. This method of creating a versatile stripped gold precursor particle amenable to functionalization by a wide range of thiols is promising as a route to nanoscale building

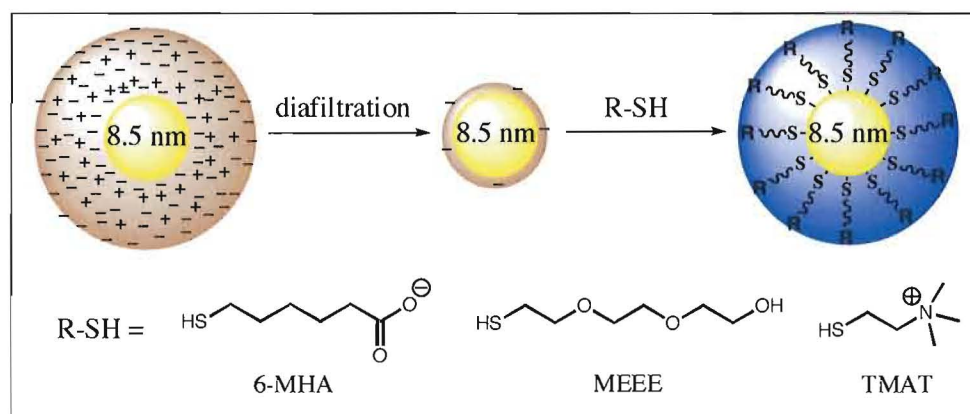


Figure 1.28. A new strategy for functionalization of citrate stabilized nanoparticles utilizes extensive diafiltration to remove most ions from the surface of the gold particle, thus allowing facile binding of an incoming thiol ligand.

blocks capable of self-assembly, much in the way that phosphine-to-thiol exchanges have increased the scope of utility for 1.4 nm triphenylphosphine stabilized nanoparticles.

Surfactant-to-thiol. This class of exchange has been discussed elsewhere throughout the review, as it is a key route to high aspect ratio nanorods and prisms. Briefly, gold clusters may be synthesized within micellar templates through reduction of gold salts by NaBH_4 . Excess surfactant molecules, usually in a tetraalkylammonium form, impart stability to the clusters while providing a ligand shell that is readily displaced by ligands capable of bonding covalently to gold, such as thiols. Although the use of surfactant in this capacity is common, subsequent displacement by thiols or other ligands has not been reported frequently, likely due to the difficulty in obtaining products free of surfactant contaminants. Surfactants have also been displaced by amines, as in the case of Gandubert and Lennox's assessment of dimethylaminopyridine's (DMAP) capability as a stabilizing agent for nanoparticles. Gold nanoparticles were synthesized in a biphasic Brust reaction, yielding TOAB-stabilized clusters suspended in toluene. The

clusters were exchanged with DMAP, which is intended to serve as a temporary stabilizer for subsequent ligand exchanges meant to yield functionalized nanomaterials.¹⁹⁸

6. Future Challenges for Greener Nanosynthesis

The emerging field of green nanoscience faces considerable research challenges to achieve the maximum performance and benefit from nanotechnology while minimizing impact on human health and the environment. The principles of green chemistry, applied to nanoscience, provide a framework for designing greener nanomaterials and developing greener nanosynthesis methods. As nanoscience emerges from the “discovery phase” to the production level, the need for larger quantities of highly purified, structurally well defined and precisely functionalized materials will require significant improvements in nanoparticle synthesis. This review highlights the growing body of research that addresses the development of these greener processes for nanomaterial synthesis. We focused primarily on the preparation of functionalized metal particles, describing advances in core synthesis, surface functionalization, and shape control that illustrate the current status and future challenges to developing greener approaches. The literature in this area illustrates a few of the many approaches that are being explored in the pursuit of greener nanosynthesis and provides some examples of how these steps can yield high performance materials with higher efficiency and enhanced safety. However, careful analysis of the examples we describe in this review suggests that there is still much to learn in developing greener nanosynthesis methods and furthermore point to a number of important research challenges that would accelerate a transition toward greener nanosyntheses.

Among the key findings thus far have been discovery of methods to produce nanoparticles and assemblies with desired properties, that (i) eliminate the use of toxic reagents and solvents, (ii) afford higher yields and fewer by-products, (iii) provide better control of particle size dispersity, (iv) reduce the need for purification or the amount of solvent needed to carry out purification, and (v) enhance material utilization (e.g. in assembly reactions). Finally, initial steps have been taken toward development of metrics by which competing production methods will be compared.

Despite the progress described within this review, there are still considerable research challenges within this field that remain to be addressed. Each of those listed below would have significant impact toward providing the research base needed to pursue greener approaches, while advancing nanoscience generally. To achieve this end it is necessary to:

1. Develop structure-activity relationships (SARs) needed to predict biological impacts, ecological impacts and degradation at end-of-life. Each of these SARs is needed to design nanoparticles that will have the desired human health and environmental performance to complement their physical properties. The materials challenge in developing these SARs is accessing diverse populations of nanostructures for investigation that have well-defined structures and purity profiles.
2. Develop new transformations and reagents that are more efficient, safer, and useful in a wider range of reaction media/solvents that will ultimately provide access to greener media. These methods should also produce materials of high

quality and purity and allow one to access the composition, size, shape, and functionality desired in a compact synthetic approach. This is a significant challenge that will require enhanced understanding of the mechanisms of nanoparticle formation and the ability to adjust reagent reactivity to address these multiple criteria. These transformations and reagents should be amenable to scale up for production level processing. Continuous-flow microreactors present such advantages for nanoparticle production and may be useful for large-scale production.

3. Gain improved understanding of product distributions, nanoparticle formation mechanisms, and reaction stoichiometries. Currently little is known about the mechanistic details of these transformations. Without knowledge of stoichiometry and mechanism, it is impossible to assess atom economy or rationally develop new synthetic methods. Without an understanding of the impurity profiles, one cannot develop new purification strategies. In terms of impact, this is one of the most important challenges, but one that is difficult, in part, because of the limitations of analytical techniques to assess nanoparticle structure, composition, and purity (*vide infra*).
4. Optimize analytical techniques that permit the routine analysis of nanoparticles for composition, structure, and purity. In the discovery phase of nanoscience, greater emphasis has been placed on the analysis of structure (e.g. core diameter of a particle by TEM) with little attention paid to the chemical composition of the stabilizing shell or the presence of small molecule impurities in the nanoparticle

samples. Availability of routine analytical methods that address these issues is a key to gaining a better understanding of the mechanisms of nanoparticle formation and reactivity. In addition, given the influence of purity on a wide range nanoparticle properties (e.g. self-assembly, ligand exchange, and toxicity) analytical techniques that can detect and quantify impurities will be important to pursuing greener approaches. Importantly, analytical techniques are needed that permit real-time, in situ monitoring to optimize production processes, thus minimizing waste and energy costs as well as providing mechanistic information.

5. Find alternatives to the use of surfactants, templates, or other auxiliary substances to stabilize and control nanoparticle shape during synthesis. A number of the examples provided in this review make use of surfactants for these purposes. Surfactants are often toxic, tend to persist as residual contaminants in the product, and must usually be replaced in order to incorporate new functionality on the particle surface. New approaches wherein the molecule used to control shape during synthesis instills permanent function (beyond initial stabilization) to the material are particularly needed. Some studies have utilized biological molecules to control the size and shape of nanoparticles, often in the absence of surfactants. These biomimetic approaches are in their infancy, but show great promise in biologically derived nanoparticle production. For these bio-based nanoparticles to be successful, it will be necessary to develop methods that are amenable to scale up, such as those used in microreactor design.

6. Further develop and assess alternative solvents and reaction media. If alternative reaction media (e.g. ionic liquids, supercritical fluids, or other new solvents) are to be exploited, the efficacy, safety, and broader implications need to be assessed to guide selection of most appropriate medium, whether it be a new material or a traditional solvent. These implications include chemical and energy utilization associated with production and use of the new reaction media.
7. Develop convenient purification methods that provide access to pure nanomaterials without generating large amounts of solvent waste. As nanoscience transitions from the discovery phase to commercialization, the availability of pure nanoparticle samples or those with well-defined impurity profiles will be needed for applications. In addition, pure materials are essential for studies aimed at developing structure-activity relationships needed to predict physical properties, reactivity, toxicity, and eco-toxicity. Current purification methods are wasteful and inadequate as described in section 2.4.2. Methods that utilize filtration technology can greatly improve purification without generating large solvent wastes and should be investigated to develop greener purification methods.
8. Identify metrics or other approaches for comparing the greenness of competing approaches¹⁹⁹ that consider the relative hazards and efficiencies of the immediately relevant transformation and the relative impacts of each method within a broader life cycle. These metrics are only beginning to be developed, but will be increasingly important in guiding method selection, particularly during

reaction scale up, and the development of new, greener approaches to nanoparticle synthesis.

As the above listing of research challenges suggests, green nanosynthesis is in its early stages and further research is warranted to develop the approach and examine the breadth of its application. There are encouraging results that suggest that the green nanoscience framework can guide design, production, and application of greener nanomaterials across the range of compositions, sizes, shapes, and functionality. Further development and application of this framework to the design and production of a growing number of classes of nanoparticle materials will provide research opportunities and challenges for this community for the foreseeable future.

7. Bridge to Chapter II

Portions of this dissertation (specifically, chapters I, II, and III) contain previously published and/or coauthored materials. The material in Chapter I originally appeared as a portion of a recent publication, reprinted from Dahl, J. A.; Maddux, B. L. S.; Hutchison, J. E. "Toward Greener Nanosynthesis" *Chemical Reviews*, **2007**, *107*, 2228-2269. The majority of the material appearing in chapter I was authored by Dahl, with contributions from Hutchison; Dahl and Hutchison shared editing tasks in preparation for publication. Chapter I provided an overview of the presence of green chemistry in the synthesis and functionalization of metal-based nanomaterials. Chapter II describes the development of a route to functionalized large gold nanoparticles, useful for their inherent optical properties. The synthesis features numerous green advantages, including innocuous reagents, mild reaction conditions, and benign purification and processing techniques.

Specifically, we have produced stable gold cores with diameters exceeding 8 nm that serve as versatile synthons for the generation of a library of functionalized particles, via functionalization by an incoming thiol. In order to define the scope of these materials and maximize the range of possible applications, the gold cores were functionalized with several water-soluble thiols, having a range of pendant functional groups useful for participation in later self-assembly processes.

CHAPTER II

FUNCTIONALIZATION OF CITRATE STABILIZED GOLD NANOPARTICLES WITH WATER SOLUBLE THIOLS

Note: Portions of Chapter II are expected to appear in an upcoming publication, co-authored by Dahl, J. A.; Jespersen, M. L.; and Hutchison, J. E. The first author made the initial discoveries described in this work, designed experiments, and carried out the majority of the laboratory work. The author also composed the manuscript corresponding to Chapter II. J. E. Hutchison provided experimental and editorial guidance, while M. L. Jespersen assisted with laboratory experiments during the later stages of this project. All syntheses and the vast majority of materials characterization were carried out at the University of Oregon, with some analysis performed at the Environmental Molecular Sciences Laboratory at Pacific Northwest National Laboratory.

1. Introduction

The demand for functionalized noble metal nanoparticles has steadily increased as the scope of these materials broadens to include a multitude of optical, electronic, and biomaterials applications.^{39,172,200-210} Realization of these materials often requires the presence of a functional ligand shell that affords control over solubility, reactivity,

stability, and self-assembly processes. Within the past decade, a number of methods for the preparation of functionalized gold nanoparticles have been reported, including the synthesis of a 1.4 nm triphenylphosphine-stabilized gold precursor nanoparticle which readily undergoes ligand exchange reactions with a wide range of thiols,^{28,38,187} while variations of the Brust synthesis provide a direct route to functionalized nanoparticles with diameters in the range of 2-8 nm.^{38,39,42,177,211,212} However, for applications that exploit strong optical characteristics arising from surface plasmon activity, such as molecular sensors,^{14,213-215} flow assays,^{216,217} and optical waveguides,^{200,205,218-220} larger particles having diameters greater than 8 nm are required, yet access to functional nanoparticles in this size regime remains limited.

Large gold nanoparticles are usually synthesized directly by citrate reduction of gold salts,^{31,32,190,221} or by seeded growth techniques^{52,95,222-224} that employ solutions consisting of a mild reducing agent, a gold salt, and a stabilizer (often a surfactant) to iteratively increase the diameter of smaller metal seed particles. While such methods offer products having desirable core sizes and optical properties, subsequent functionalization attempts often lead to materials that are poorly defined in terms of surface chemistry and purity.

Although ligand exchange reactions are proven to be a reliable means of functionalizing smaller nanoparticles, similar transformations of citrate stabilized gold nanoparticles are largely unsuccessful due to the tendency for the particles to aggregate in the event of modest variations to solution conditions. Small changes in pH and ionic strength are sufficient cause for irreversible precipitation. Specifically, electrostatic

repulsion between particles is lost under acidic conditions, as ionized carboxylate groups are re-protonated. While better tolerated than acidic solutions, basic environments disrupt the stabilizing electrolyte gradient around the gold cores, leading to precipitation.

Although excess ions (in the form of NaCl, buffers, or even excess citrate) do not interact directly with the surface of the nanoparticles, their presence causes aggregation by promoting a loss in electrostatic screening.^{191,225}

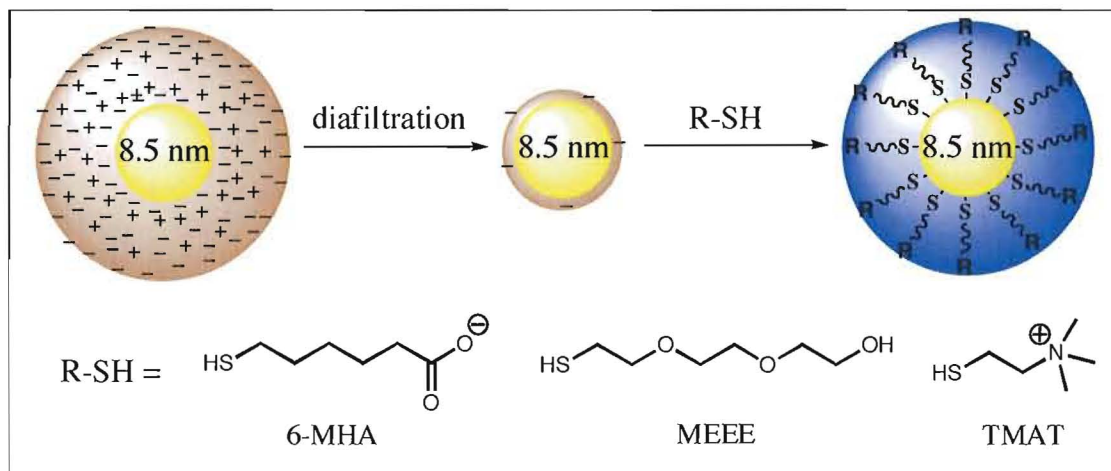
A closer look at the synthesis and surface chemistry reveals both the green merits and functionalization challenges of citrate stabilized nanoparticles. The citrate reduction route remains an attractive, reliable, green method of nanosynthesis, using benign reducing agents, solvents (water) and no additional passivating ligand, yielding gold nanoparticles within the size range of 8-100 nm with relatively monodisperse size distributions.^{31,32} Control over nanoparticle size is fairly straightforward and related to the ratio of reagents used, yet a single citrate molecule can undergo multiple oxidations in this non-stoichiometric reaction. As a result, the surface chemistry is confounded by the formation of a complex, negatively charged, multilayered stabilizing shell composed of excess citrate anions in various oxidation states. It is known that deprotonated citrate and dicarboxyacetone species form stable complexes with surface gold atoms,¹⁸⁹⁻¹⁹¹ yet the precise extended structure surrounding the core of a citrate stabilized gold nanoparticle remains ambiguous since it varies with the ratio of reagents used, the size of the gold cores, and the relative solution concentration. The presence of the multilayered stabilization shell creates an electrostatic barrier to functionalization by incoming ligands. The stability of the particle solution is limited to a narrow range of conditions, many of

which do not permit the presence of an incoming ligand. Taken together, such qualities pose a significant barrier to subsequent functionalization efforts, with the consequence of limiting their utilization in more advanced applications.

Despite a general intolerance for changes in solution characteristics, a few reports of thiol functionalization have emerged recently, sharing common features based on the character of incoming ligand, including ligands with anionic pendant groups and thiolated macromolecules. The first case involves thiols having anionic pendant groups (usually carboxylate or sulfonate)^{195-197,215,226-231} which form a covalent Au-S bond without significant destabilization, suggesting that it is crucial to maintain the electrostatic environment afforded by the stabilizing citrate anions as they are replaced by new ligands. The second case involves the use of macromolecules in the form of thiolated polymers^{157,232-236} or biomolecules.^{157,192,237-239} Large gold nanoparticles stabilized by charge-neutral water-soluble thiol ligands have been pursued for use in biological applications, as such a ligand shell offers excellent biocompatibility and solubility in biological media while hindering unwanted non-specific interactions. Thiolated biomolecules, poly(ethylene glycol), and thiol end-capped polymers readily bind to gold, although dense surface coverage of nanoparticles remains elusive. In these instances, solubility is dictated by the biomolecule, rather than the nanoparticle. Such materials are often lacking aggressive purification efforts, leaving small amounts of unbound materials in solution, enhancing the stability of such nanoparticles while hindering complete characterization of the surface chemistry and masking the need for more extensive functionalization.

Instead of accommodating the inherent difficulties of citrate stabilized gold nanoparticle solutions, isolating the gold cores by removing excess ions may hold the promise of successful functionalization. In general, ligand exchange reactions rely upon two key factors: the outgoing stabilizing material must be labile enough to be displaced, while being stable enough to support the particles during ligand exchange. Additionally, the incoming ligand must have a greater affinity for the gold surface than the outgoing ligand. Hence, citrate stabilized nanoparticles should be capable of participating in ligand exchange reactions if the native stabilizers (excess citrate ions) can be removed, clearing the path for a stronger ligand (i.e. thiol) to bind with the gold surface. Recent reports describe how citrate stabilized gold nanoparticles are more readily functionalized in solutions of low ionic strength,²⁴⁰ suggesting that removal of excess citrate prior to functionalization promotes denser ligand coverage. Rather than simply diluting nanoparticle solutions to tailor ionic strength, a more powerful means of controlling the electrostatic environment can be found in diafiltration. Capable of removing ions, unreacted materials, and other small molecules from aqueous nanoparticle solutions, diafiltration does not disturb ligands that are either covalently bound or strongly complexed with a nanoparticle.⁹² Previously identified as a superior means of purifying nanomaterials, we discovered that diafiltration could also strip excess ions away from nanoparticles prepared by the citrate route without compromising their stability in aqueous solutions.

Here, we report a new approach to the functionalization of citrate stabilized gold nanoparticles where unbound citrate anions are completely removed from the particles by



Scheme 2.1. Strategy for functionalizing citrate stabilized gold nanoparticles with water-soluble thiols featuring anionic, cationic, and neutral pendant groups. Excess citrate species are first removed from the surface of the gold nanoparticles, leaving behind a gold core that is readily functionalized by an incoming thiol.

extensive diafiltration, leaving behind stable, well-defined gold cores having only a sparse monolayer of dicarboxyacetone bound to the surface (scheme 2.1). The improved reactivity of the stripped gold cores is demonstrated in scalable ligand exchange reactions with simple water-soluble thiols having a range of pendant functional groups, including anionic, neutral, and cationic moieties, leading to readily characterized products with unambiguous compositions.

The entire fabrication process features the use of greener methods starting with nanoparticle synthesis, isolation of the gold cores, ligand exchange, and purification. The techniques described here facilitate dense binding of an incoming thiol ligand to gold cores prepared by the citrate reduction method, without the usual constraints imposed by the presence of excess ions. By this route, citrate stabilized gold nanoparticle solutions may be transformed into versatile synthons, leading to well-defined functional

nanomaterials upon reaction with thiols, thus enabling applications that demand products with strong optical properties and specific functional groups.

2. Experimental

Ultrapure water (minimum 18.2 M Ω •cm resistivity) was provided by a Barnsted Nanopure water filtration system and used in all stages of glassware cleaning, ligand synthesis, sample preparation, and purification. Hydrogen tetrachloroaurate trihydrate (HAuCl₄•3H₂O, 99.9%) was purchased from Strem Chemicals, Inc., and used as received. Trisodium citrate dihydrate (Na₃C₆H₅O₇•2H₂O) was purchased from Fisher Scientific and used as received. Polyethylene glycol 200 (PEG-200, average molecular weight 190-210) was purchased from J. T. Baker and used as received. Thiol ligands (6-mercaptohexanoic acid, 2-ethanol, and (trimethylammonium)ethane thiol iodide) were prepared according to known procedures.^{98,167,187} Buffer solutions (pH = 4, 7, and 10, 0.025 M) were purchased from VWR and used as received. Diafiltration membranes (Minimate 70 kDa, polysulfone) were purchased from Pall, Inc. All other reagents and solvents were obtained from Aldrich and Mallinckrodt and used without further purification. Standard glassware and stir bars were cleaned with aqua regia; fritted funnels were cleaned with bleach/HCl. All glassware was rinsed with copious amounts of ultrapure water prior to use.

UV-visible absorption spectra (UV-vis) were collected using an Ocean Optics USB2000 spectrometer and a quartz cuvette, which was cleaned with aqua regia and rinsed with ultrapure water prior to use. Spectra were normalized at an arbitrary wavelength of 450 nm and displayed in an offset overlay format for clarity. Transmission

electron microscopy (TEM) was used to collect images of nanoparticles with a Philips CM-12 microscope operating at an accelerating voltage of 120 kV. Nanoparticles were aerosoled from dilute solutions onto SiO_x coated copper TEM grids (400 mesh, Ted Pella) and allowed to dry under ambient conditions prior to image collection. Image processing and size analysis were performed with Image J software. X-ray photoelectron spectroscopy (XPS) and thermogravimetric analysis (TGA) were used to analyze lyophilized nanoparticle samples in powder form. XPS was performed on a Kratos Axis 165 instrument with an operating pressure of 10⁻⁹ mmHg using monochromatic Al K α radiation at 10 kV and 20 mA. Dry nanoparticle powders were pressed onto indium foil affixed to a copper sample holder with carbon tape. Charge neutralization was applied to the samples during analysis, and the resulting spectra were referenced to C 1s at 284.5 eV. TGA was performed with a Hi Res TGA 2950 thermogravimetric analyzer equipped with a nitrogen purge. Powder samples were applied to calibrated aluminum pans at ambient temperatures, heated at 5 °C/min to 110 °C, whereupon isothermal conditions were maintained for 10 minutes to ensure removal of residual solvent. The samples were then heated at 5 °C/min to 500 °C, and held under isothermal conditions for twenty minutes to ensure that mass loss due to ligand removal was complete.

The use of diafiltration for nanoparticle purification has been described in detail elsewhere. Here, diafiltration is used to concentrate particle solutions, strip away excess ions, and purify thiol functionalized nanoparticles. Briefly, aqueous solutions of nanoparticles may be concentrated via diafiltration by feeding particle solutions into a sample reservoir, and a peristaltic pump drives the crude sample through a diafiltration

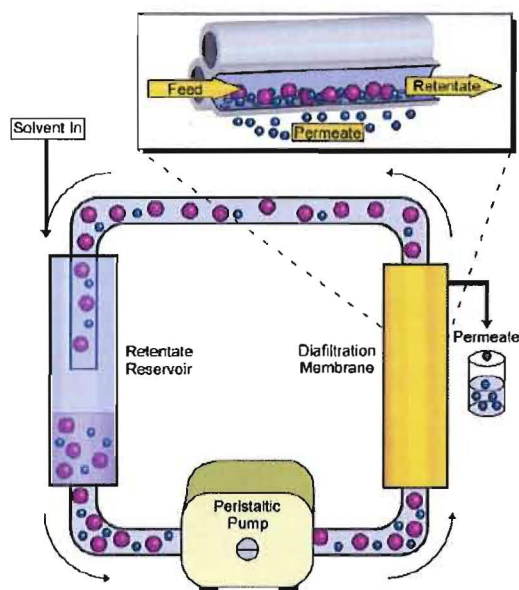


Figure 2.1. Schematic of the diafiltration apparatus. As nanoparticle solutions are driven through the filtration membrane by a peristaltic pump, solvent, ions and small molecules pass through the pores of the membrane, iteratively reducing the concentration of such species in the retentate. Larger materials such as nanoparticles are retained, and solution volume is maintained by adding fresh solvent as diafiltration progresses. (Reprinted with permission from: Sweeney, S.F.; Woehle, G. H.; Hutchison, J. E. *J. Am Chem. Soc.*, **2006**, *128*, 3190. Copyright 2006 American Chemical Society.)

membrane at a constant pressure of 100 kPa. Excess solvent, ions, and small molecules are eluted as filtrate, while the nanoparticles are returned to the sample reservoir as retentate (figure 2.1). A constant retentate volume (V_r) is maintained by feeding additional crude nanoparticle solution to the retentate reservoir as excess solvent and small molecules are eluted, eventually reducing the volume of the nanoparticle sample while retaining initial nanoparticle sample mass. (Here, a batch of nanoparticles that has been reduced in volume to 40 mL will be referred to as “concentrated.”) Diafiltration progress is generally expressed in volume equivalents (V_{eq}) of filtrate, where $1 V_{eq} = V_r$. To strip excess ions away from the gold cores diafiltration is continued on a concentrated sample of citrate stabilized gold nanoparticles, introducing fresh solvent (ultrapure water)

to the retentate reservoir to maintain constant sample volume during processing (for details, *vide infra*). To purify thiol functionalized particles, nanoparticle samples are concentrated in the retentate reservoir, and ultrapure water is added to maintain sample volume as diafiltration progresses until $20 V_{eq}$ of retentate have been collected.

Citrate stabilized gold nanoparticles having average diameters of 8.5 nm were synthesized via an adaptation of the method reported by Turkevich. Briefly, 0.17 g of $\text{HAuCl}_4 \cdot 3\text{H}_2\text{O}$ was added to 300 mL ultrapure water in a 500 mL round-bottom flask equipped with a magnetic stirrer. The solution was brought to reflux, whereupon 0.44 g $\text{Na}_3\text{C}_6\text{H}_5\text{O}_7 \cdot 2\text{H}_2\text{O}$ dissolved in 10 mL ultrapure water was added and allowed to reflux for 20 minutes. The resulting ruby red solution of nanoparticles was rapidly cooled to room temperature using an ice bath, and filtered through a medium ceramic frit. The solution was immediately concentrated to a volume of 40 mL using a diafiltration apparatus as described above. The concentrated solution of nanoparticles was stripped of excess ions by continuing diafiltration with a continuous feed of ultrapure water supplied to the retentate reservoir to maintain volume. The progress of anion (citrate) removal was monitored by UV-vis spectrometry, tracking of the presence of citrate in the filtrate, rather than the retentate, of a sample as it is being stripped of ions. Aliquots of filtrate were collected from the diafiltration apparatus, and the stripping process was deemed complete by the loss of citrate's signature absorption at 210 nm, which usually occurred after 10-15 V_{eq} of filtrate had been collected. (A detection limit of 10 μM was first established by tracking the spectra of increasingly dilute trisodium citrate solutions of known concentrations.)

To functionalize the gold cores, concentrated nanoparticle solutions (20 mL) were redispersed in ultrapure water to reach a volume of 130 mL. A twenty-fold excess (based upon potential binding sites relative to the surface area of the gold cores) of water soluble thiol ligands was dissolved in 20 mL of either ethanol or ultrapure water and introduced to the stirring nanoparticle solution. After stirring for at least 8 hours, the nanoparticle solutions were concentrated to a volume of 20 mL and subject to constant volume diafiltration until $20 V_{eq}$ of filtrate were obtained. The purified samples were allowed to remain in solution for analysis by TEM and UV-Vis, or lyophilized to a dry powder and stored under vacuum for analysis by TGA and XPS. Slight modifications to this general method were employed to accommodate the solubility characteristics of imparted by various ligands:

- 1) Cationic Ligands. The use of (trimethylammonium)ethane thiol iodide (TMAT) did not require any modifications to the general functionalization described above.
- 2) Anionic Ligands. Bare gold nanoparticles were allowed to react with 6-mercaptohexanoic acid (6-MHA) by the functionalization procedure described above, although pH adjustments were made as follows to ensure complete ligand ionization: prior to introduction of the ligand, the pH of the nanoparticle solution was adjusted to pH = 10 with 2M NaOH. After the ligand was introduced as an ethanolic solution to the stirring nanoparticles, the pH was once again adjusted.

- 3) Neutral Ligands. To prevent ligand interdigitation, a small amount (5-fold excess, relative to thiol) of PEG-200 was added to the solution of bare gold nanoparticles prior to the introduction of 2-[2-(2-mercaptoethoxy)ethoxy]ethanol (MEEE). The ultrapure water used for diafiltration of the functionalized particles was spiked with a similar concentration of PEG-200 to prevent agglomeration during diafiltration.

3. Results and Discussion

Functionalization of citrate stabilized gold nanoparticles by thiols featuring charged pendant groups was successful after complete removal of the citrate anion stabilizing shells by extensive diafiltration. Dense functionalization was achieved using anionic (6-MHA), neutral (MEEE), and cationic (TMAT) ligands. With slight modifications to enhance ligand solubility (described above), the particles remained in solution, subject to none of the constraints (primarily ionic strength and electrostatics) formerly imposed by excess citrate anions. Following functionalization, diafiltration was employed once again to purify the modified nanomaterials, removing unbound ligands, salts, and other liberated materials. To gain a better understanding of the surface chemistry enabling these functionalizations, both the stripped gold nanoparticles and the functionalized materials were characterized using TEM, UV-vis, TGA, and XPS, highlighting surface transformations due to the removal of excess ions and the subsequent binding of thiols.

We discovered a new application of diafiltration that enables otherwise difficult functionalization chemistry by removing ions and molecules that hinder the binding of

incoming ligands if left intact. Since previous reports suggest that efforts to remove excess citrate lead to unstable gold cores,²⁴¹ a means of monitoring the ion removal process was required to ensure that all excess ions have been removed without compromising the general stability and quality of the gold cores. Diafiltration is a continuous flow filtration method where the retention and elimination of materials corresponds to the pore size of the membrane material, analogous to standard dialysis. However, diafiltration features a dynamic system driven by a peristaltic pump to increase the speed and efficiency of purification, while tangential flow prevents membrane fouling associated with dialysis. Previous reports have demonstrated that diafiltration is superior to classic nanomaterials purification methods, including dialysis, ultracentrifugation, and chromatography, yielding products free of unbound ligands, unreacted materials, and other small molecules.⁹² In our application, nanoparticle products remain dissolved in the retentate, while unbound materials are collected in the filtrate. We found that the immediate removal of citrate by diafiltration is critical to the success of this method, since aged nanoparticles are known to be less reactive in ligand exchange reactions, presumably due to the decreased lability of the outgoing ligands.²⁴² As crude citrate stabilized gold nanoparticles were stripped of ions via diafiltration, the presence of citrate in the filtrate was tracked at regular intervals. Once the absorption at 210 nm was no longer detected in the filtrate (see figure 2.2), the stripping of noncoordinated ions from the surface of the particles was complete, and the particles were ready for functionalization.

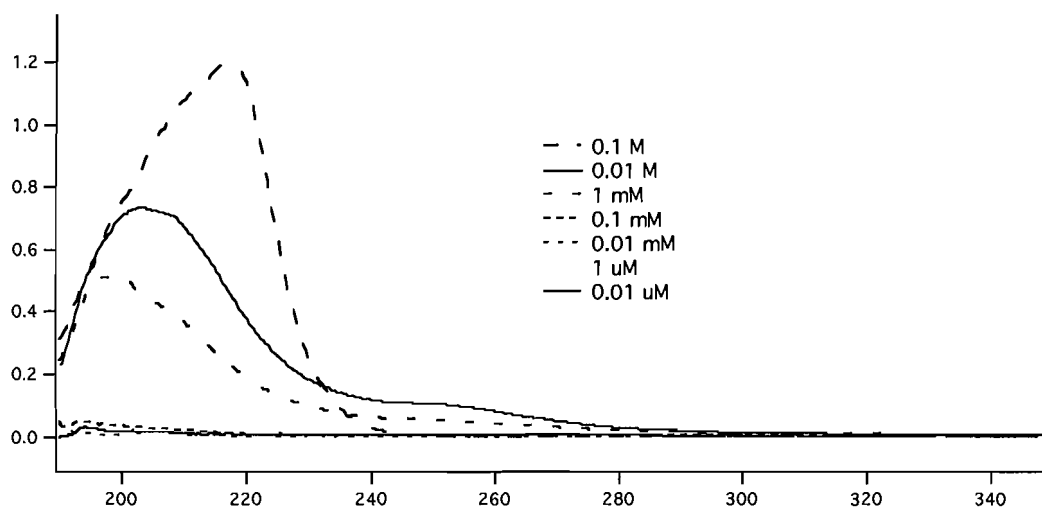


Figure 2.2. UV-vis monitoring of citrate molecules in solution. Known concentrations of citrate ions were analyzed to determine the detection limit, enabling an in-line monitoring process for determining complete removal of citrate ions from a solution of gold nanoparticles.

Full characterization of the stripped gold cores provided a better understanding of particles transformations that occur during the ion removal process, revealing that diafiltration completely removes noncoordinated ionic stabilizers, leaving behind a partial monolayer of dicarboxyacetone. Previous reports of citrate removal by washing with acetone or by reduction with NaBH_4 suggest that the exposed gold cores are unstable.²⁴¹ We found that the stripped cores prepared by our technique remain in solution for at least six months even in the absence of other stabilizing agents, likely due to the remaining dicarboxyacetone species tethered to the surface, which affords electrostatic stability and solubility. Stability is often judged in terms of agglomeration (the reversible clustering of particles due to decreased repulsion) and aggregation (the fusion of nanoparticles upon contacting another completely unpassivated particle). TEM images (figure 2.3) demonstrate that the as-synthesized particles are monodisperse (8.5 ± 1.2 nm) and

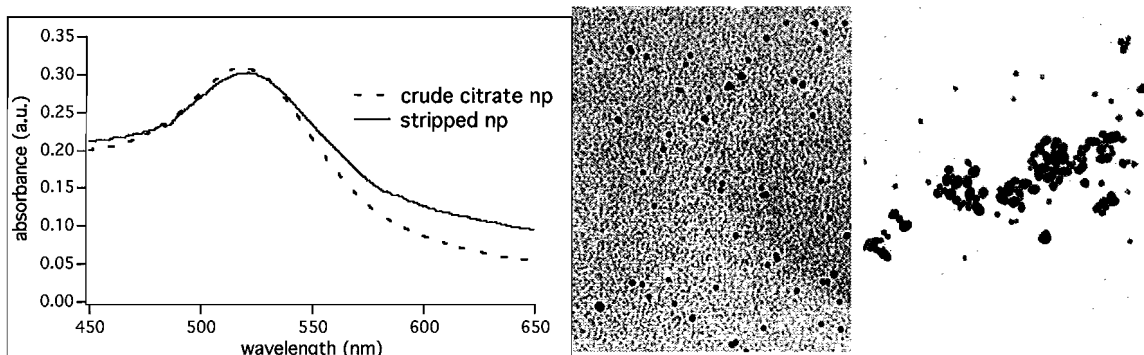


Figure 2.3. (left) UV-vis extinction spectra of nanoparticle solutions. The position of the surface plasmon peak changes little after the nanoparticles are stripped of excess ions. TEM images of citrate stabilized gold nanoparticles, (middle) as synthesized, and (right) stripped gold cores (200,000x magnification)

unaggregated. After extensive diafiltration, the particles agglomerate (rather than aggregate) since most of the citrate has been removed, and interparticle repulsions are minimized. Despite the fact that the stripped particles have a tendency to settle to the bottom of a flask after standing for extended periods, they redispersed immediately with gentle swirling. Although TEM images of the stripped particles suggest aggregation, UV-Vis spectra corresponding to these samples (figure 2.3) show the surface plasmon band position is only slightly shifted, indicating that the nanoparticles are simply agglomerated.

Thermogravimetric analysis (TGA) provides an estimate of the organic portion of a functionalized nanoparticle, with distinct step-like mass losses corresponding to simple pyrolysis reactions associated with the combustion of ligands. TGA curves of the stripped particles confirmed that a very modest amount of organic material remains attached to the particle, showing a mass loss corresponding to a monolayer of dicarboxyacetone, rather than larger amounts of citrate derivatives. Comparison of TGA data derived from

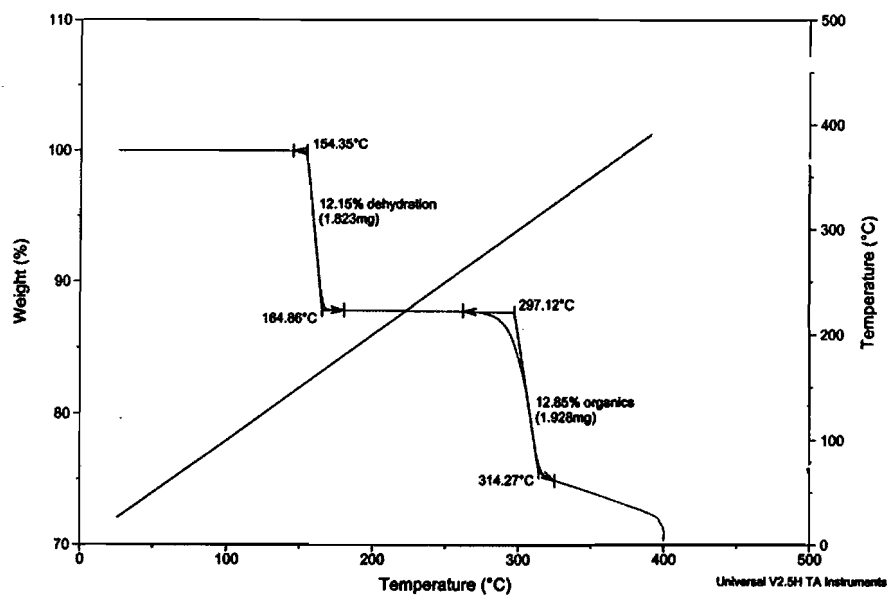


Figure 2.4. Thermogravimetric analysis of trisodium citrate reagent. Mass loss occurs in two distinct steps, due to the loss of waters of hydration and subsequent elimination of CO_2 attributed to the three carboxylate moieties.

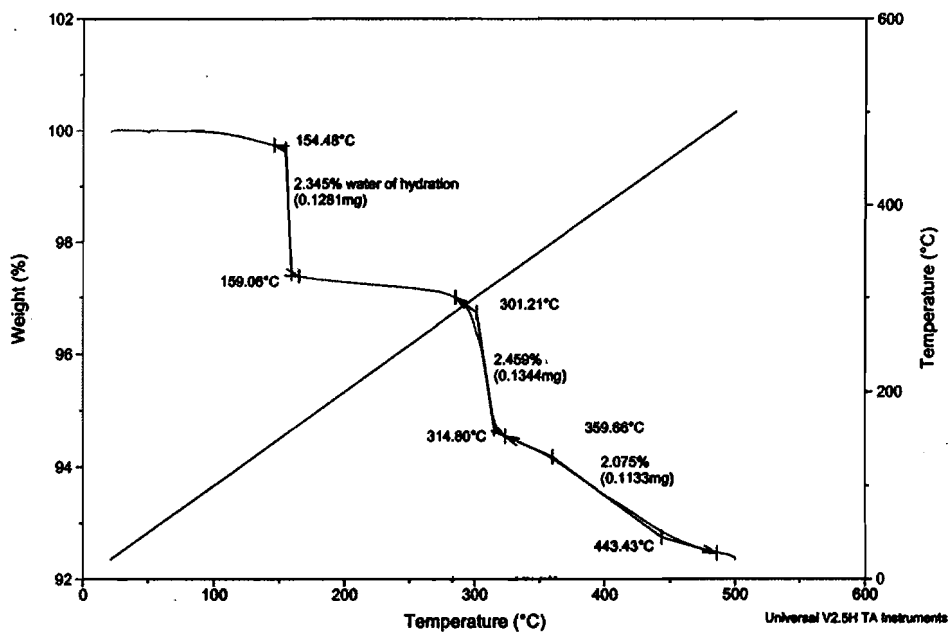


Figure 2.5. Thermogravimetric analysis of gold nanoparticles with excess citrate. The features of the curve are dominated by the presence of pure trisodium citrate.

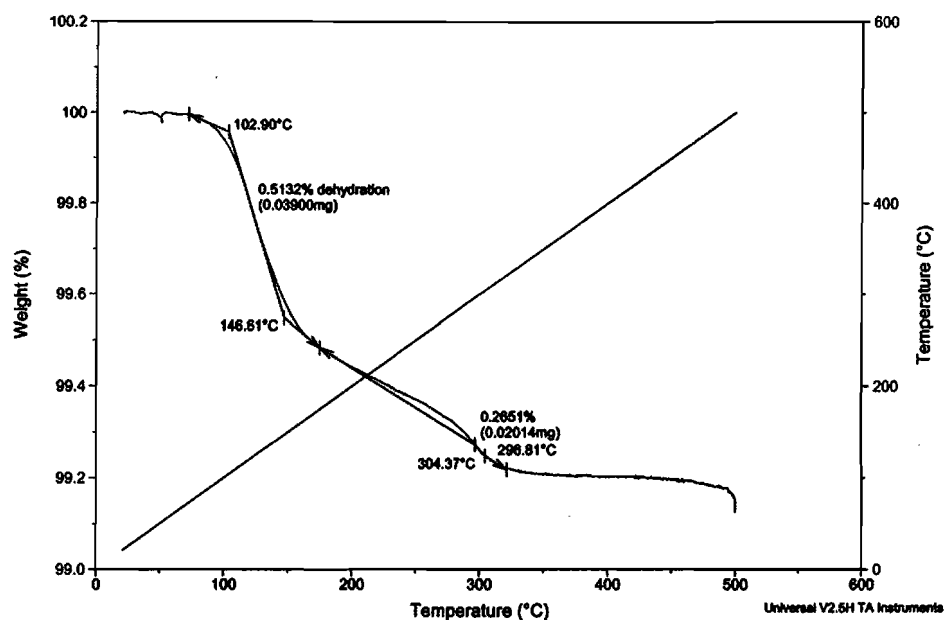


Figure 2.6. Thermogravimetric analysis of stripped gold cores. The mass loss features of free citrate (specifically, the loss of CO₂) are absent from the curve, indicating that citrate is not the chemical species remaining on the surface of the particles after processing.

stripped particles, as-synthesized citrate-stabilized nanoparticles, and trisodium citrate reagent (figures 2.4-2.6) reveals a unique mass loss curve for the stripped particles attributed to a partial monolayer of dicarboxyacetone, confirming that citrate is neither bound to nor associated with the surface of the stripped particles (see table 2.1).

X-ray photoelectron spectroscopy (XPS) was performed before and after pyrolysis of organic components associated with the stripped gold cores. Carbon species were present on the surface of the particles prior to pyrolysis, with C 1s binding energies consistent with carboxylate and ketone species. Sodium counterions were not detected, suggesting that all carboxylate groups are complexed with the surface of the gold

Table 2.1. Summary of nanoparticle functionalization.

Particle type	Surface plasmon band max position (UV-vis)	S: Au ratios (XPS)	Ligands as percent of total mass (TGA)	Extent of Ligand Coverage
Stripped, excess citrate removed	521 nm	N/a	0.28%	96.0%
Particles functionalized with 6-MHA (anionic)	531 nm	0.18 ± 0.05	7.38%	98.1%
Particles functionalized with MEEE (neutral)	537 nm	0.15 ± 0.07	6.41%	75.9%
Particles functionalized with TMAT (cationic)	532 nm	0.14 ± 0.08	3.99%	65.5%

Notes: The surface plasmon band is red shifted in the case of functionalized particles, reflecting the change in the dielectric environment upon binding. S: Au ratios determined by XPS show a clear trend in thiol ligand coverage, while TGA reveals the relative ligand coverage based on the particles surface area and the number of possible binding sites.

particles. No organic material was detected after pyrolysis, confirming that the amount of ligand detected by TGA corresponds to a complete and quantitative assessment of ligand coverage.

A second round of characterization was performed on the functionalized materials after reaction with thiols and subsequent purification. XPS and TGA were used to establish the surface chemistry and extent of functionalization, while TEM and UV-vis provided information related to overall structural integrity. We discovered a clear trend in the extent of functionalization based on the nature of the pendant group of the thiol ligand (summarized in table 2.1). The Au: S atomic ratios detected by XPS (figure 2.7) provide a comparison of ligand coverage density. Here, integrated peaks corresponding to photoelectrons emitted from the S 2p and Au 4f were compared to discern the relative amounts of these elements present in each sample. We found that 6-MHA binds most

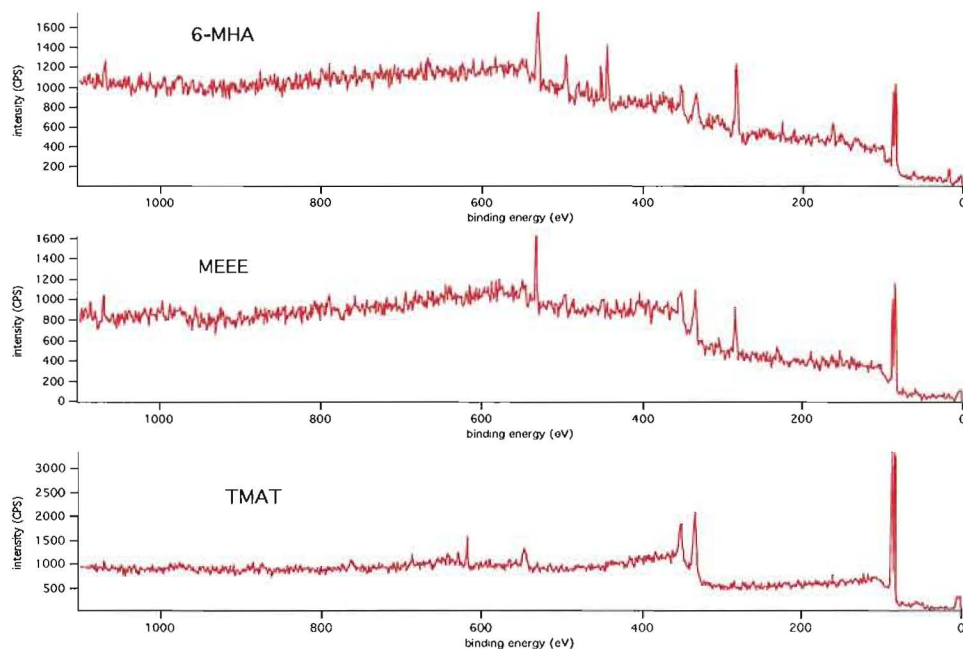


Figure 2.7. XPS survey scans of gold nanoparticles functionalized with (top) 6-MHA, (middle) MEEE, and (bottom) TMAT.

readily, followed by MEEE and TMAT. Corresponding TGA data revealed a similar trend for the relative amounts of ligand lost through pyrolysis, allowing additional comparisons of the amount of ligand detected to the theoretical amount of ligand required to fully functionalize the particles. Nearly full coverage was achieved for 6-MHA, but lesser amounts of ligand were bound to the gold cores for the cases of MEEE and TMAT. Full coverage by 6-MHA was expected based on literature precedent, since it has been proposed that the addition of the anionic ligand shouldn't disrupt the overall electrostatic environment of the nanoparticles, ensuring stability as the functionalization proceeds. However, in the case of MEEE, interparticle repulsions are reduced as the nonionic ligand is added to the surface. As a result, complete ligand coverage is progressively hindered by the increased likelihood of particle interaction and ligand

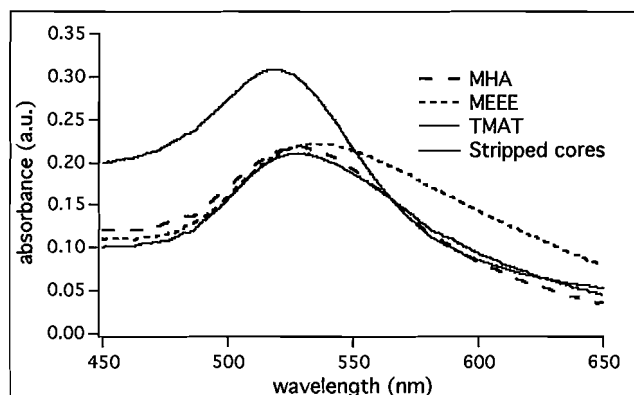


Figure 2.8. UV-vis extinction spectra of gold nanoparticles before and after functionalization with water-soluble thiols. Modest red shifting is observed as the dielectric environment at the surface of the particle changes in response to the binding of thiols.

interdigitation. For the case of ligand exchange with TMAT, it is probable that the pendant quaternary ammonium groups of the particle-bound ligand induced moderate cross-linking with neighboring particles through electrostatic interaction with residual dicarboxyacetone moieties.

These hypotheses are further supported by UV-vis and TEM images of the functionalized nanoparticles, where the assemblies of particles reflect the nature of interactions proposed above. UV-vis data confirm that the particles retain their inherent optical properties after functionalization, showing a modest red shift of the surface plasmon band due to ligand binding, rather than the dramatic red shifts indicative of aggregation (figure 2.8). Nanoparticles functionalized with 6-MHA were once again completely dispersed, reflecting a similar degree of interparticle repulsion compared to the as-synthesized citrate nanoparticles due to ionized carboxylate species. The size (8.9 ± 1.5 nm) and shape of the gold core is virtually unchanged after stripping and functionalization, despite the stripped particles appearing heavily aggregated prior to

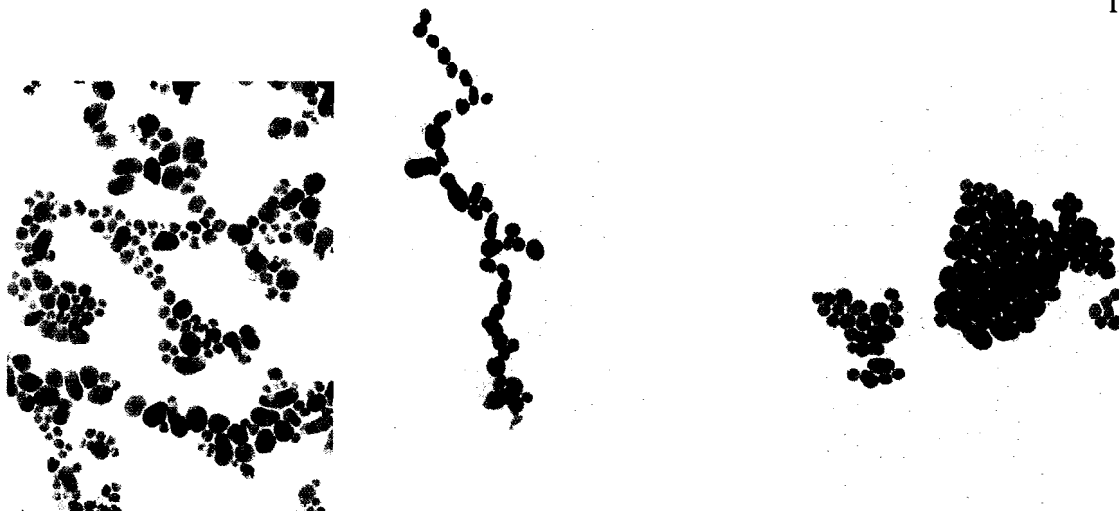


Figure 2.9. TEM images of particles functionalized with: TMAT (left) 24 hours of stirring (center) TMAT, 48 hours, and (right) MEEE (200,000x magnification)

functionalization. Nanoparticles functionalized with MEEE interact in a manner that suggests a lack of interparticle repulsion, much like the stripped citrate particles. Ligand interdigitation was confirmed by adding a small amount of low-molecular weight (poly)ethylene glycol (PEG-200) to solutions of MEEE-functionalized particles. Based on our observations, we propose that the otherwise unreactive PEG interacts with bound MEEE, reversing any agglomeration caused by interdigitated particles. TMAT functionalized nanoparticles form end-to-end structures suggestive of mild cross-linking. Regardless of the apparent nanoparticle interaction observed by TEM (figure 2.9), the nanoparticles retain their optical properties, showing only small red shift in the surface plasmon band upon functionalization, consistent with solution stability and little aggregation.

To delineate whether successful functionalization is dependent upon the either the low ionic strength of the stripped nanoparticle solutions or simply the loss of the multilayered citrate stabilizing shell, the same functionalization conditions were applied

to 1) as-synthesized “crude” citrate nanoparticles dissolved in ultrapure water and 2) stripped nanoparticles dissolved in buffer solutions having pH = 4, 7, or 10. For all cases introduction of MEEE and TMAT to the crude solutions led to irreversible aggregation, while modest amounts of 6-MHA were able to bind to the nanoparticles. With the exception of 6-MHA, aggregation and subsequent precipitation was most rapid for the crude citrate nanoparticles, whereas the stripped particles dissolved in buffer solutions were slower to precipitate, with the exception of the rather unstable acidic solution of particles. These results underscore the importance of complete removal of excess citrate anions, as these failed functionalizations confirm that both high ionic strength of the solution as well as the presence of the full citrate ligand shell hinder efficient functionalization by thiol ligands.

4. Conclusions

We have developed a facile route to the functionalization of large gold nanoparticles prepared by the citrate reduction method. Complete stripping of the anionic citrate stabilizing shell by extensive diafiltration leads to a versatile gold core, unhindered by the presence of noncoordinated ions. The stripped gold cores are stabilized by a monolayer of dicarboxyacetone, rather than an extended stabilizing shell of excess citrate anions, and are thus amenable to functionalization by a range of water-soluble thiol ligands. Overall size and shape of the particles is preserved throughout this process, and the particles retain their optical properties regardless of the pendant functionality of the thiol ligand shell. The extent of ligand coverage is based on the character of the pendant groups, highlighting the importance of maintaining electrostatic repulsion between

particles and avoiding the possibility of cross-linking between reactive surface functional groups. This ability to control the surface chemistry of nanoparticles prepared by the citrate reduction route is likely to facilitate the utilization of these materials in applications dependent upon the optical properties associated with surface plasmon activity, paving the way for the development of new chemical sensors, bioassay materials, and optical devices.

5. Bridge to Chapter III

Chapter II discussed the preparation of a large gold nanoparticle core amenable to functionalization by an incoming thiol, yielding stable materials with known surface chemistry. While the work detailed in Chapter II provides a versatile precursor to functionalized nanoparticles, offering a wide range of options in terms of surface chemistry, a simple direct route is useful when specific materials are needed, rather than a library of analogs. Chapter III describes such a direct route to well-defined nanomaterials, yielding functionalized, water-soluble gold nanoparticles in a single reaction step. By reducing a gold salt in the presence of a capping agent, functionalized nanoparticles are produced without the need for addition processing or ligand exchange reactions. As an alternative to the thiols used in more traditional preparations, we used Bunte salts as a capping agent for the work comprising Chapter III. Bunte salts are easily synthesized, odorless, and shelf-stable, eliminating the need for the sometimes complicated syntheses and careful handling of thiols.

CHAPTER III

DIRECT AQUEOUS SYNTHESIS OF LARGE GOLD NANOPARTICLES USING BUNTE SALTS

Note: Portions of Chapter III are expected to appear in an upcoming publication co-authored by Lohse, S. E.; Dahl, J. A.; and Hutchison, J. E. The author of this dissertation made the initial discoveries reported in Chapter III, guided the later experiments of the project, and co-authored a manuscript. J. E. Hutchison provided research guidance and editorial assistance, while S. E. Lohse performed and designed many of the experiments in the later stages of this project, in addition to co-authoring a manuscript for publication.

1. Introduction

The size-dependent electronic and optical properties of spherical gold nanoparticles have generated interest in gold nanoparticle-based devices including microelectronic and optical devices, as well as *in vitro* sensors.^{6,167,171,243} Gold nanoparticles (AuNPs) smaller than 2.0 nm in diameter may display non-linear current vs. voltage behavior at room temperature,^{90,167} while those larger than 5.0 nm in diameter possess strong optical properties due to the resonant behavior between visible light and

surface electrons (plasmons), characterized by an optical absorbance at 520 nm.^{6,244-246} Functionalized nanoparticles hold a green advantage as device components, due to their ability to act as nanoscale “building blocks” of higher-ordered structures. Devices assembled using a bottom-up fabrication approach via the self-assembly of AuNPs provide superior lithographic resolution and are less materials intensive in their construction compared to devices produced by etching or other top-down production methods.^{167,244} Successful bottom-up device fabrication requires the nanoparticles to have specific functional groups, serving as anchor points between the particles and the substrate. Thus, the realization of these materials applications requires the development of syntheses that provide precise control over nanoparticle core diameter and facile functionalization methods.

Although a number of AuNP syntheses have been developed that provide very precise control over nanoparticle core diameter between 0.8 and 10.0 nm, many of these routes do not provide effective methods for functionalizing the surface of the nanoparticle, particularly in the case of AuNPs with $d_{\text{core}} > 5.0$.^{31,32,98,247-249} The Brust method provides a direct synthesis route which imparts control over both functionality and size,^{212,250-253} while ligand exchange reactions allow for modification of existing nanomaterials post-synthesis.^{98,166,168,188,196,254,255} However, both methods have significant drawbacks that limit their utility in the general synthesis of functionalized AuNPs. The Brust prep is most effective in the synthesis of AuNPs less than 5.0 nm in diameter, while nanoparticles greater than 5.0 nm in diameter are typically synthesized using charged ligands, such as citrate^{31,32} or tetraoctyl ammonium bromide (TOAB),^{195,256} making the

introduction of certain ligands (e.g. thiols) during ligand exchange challenging. Additionally, the use of materials stabilized by TOAB compromises the green merits of subsequent device assembly, as TOAB is a persistent contaminant having significant cytotoxicity. Furthermore, both of these methods require the synthesis of functionalized thiols, which have very short shelf lives and often require complex syntheses to produce. The development of a direct synthesis method for AuNPs in a variety of size regimes having intact thiol-based ligand shells would greatly simplify the synthetic process required to produce nanoparticle-based devices or in-solution sensors, reducing the overall number of steps, the amount of materials used, and the need for purification throughout the process.

Recently, Murray proposed alkylthiosulfates (Bunte salts) as alternatives to functionalized thiols for the direct synthesis of gold nanoparticles. Functionalized Bunte salts are synthetically more straightforward to prepare than most functionalized thiols, and can be stored for long periods of time without oxidizing to disulfides.²⁵⁷⁻²⁵⁹ When used in gold nanoparticle synthesis, the Bunte salt first physically adsorbs to the surface of the developing nanoparticle, and then eliminates sulfite to form a thiolate linkage to the gold core (Figure 3.1).

The potential for Bunte salts as ligand precursors for the synthesis of large functionalized AuNPs has not been extensively investigated, however. Although it is known that Bunte salts passivate growth at the nanoparticle surface more slowly than thiols, no attempt has yet been made to use Bunte salts as ligand precursors in the direct synthesis of AuNPs greater than 5.0 nm in diameter, nor has any one study demonstrated

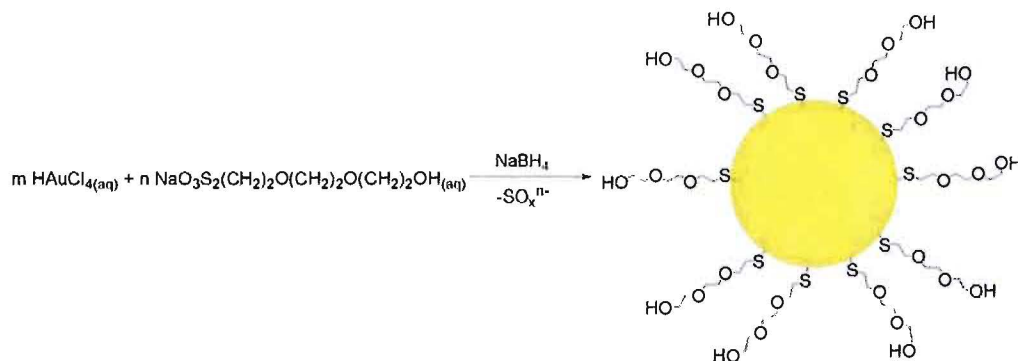


Figure 3.1. Reaction scheme for the synthesis of gold nanoparticles using Bunte salts as ligand precursors. Following adsorption to the gold surface, the ligand precursor eliminates an oxidized sulfur species to provide a thiolate attachment to the surface of the gold nanoparticle (AuNP).

the versatility of Bunte salts as a method for introducing a wide array of functional groups onto the AuNP surface.²⁵⁷⁻²⁶⁰

In this study, we demonstrate that the use of Bunte salts as ligand precursors can be utilized in the synthesis of gold nanoparticles as large as 9.0 nm, while simultaneously imparting a number of hydrophilic functionalities to the surface of the particles, including neutral, cationic, and anionic moieties. We also show that a range of core diameters can be accessed (much as in the Brust prep) by varying the L: Au ratios used in the reaction mixture. The potential for simultaneous size and functionality control provided by this synthetic method make it a powerful tool for the direct synthesis of functionalized gold nanoparticles, which has hitherto been unavailable for AuNPs $d_{\text{core}} > 5.0$ nm in diameter.

2. Experimental

Ultrapure water (minimum 18.2 MΩ•cm resistivity) was provided by a Barnsted Nanopure water filtration system and used in all stages of glassware cleaning, ligand synthesis, sample preparation, and purification. Hydrogen tetrachloroaurate trihydrate ($\text{HAuCl}_4 \cdot 3\text{H}_2\text{O}$, 99.9%) was purchased from Strem Chemicals, Inc., and used as

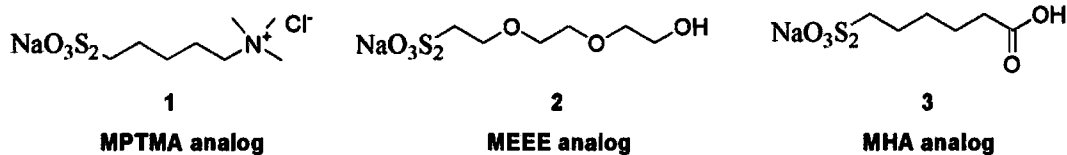


Figure 3.2. The Bunte salts used in this study.

received. 5-bromopentyl(trimethylammonium bromide) (BPTMA) (99%), 2-[2-(2-chloroethoxy)-ethoxy]ethanol (99%), and 6-bromomercaptohexanoic acid (BMHA) were purchased from Aldrich and used as received. Diafiltration membranes (Minimate 10 kDa, polysulfone) were purchased from Pall, Inc. All other reagents and solvents were obtained from Aldrich and Mallinckrodt and used without further purification. Standard glassware and stir bars were cleaned with aqua regia; fritted funnels were cleaned with bleach/HCl. All glassware was rinsed with copious amounts of ultrapure water prior to use.

Bunte salts (figure 3.2) were synthesized using known methods adapted from Murray and others.²⁵⁹⁻²⁶² Briefly, 2.0 g of the organohalide precursor was added to a stirring solution containing 0.8 molar equivalents of sodium thiosulfate ($\text{Na}_2\text{S}_2\text{O}_3$) and 150 mL ultrapure water. The solution was heated to reflux for four hours, cooled to room temperature, and the solvent was removed via rotary evaporation. Due to differences in solubility, purification methods were customized as follows:

- 1) *Purification of the Bunte Salt of MPTMA I.* The crude product was dried *in vacuo* overnight. To remove excess starting material, the product was triturated 2x with 50 mL acetone. The remaining solid was dissolved in ultrapure water and sonicated for 30 min with 10 molar equivalents of solid NaCl to promote ion

exchange. Excess water was removed via rotary evaporation, and triturated once more with 50 mL acetone to remove liberated bromide. The remaining solids were filtered and dried briefly *in vacuo*, and the product was taken up with dry ethanol. The solution was filtered and the solvent was removed to yield an oily white solid. $^1\text{H NMR}$ (300 MHz, D_2O): δ 3.30 ($(\text{CH}_3)_3\text{-N}$, s, 9H); 3.24 ($(\text{CH}_3)_3\text{-N-CH}_2$, t, 2H); 2.56 ($\text{CH}_2\text{-S-SO}_3$, t, 2H); 1.73 ($(\text{CH}_3)_3\text{-N-CH}_2\text{-CH}_2$, m, 2H); 1.59 ($\text{CH}_2\text{-CH}_2\text{-S-SO}_3$, m, 2H); 1.29 ($(\text{CH}_3)_3\text{-N-CH}_2\text{-CH}_2\text{-CH}_2$, m, 2H).

- 2) *Purification of the Bunte Salt of MEEE 2*. Following reflux heating, the water was removed by rotary evaporation, followed by overnight drying *in vacuo*. The crude product was recrystallized in ethanol. $^1\text{H NMR}$ (300 MHz, D_2O): δ 3.70 ($\text{CH}_2\text{-OH}$, q, 2H); 3.65 ($\text{CH}_2\text{-O-CH}_2$, m, 8H); 3.36 ($\text{CH}_2\text{-S-SO}_3$, t, 2H); 2.31 (OH , t, broad, 1H).
- 3) *Purification of the Bunte Salt of MHA 3*. Following reflux heating of the reaction mixture, the water was removed by rotary evaporation, followed by overnight drying *in vacuo*. The crude product was purified by recrystallization in ethanol, retaining excess NaBr side product. (The final product was determined via acid-base titration to be 60% by weight of the desired Bunte salt. The presence of excess NaBr in the reaction mixture was found to have no effect on particle size.) $^1\text{H NMR}$ (300 MHz, D_2O): δ 2.39 ($\text{CH}_2\text{-S-SO}_3$, t, 2H); 2.24 ($\text{CH}_2\text{-COOH}$, t, 2H); 1.45 ($\text{CH}_2\text{-CH}_2\text{-CH}_2$, m, 4H); 1.27 ($\text{CH}_2\text{-CH}_2\text{-CH}_2$, m, 2H).

Gold nanoparticles were synthesized using a modified procedure from that given by Murphy et al. Briefly, 0.1 mmol of hydrogen tetrachloroaurate hydrate (Strem) were

combined in a potassium hydroxide solution (pH=10) with varying amounts of the chosen organothiosulfate, yielding solutions ranging in appearance from clear and colorless to light orange or brown in the case of higher L: Au ratios. The use of sodium hydroxide is necessary to ensure complete ionization of the MHT analog, and to prevent to formation of Au(III)-(MPTMA)₃ complexes, which are insoluble under neutral or acidic conditions. The reaction mixture was allowed to stir for five minutes prior to the addition of 2.0 molar equivalents (with respect to HAuCl₄) of aqueous NaBH₄ (0.1 M). This addition immediately induced a color change to deep red (at lower L: Au ratios) or dark brown (at higher L: Au ratios). The particle solutions were left to stir for an additional 3 hours, filtered through a coarse ceramic frit, and diafiltered with 20 volume equivalents of ultrapure water to remove the excess free organothiosulfate and unreacted gold salt.⁹²

UV-visible absorption spectra (UV-vis) were collected using an Ocean Optics USB2000 spectrometer and a quartz cuvette, which was cleaned with aqua regia and rinsed with ultrapure water prior to use. Spectra were normalized at an arbitrary wavelength and displayed in an offset overlay format for clarity. Transmission electron microscopy (TEM) was used to collect images of nanoparticles with a Philips CM-12 microscope operating at an accelerating voltage of 120 kV. Nanoparticles were aerosoled from dilute solutions onto SiO_x coated copper TEM grids (400 mesh, Ted Pella) and allowed to dry under ambient conditions prior to image collection. Image processing and size analysis were performed with Image J software. Thermogravimetric analysis (TGA) was used to quantify the relative organic content of lyophilized nanoparticle samples in

powder form. Analysis was performed with a Hi Res TGA 2950 thermogravimetric analyzer equipped with a nitrogen purge. Powder samples were applied to calibrated aluminum pans at ambient temperatures, heated at 5 °C/min to 110 °C, whereupon isothermal conditions were maintained for 10 minutes to ensure removal of residual solvent. The samples were then heated at 5 °C/min to 500 °C, and held under isothermal conditions for twenty minutes to ensure that mass loss due to ligand removal was complete.

3. Results and Discussion

Gold nanoparticles were synthesized by reducing Au(III) with sodium borohydride in the presence of a Bunte salt. As a capping agent, Bunte salts act in a manner similar to thiols, while having the advantages of easy preparation, shelf-stability, and versatility. Bunte salts stabilize gold nanoparticles via the formation of a monolayer at the surface of the particle, first associating through the thiosulfate headgroup, followed by the elimination of sulfite to yield a stable gold-thiolate system. Because monolayer formation occurs in two steps, nanoparticle synthesis in the presence of Bunte salts was expected to differ from analogous reactions with thiols in terms of kinetics. Since the average size of the nanoparticle products is not only a function of reagent ratios but also passivation rates, a change in the kinetics of monolayer formation (passivation) should have an impact on particle growth. Thus, if the two-step monolayer formation of Bunte salts results in slower passivation, nanoparticles should be able to grow beyond sizes accessed by the Brust prep using similar reagent ratios. On the other hand, if the thiosulfate headgroup passivates nanoparticle growth as well as a thiol, the average core

size of the products should be unaffected, despite the transient nature of this arrangement. Beyond investigating the nature of the ligand shell, we demonstrate the versatility of Bunte salts in nanoparticle synthesis by synthesizing particles with a range of core sizes and functional groups, providing access to nanoparticles in size regimes associated with useful electronic or optical properties through a single direct synthesis route.

Our general preparation method used Bunte salts prepared from organobromide precursors having a range of water-soluble functional groups, including those with neutral, cationic, or anionic characteristics. The ratio of gold salt (HAuCl_4) to Bunte salt was varied to yield products with different average core diameters. The reducing agent concentration was kept fairly low, as it is suspected that excess borohydride ions may act as a surface passivant, rapidly arresting nanoparticle growth and interfering with the formation of Au-thiolate bonds. We also regulated solution pH with hydroxide ions, to ensure complete ionization of carboxylates and prevent to formation of unreactive solids prior to the addition of borohydride. Diafiltration was used to remove any unreacted materials from the nanoparticle solutions prior to analysis.

Immediately following synthesis, the AuNPs were analyzed using UV-vis absorption spectroscopy to gain a first approximation of the gold core diameter, and thus the relative impact of the ligand to gold (L: Au) ratio on the core size (Figure 3.3). We expected that higher ratios of L: Au would yield smaller particles, as excess ligands will quickly passivate the particles after nucleation, while lesser amounts of ligand should permit further particle development. As predicted, AuNPs synthesized using L: Au ratios less than 4:1 showed SPR (surface plasmon resonance) absorbances at approximately 520

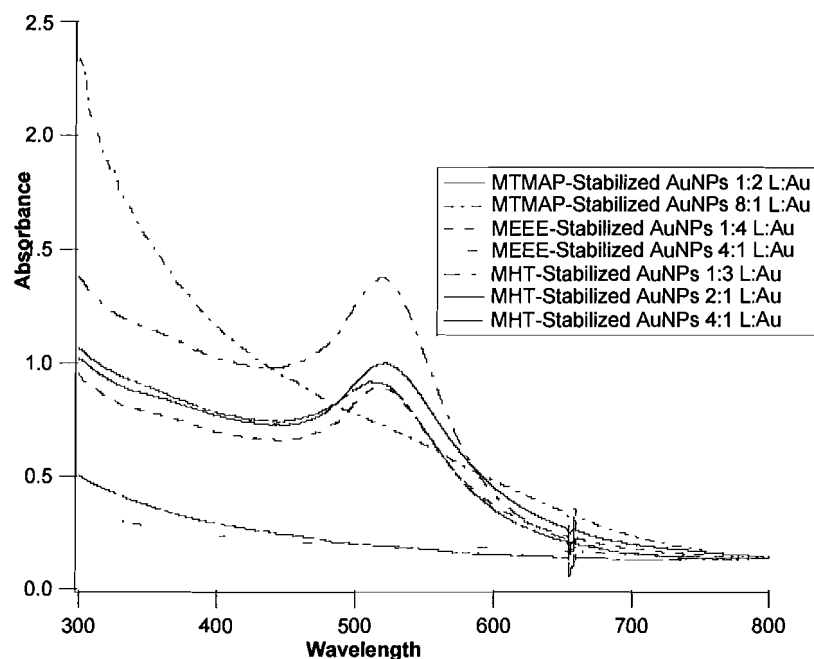


Figure 3.3. UV-vis spectra of AuNPs_(aq) generated from thiosulfate analogs of the following thiols (a) mercaptotrimethylaminopentane (MPTMA), (b) mercaptoethoxyethoxyethanol (MEEE), (c) mercaptohexanoate (MHA). Spectra were taken 3h after the addition of the reducing agent to HAuCl₄/Bunte salt reaction mixture. The ligand:gold (L: Au) ratio used in the corresponding reaction mixture is given in the legend.

nm, suggesting that these red solutions contain particles greater than 5.0 nm in diameter.

In contrast, when reagent ratios exceeded 4:1 L: Au, the surface plasmon absorbance broadens and loses intensity, consistent with the formation of particles 2.0-2.5 nm in diameter.⁶ This trend was especially apparent in the case of the anionic MHT-stabilized particles. Particles resulting from 2:1 L: Au conditions show a blue-shifted absorbance compared to the 1:3 L: Au particle solution, indicating that the solution contains particles of intermediate size. These results suggest that fine size control can also be achieved by varying the L: Au ratio used in the reaction mixture.

TEM analysis of the purified particle solutions supports the size trend suggested by the UV-vis data (Table 3.1). At lower L: Au ratios, the synthesized nanoparticles are

Table 3.1. Summary of nanoparticle properties.

Ligand	L:Au Ratio	d_{core} (nm)	SPB _{max}	Percent Organic (TGA)
MTMAP	1:2	6.4 ± 2.8	525 nm	6.1%
MTMAP	8:1	2.0 ± 1.3	--	12.7%
MEEE	1:4	6.9 ± 3.2	526 nm	3.5 %
MEEE	4:1	1.8 ± 0.8	--	14.5 %
MHT	1:3	8.4 ± 3.2	520 nm	3.6 %
MHT	2:1	6.5 ± 3.1	511 nm	*
MHT	4:1	2.0 ± 0.7	--	7.6 %

larger than 5.0 nm in core diameter, while those synthesized at higher L:Au ratios are approximately 2.0 nm in diameter. This confirms that the L:Au ratio used in this direct synthesis provides core diameter control at room temperature, which extends to a size range beyond that provided by the Brust prep. Interestingly, when similar L:Au ratios are used in the Brust prep and in our reaction, gold nanoparticles of comparable core diameters are produced, suggesting that Bunte salts passivate nanoparticle growth at an overall rate similar to that of thiols, yet the Brust prep cannot be extended to larger particles. TGA of the lyophilized particles suggests that the product AuNPs are covered with a monolayer-like ligand shell comparable that of nanoparticles in the same size range, synthesized with similar Au:thiol ratios via the Brust route. However, in the case of the MPTMA analog, a much higher L:Au ratio is required to achieve the smaller core diameters, suggesting that the quaternary ammonium functionalized ligand is not passivating the nanoparticle growth with the same efficacy as the other two Bunte salts.

This may be due to solubility differences among the ligands- the MTMAP analog possesses a quaternary ammonium functionality and a long hydrocarbon chain, making it the least hydrophilic of the functionalities investigated. Alternatively, the steric demands of this bulky head group may hinder ligand association. If so, this effect would be greatest in the case of the smallest particles, due to the pronounced curvature of the surface, and so increased L:Au ratios are required to force sufficient coverage of the nanoparticle surface.

TEM analysis also suggests that the core diameter of the synthesized nanoparticles show significant dispersity. For particles above 5.0 nm in diameter, the polydispersity approaches 40% in some instances, while in the case of the smaller particles, the polydispersity has decreased somewhat to approximately 30%. It can be seen from the size distribution histograms (Figure 3.4) that this relatively large polydispersity is, in part, due to a large population of particles ~ 2.0 nm in diameter, the relative population of which increases as the L:Au ratio increases.

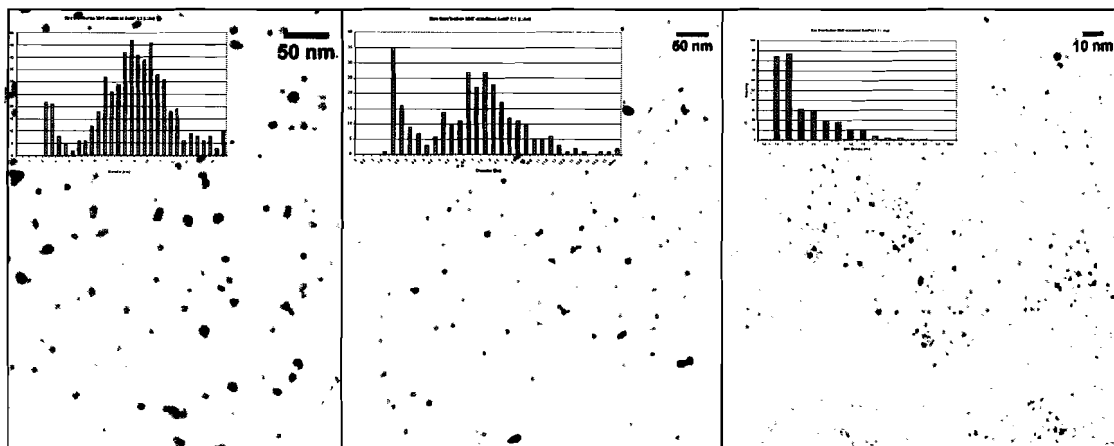


Figure 3.4. TEM images of MHT-stabilized AuNPs. (left) 1:3 L:Au [140 kx magnification], (middle) 2:1 L:Au [140 kx], (right) 4:1 L:Au [260 kx].

Further size control could be exerted during purification by increasing the pore diameter of the diafiltration membrane, allowing the smaller diameter particles to be eluted in the filtrate, thus decreasing the polydispersity of the sample. For the purposes of this study, the smaller particles were retained to provide an accurate picture of the reaction products by performing diafiltration with a small pore diameter (10 kDa) membrane. It should also be noted that the somewhat bimodal nature of the size distribution does not significantly impact the reported mean diameter for the samples, which still reflects the approximate modal diameter well in all cases.

It should be emphasized that varying the L: Au ratio used in the reaction mixture also provides access to products with intermediate core diameters. This is demonstrated in Figure 3.3, where an increase in the L: Au ratio used in the synthesis of MHT-stabilized AuNPs from 1:3 to 2:1 L: Au causes a core diameter decrease from 8.4 nm to 6.5 nm. This core diameter decrease is apparent in both the UV-vis analysis, where the bulk surface plasmon absorbance changes from 520 nm to 511 nm, as well as TEM analysis. This makes the direct synthesis of AuNPs using Bunte salts as ligand precursors a powerful technique for both “coarse” and “fine” size control, which can potentially extend across a number of useful core diameters from 10.0-2.0 nm. The nanoparticles generated by this method can be manipulated (post-synthesis) as single molecules- that is the particles can be dried out and re-suspended in solution, or stored in the freezer and reconstituted later. Such properties are characteristic of AuNPs protected with a thiolate-stabilized monolayer. This is consistent with previous XPS studies of Bunte salt-derived monolayers on both planar gold surfaces and AuNPs, which describe how Bunte salts

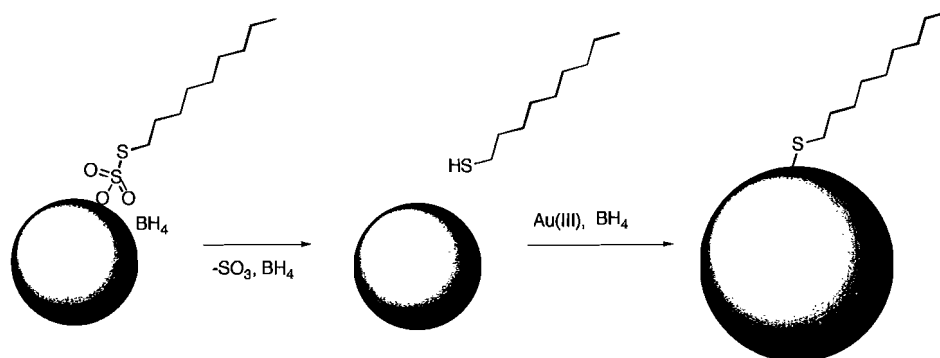


Figure 3.5. A possible mechanism of nanoparticle growth with Bunte salt passivants. While the thiosulfate headgroup associates rapidly with growing nuclei, the concurrence of borohydride creates a poorly passivated surface. As sulfite and borohydride are eliminated, the surface of the particle is exposed, presenting an opportunity for further growth before Au-thiolate bonds are formed.

eliminate sulfite following interaction with the gold surface to provide a thiolate-gold bond.

The observed polydispersity is believed to be a consequence of the unique passivation kinetics of Bunte salts. The initial passivation is accomplished by physical adsorption of the thiosulfate and borohydride to the nanoparticle surface, followed by elimination of sulfite to provide a thiolate linkage to the gold nanoparticle surface.^{259,261,262} It is possible that the surface of the particle is briefly unprotected as the sulfite and borohydride are eliminated, allowing the particle to grow a bit more before the Au-thiol linkage is established (figure 3.5).

Although the overall rate of passivation is similar to that of thiols, Bunte salt passivation may consist of two relatively fast steps, giving the appearance of kinetics having rates similar to thiols, but an entirely different mechanism.

4. Conclusions

In conclusion, we have extended the direct synthesis of functionalized spherical AuNPs using Bunte salts as stabilizing ligands to core diameters greater than 5.0 nm, and demonstrated the versatility of Bunte salts as a delivery vehicle for imparting hydrophilic functional groups. This synthesis provides simultaneous control of both size and functionality. Size control is provided during synthesis by varying the ligand: Au ratio, in a similar manner to the Brust prep, but provides access to a wider variety of core diameters ranging from 2.0 to 9.0 nm. The nanoparticles produced by this method show some significant polydispersity in core diameter- likely a consequence of the passivation kinetics of Bunte salts. The observed polydispersity could be decreased by making small adjustments to the purification method, or by varying other synthetic parameters, such as reducing agent concentration or reaction temperature. Improving the dispersity of the product core diameters is the focus of our current investigations, and will be key for realizing the full synthetic power of this technique.

5. Bridge to Chapter IV

Chapters II and III described two unique routes to synthesizing functionalized large gold nanoparticles. These materials are known to have useful optical properties, owing to the dimensions of the gold cores. The presence of a ligand shell, whether it originates from exchanged thiols or transformed Bunte salts, imparts the functional groups needed to drive assembly into a coherent structure. Chapter IV describes the assembly of nanoparticles produced by the citrate route upon a biomolecular scaffold. Previous work with appropriately functionalized 1.4 nm gold particles demonstrated that

periodic 1-D arrays and other extended structures may be composed if the particles are allowed to assemble upon DNA scaffolds, either in situ or when the DNA has been pre-arranged on a solid substrate. By analogy, larger particles featuring similar surface chemistry are expected to interact with DNA, yielding arrays that may be useful for waveguiding applications, since the surface plasmons of neighboring particles are known to couple efficiently when excited by incoming light.

CHAPTER IV

NANOPARTICLE ASSEMBLY ON BIOMOLECULAR SCAFFOLDS

1. Introduction

Note: Chapter IV was authored entirely by J. A. Dahl, and the work was shared amongst J. A. Dahl and G. E. Kearns. J. E. Hutchison provided research guidance and editorial assistance.

In order to take full advantage of the unique physical properties of nanomaterials, it must be possible to assemble particles into higher-ordered structures, with 1-, 2-, and 3-dimensional architectures. Most applications in the fields of optics, electronics, and sensing require controlled interactions between the individual components of an ordered structure. For example, nanoparticle based electronic devices that operate by tunneling and Coulomb blockade characteristics must be arranged such that the nanoparticle “building blocks” are spaced in a relatively uniform manner, in close proximity to each other (separated only by tens of angstroms). Likewise, the optical characteristics of arrays of larger nanoparticles arise from distance-dependent plasmon interactions. Nanoparticle based sensing devices, regardless of whether they provide an optical or electronic

response, operate as a function of spatial proximity. The ability to manipulate functional materials at the nanoscale is critical for realizing the promise of green nanoscience.

If arranged properly, large ($d > 5$ nm) gold nanoparticles may serve as optical waveguides. Noble metal nanoparticles ($d = 5$ -100 nm) have unique optical characteristics due to the highly polarizable valence electrons at the periphery of the particle, commonly referred to as surface plasmons. Plasmons are capable of interacting with light in the visible regime, leading to very strong absorptions with extinction coefficients exceeding 10^6 . One-dimensional nanoparticle arrays have demonstrated highly efficient waveguiding properties via the coupling of dipolar plasmon oscillations amongst particles in the array, even though the smallest dimension of the array is much smaller than the impinging light. In such an array, light interacts with the surface plasmons, simultaneously polarizing the nanoparticles electric field (figure 4.1). This creates an effective restoring force that initiates a dipolar oscillation of the surface plasmons on the particle. This oscillation in turn induces subsequent oscillation of the plasmons of a neighboring particle. In this manner, a collective, coherent oscillation is

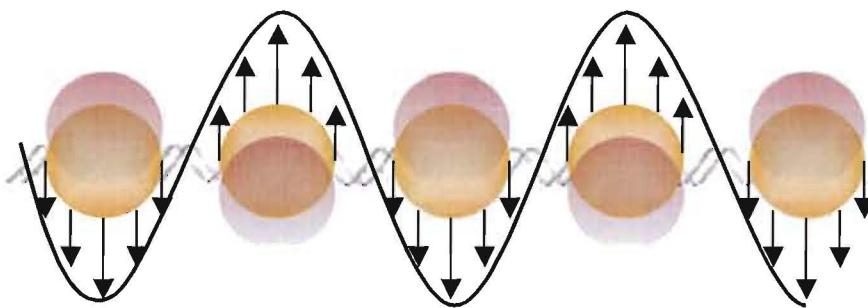


Figure 4.1. Surface plasmon resonance in a 1-D array. As the plasmons of a particle oscillate in response to light (ca. 500-550 nm), the electric field around the particle is offset accordingly. This electronic offset is capable of influencing the field of a neighboring particle, inducing a similar oscillation, effectively guiding light along the array.

created along the nanoparticle array, and light is effectively guided along a structure having a dimension $d \ll \lambda$, thus circumventing the diffraction limit of light.

Nanoparticle arrays have additional optical qualities that define them as a superior alternative to existing optical devices. It has been shown that energy is tightly confined to the array, minimizing radiation losses. Because wave propagation occurs primarily through nearest-neighbor plasmon coupling, it is possible for light to be guided around 90° bends.^{200,202,263,264} Typical optical devices suffer significant radiation losses if similar changes in geometry are encountered. The ability to manipulate the position of nanoparticles in solid-state arrays is the key to fabricating novel waveguides.

Assemblies of nanostructures can be achieved through three main routes, including interparticle linkage, binding to a functionalized surface, or binding to a fixed template. The primary interactions responsible for the construction of robust nanoarchitectures can be classified as either electrostatic attractions or covalent bonding, and thus good control over the surface chemistry is critical. The ability to impart specific functionality to the surface of a nanoparticle provides a means of exploiting such interactions to generate higher-order structures.

Self-organizational processes enable bottom-up approaches toward device fabrication, which is an inherently greener approach than the wasteful top-down techniques (figure 4.2) currently employed in commercial micro- and nanodevice production, although other techniques such as atomic layer deposition and lithographic methods are finding their place within nanoscience as they become more refined and less resource intensive. Self-assembly stands as the greenest method of creating ordered

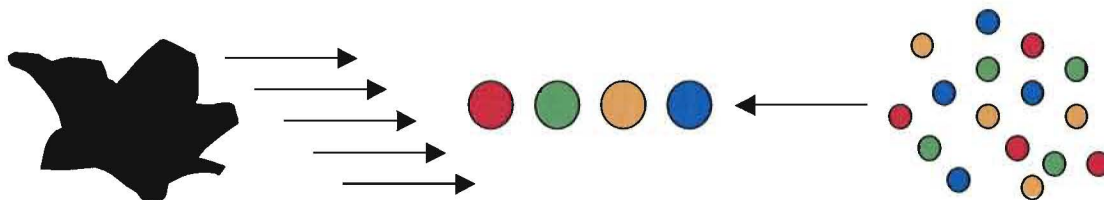


Figure 4.2. Top down vs. bottom up approaches to materials assembly. Top down approaches (left side) begin with relatively amorphous materials and employ a series of additive and subtractive processing steps to arrive at an ordered structure, generating various amounts of waste with each step. Bottom up strategies (right side) take advantage of functionalized precursor materials combined by additive processes to create a higher-order structure, requiring little processing support while sacrificing minimal amounts of starting materials.

structures, as it uses minimal materials, consumes negligible amounts of energy, and is often self-passivating, with a tremendous ability to correct defects as the most thermodynamically stable configuration is achieved.

Chemical modification of the substrate may be needed to drive interactions with nanomaterials and can be achieved through simple monolayer chemistry.²⁶⁵⁻²⁶⁸ Common examples include dithiol functionalized gold surfaces, capable of capturing gold nanoparticles, and amine functionalized surfaces that drive electrostatic assemblies of nanoparticles having carboxylate and sulfonate groups at their periphery. Conversely, monolayers with inert pendant groups can be used to passivate surfaces and prevent nanoparticle adhesion: alkylsilane films have been used for such purposes. The work featured in this chapter uses this a combination of these strategies, as nanoparticles functionalized with ionic functional groups are assembled upon DNA scaffolds.

DNA stands as the most common biomolecular substrate employed for assembling nanoparticle linkages^{192,208,269-272} and arrays.^{166,209,273-275} A wide range of biologically derived substrates have proven useful, including RNA,²⁷⁶⁻²⁷⁸ viruses,²⁷⁹⁻²⁸⁶ and proteins/peptides.^{214,287-294} Manipulation of the biomolecule prior to self-assembly

reactions with nanomaterials allows one to control the morphology of the assembled array, as the final structure typically mimics that of the substrate. Thus, planar substrates may support two-dimensional arrays, whereas substrates having a relatively linear structure (such as a biomolecule) are best suited to one-dimensional structures.

Here, molecular combing techniques are used to stretch DNA into a linear arrangement upon the surface of an alkylsilane passivated SiO_2 TEM grids (figure 4.3). Citrate-stabilized gold nanoparticles were stripped of excess ions and functionalized by an incoming thiol, trimethyl(ammonium)ethanethiol iodide (TMAT). Solutions of functionalized nanoparticles were incubated with the DNA-containing grids to create one-dimensional arrays, which have the potential to act as optical waveguides, owing to the optical properties of larger gold nanoparticles.

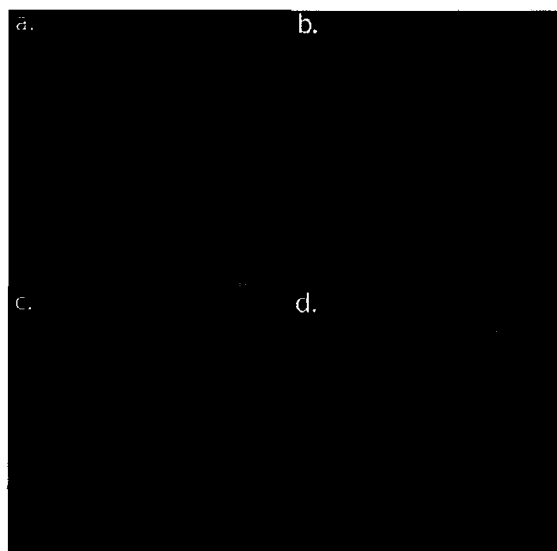


Figure 4.3. SEM images of Si/SiO_2 TEM grids. a.) top view of windows, b.) a single window with a dust particle, c.) back view showing converging $\text{Si}(111)$ etch planes, and d.) closer back view of an individual window. (Reprinted with permission from Kearns, G. J.; Foster, E. W.; Hutchison, J. E. *Anal. Chem.* **2006**, 78, 298, Figure 1. Copyright 2006 American Chemical Society.)

2. Experimental

Ultrapure water (minimum $18.2 \text{ M}\Omega\cdot\text{cm}$ resistivity) was provided by a Barnsted Nanopure water filtration system and used in all stages of glassware cleaning, ligand synthesis, sample preparation, and purification. Hydrogen tetrachloroaurate trihydrate ($\text{HAuCl}_4\cdot 3\text{H}_2\text{O}$, 99.9%) was purchased from Strem Chemicals, Inc., and used as received. Trisodium citrate dihydrate ($\text{Na}_3\text{C}_6\text{H}_5\text{O}_7\cdot 2\text{H}_2\text{O}$) was purchased from Fisher Scientific and used as received. (Trimethylammonium)ethanethiol iodide was prepared according to known procedures.^{98,167,187} SiO_2 TEM grids were prepared by known procedures.⁹⁰ Octyltrichlorosilane was purchased from Aldrich and used as received. MES buffer solutions (50 mM, (2-(N-morpholino)ethanesulfonic acid) was freshly prepared prior to use. Diafiltration membranes (Minimate 70 kDa, polysulfone) were purchased from Pall, Inc. All other reagents and solvents were obtained from Aldrich and Mallinckrodt and used without further purification. Standard glassware and stir bars were cleaned with aqua regia; fritted funnels were cleaned with bleach/HCl. All glassware was rinsed with copious amounts of ultrapure water prior to use.

Citrate stabilized gold nanoparticles having average diameters of 10 nm were synthesized via an adaptation of the method reported by Turkevich. Briefly, 0.17 g of $\text{HAuCl}_4\cdot 3\text{H}_2\text{O}$ was added to 300 mL ultrapure water in a 500 mL round-bottom flask equipped with a magnetic stirrer. The solution was brought to reflux, whereupon 0.44 g $\text{Na}_3\text{C}_6\text{H}_5\text{O}_7\cdot 2\text{H}_2\text{O}$ dissolved in 10 mL ultrapure water was added and allowed to reflux for 20 minutes. The resulting ruby red solution of nanoparticles was rapidly cooled to room temperature using an ice bath, and filtered through a medium ceramic frit. The

solution was immediately concentrated to a volume of 40 mL using a diafiltration apparatus, described elsewhere.⁹² The concentrated solution of nanoparticles was stripped of excess ions by continuing diafiltration with a continuous feed of ultrapure water supplied to the retentate reservoir to maintain volume, until 15 V_{eq} were collected. Complete removal of citrate was assessed by analyzing an aliquot of filtrate by UV-vis spectrometry, confirming the disappearance of citrate's signature absorption at 210 nm. The resulting solution of bare gold nanoparticles cores was concentrated to 20 mL and redispersed in ultrapure water to reach a volume of 130 mL. A twenty-fold excess (based upon potential binding sites relative to the surface area of the gold cores) of TMAT was dissolved in 20 mL of ultrapure water and introduced to the stirring nanoparticle solution. After stirring for at least 8 hours, the nanoparticle solution was concentrated to a volume of 20 mL and subjected to constant volume diafiltration until 20 V_{eq} of filtrate were obtained, removing all unbound TMAT to yield a pure solution of functionalized particles.

SiO₂ TEM grids were cleaned a 15 minute treatment in a UV-ozone cleaner, followed by rinsing with copious amounts of ethanol followed by ultrapure water. The grids were allowed to dry and mounted on double sided tape, allowing only the edges of the grids to make contact with the adhesive material. The mounted grids were placed in a small dessicator containing a beaker with 300 μ L of octyltrichlorosilane. Vapor phase silanization continued overnight to create a hydrophobic monolayer on the surface of the grids. Prior to deposition upon the TEM grids, genomic λ -DNA (Hind III digest) was diluted to 5 μ g/mL in 0.25 mM MES buffer solution, pH pre-adjusted to 5.5 with 0.1 M

NaOH. A fine tip forceps bearing a vertically oriented silanized TEM grid was attached to a motorized pulley, and dipped into the DNA solution. The TEM grid was allowed to incubate in the solution for 5 minutes, and was removed by pulling the grid vertically, windows orthogonal to the solution meniscus, at a rate of 300 $\mu\text{m/s}$. The grids, containing fixed strands of DNA, were rinsed with ultrapure water prior to soaking with a 10 μL droplet of TMAT-functionalized nanoparticle solution for one hour. The grids were then rinsed with copious amounts of ultrapure water and blown dry with a stream of argon gas in preparation for collection of TEM images. Images of DNA-nanoparticle composites were collected with a Philips CM-12 microscope operating at an accelerating voltage of 120 kV. Image processing was performed with Adobe Photoshop and Image J software.

3. Results and Discussion

In this work, a combination of surface treatments was used to generate DNA-nanoparticle composites supported on SiO_2 TEM grids. Gold nanoparticles were functionalized with the cationic ligand TMAT in order to promote electrostatically driven self-assembly upon the anionic phosphate-containing backbone of DNA. Prior to the introduction of nanoparticles, the SiO_2 grids were treated with vapor phase OTS to form a hydrophobic monolayer intended to limit non-specific interactions with charged moieties present on the functionalized particles. DNA was then arranged on the modified surface of the grids using biomolecular combing techniques pioneered by the Bensimon group.²⁹⁵ Here, biomolecules were stretched over the grids as they were removed from a buffered DNA solution, with the receding solution meniscus effectively pulling the strands of

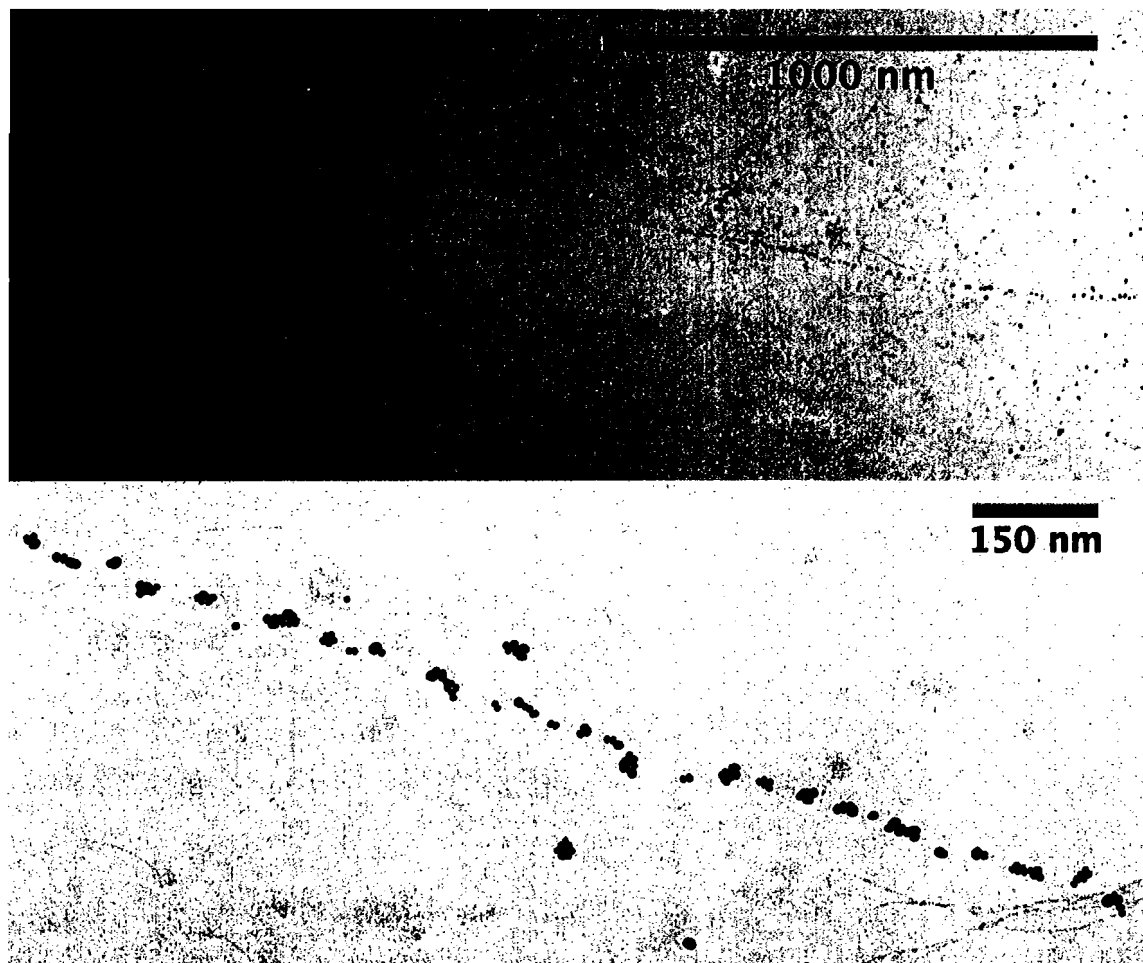


Figure 4.4. Arrays of nanoparticles supported on DNA scaffolds. While the arrays extend for microns (top), the structures lack periodicity due to the deposition of clusters, rather than individual particles (bottom).

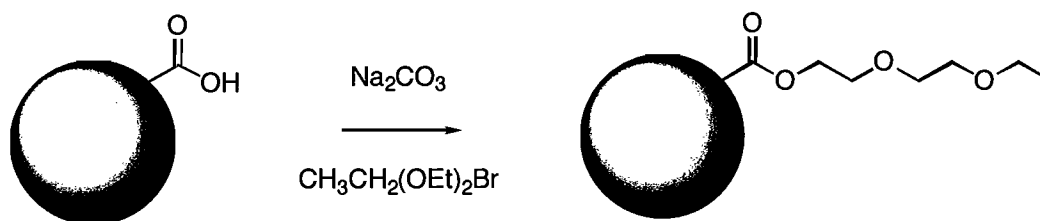
DNA downward into a parallel arrangement. Functionalized particles were allowed to assemble on the biomolecular scaffolds to yield composite structures.

TEM images reveal linear structures at low magnification, while higher resolution images reveal that the nanoparticle arrays are not continuous (figure 4.4). The particles appear to be grouped in clusters, lacking distinct interparticle spacing rather than in a periodic array. Previous work using pure 1.5 nm TMAT-functionalized particles resulted in DNA-nanoparticle “ribbons” with about 5-6 particles making up the width of the

structure.⁹⁰ These structures are believed to be the result of ultrapure particles spanning the width of the DNA scaffold. In the present case, 10 nm TMAT functionalized particles exceed the width of individual DNA strands, making it unlikely that the clustering of the large particles is due to the dimensions of the biomolecular scaffold.

The structures produced here may be understood by reviewing the nature of the nanoparticle “building blocks” prepared by the citrate route. It has been confirmed that even after excess citrate anions are removed by diafiltration, a partial monolayer of dicarboxyacetone remains, presenting free carboxylate groups. The extent of functionalization of the gold cores by incoming thiol ligands appears to be dependent upon the nature of the pendant moiety: ligands with trimethylammonium groups are incapable of forming complete monolayers since they are capable of cross-linking with free carboxylate groups of nearby particles in solution. As a result, surface coverage by the incoming ligand is limited, since cross-linking partially blocks potential binding sites. Consequently, the particles exist in clusters and present fewer pendant functional groups than otherwise expected.

The TEM images of DNA-nanoparticle composites presented here have features consistent with previously observed cross-linked particles resulting from reactions with TMAT. In order to use these structures as optical waveguides, individual particles must be arranged in a periodic structure, free of cross-linked clusters and irregular spacing. A possible solution to the problem of cross-linking could involve capping the free carboxylate groups of gold cores prepared by the citrate reduction route. Esterification under mild conditions is promising, as it can be performed in aqueous media with a



Scheme 4.1. Mild esterification reactions can be used to cap free carboxylates prior to functionalization by TMAT. The suggested conditions are compatible with the gold cores, and the ester should help maintain water solubility.

slightly basic pH by the route proposed in scheme 4.1. The esterified gold cores should remain stable and water soluble under these conditions, permitting the binding of incoming TMAT without the possibility of cross-linking.

4. Conclusions

DNA was arranged on silanized TEM grids to create aligned scaffolds for nanoparticle self-assembly. Electrostatic interactions between cationic quaternary ammonium groups present on the surface of functionalized gold nanoparticles drove electrostatic interactions with the DNA, leading to linear arrays. However, these arrays lack the periodicity necessary for their application as optical waveguides, due to apparent cross-linking amongst particles occurring during the functionalization process.

The application of efficient particle assembly methods will remain an area of focus in the pursuit of waveguides produced by green chemistry inspired routes. Continued challenges in this area are likely to include refinement of functionalization methods such that the particles remain free in solution prior to and during assembly upon a DNA scaffold. In the absence of cross-linking, DNA-nanoparticle composites may rival analogous waveguides produced by materials- and energy-intensive lithographic

techniques. Molecularly defined substrates will enable this level of sophistication in self-assembly, allowing the total application of green nanoscience throughout product fabrication, beginning with greener syntheses of nanoparticle building blocks and finishing with processing steps that yield completely green, innovative nanoproducts.

5. Bridge to Chapter V

Chapter IV described the assembly of large gold nanoparticles on DNA scaffolds, in an attempt to fabricate waveguiding materials using greener techniques. Additional studies are needed to refine the nanoparticle “building blocks” in order to obtain the desired periodic structures. Chapter V concludes this dissertation, providing the outlook for the future of all the work described in previous chapters, as well as offering possible solutions to some of the challenges encountered throughout.

CHAPTER V

OUTLOOK AND CONCLUSIONS

Although nanoscience has recently emerged as a unique discipline of research, the technology is still fairly young and the field remains loosely defined, presenting an opportunity to incorporate new concepts within the existing methodology. Utilizing green chemistry principles in both the design and application of nanomaterials ensures that this technology is approached in a responsible manner, minimizing risks to health and the environment while improving overall efficiency without compromising quality and performance. Because the field is still in its infancy, the circumstances favor the acceptance of greener ideas and principles within the scientific community, since their incorporation is not necessarily coupled to the replacement or retrofitting of well-established synthetic techniques. The benefits of greener nanosynthesis are likely to extend well beyond the laboratory, since green principles are viewed favorably by the public, and thus their implementation will aid public perception of nanotechnology.

Chapter I introduced the basic premise of greener nanosynthesis, describing the principles of green chemistry and the immediate benefits of their application to the synthesis of metal nanoparticles. Because green nanosynthesis is novel concept rather

than an existing field, proposing ways to incorporate green chemistry whenever possible is necessary to fuel the imaginations of those currently performing nanosynthesis by more traditional methods. To further inspire the interested reader, the serendipitous presence of green chemistry principles in recent literature was reviewed, demonstrating how simple changes in reagents, solvent systems, and reaction conditions can be combined to improve existing methods, yielding greener products from a benign origin. While the production of optimal materials through entirely is a noble goal, the chance to improve the syntheses of materials with unfortunate (yet accepted) side-properties should not be overlooked. To this end, the somewhat unlikely coupling of greener nanosynthesis with inherently toxic synthetic targets (such as quantum dots) was presented, highlighting the role of green chemistry in minimizing negative aspects of materials production. Finally, functionalization chemistry was reviewed, providing a means of controlling how nanomaterials interact with their environment. The ability to control the surface chemistry is a key design aspect that must be addressed in order to use nanomaterials in more advanced applications.

In Chapter II, the production of large, functionalizable gold cores from greener methods was presented. Gold nanoparticles have been synthesized by the citrate reduction route for decades, yielding relatively monodisperse particles with desirable optical properties. Citrate-stabilized gold nanoparticles are produced by an entirely green method, requiring only citrate, water, and a gold salt, but their utilization has been greatly limited by the presence of a poorly defined surface. We discovered that extensive functionalization by incoming thiols is possible after excess ions are removed, revealing a

more tractable gold core. After treatment with a range of water-soluble thiols, we found that the extent of functionalization was influenced by both the presence of a native dicarboxyacetone monolayer as well as the nature of the incoming ligand. Rather than treating it as an exchangeable ligand, future work could take advantage of the intact dicarboxyacetone species, which presents free carboxylate moieties useful for coupling reactions under mild conditions. The concept of removing unwanted ligands by diafiltration in order to facilitate secondary functionalization could be extended to other nanomaterials having weakly bound stabilizing shells. Silver nanoparticles produced by citrate reduction are an obvious choice, since they feature optical properties similar in nature to those of gold, as are metal particles created by reduction with other mild organic acids and carbohydrates. Anisotropic nanoparticles could also benefit from this method, as they are often stabilized by large amounts of surfactant, hindering ligand exchange. The removal of surfactants provides another green benefit, ensuring that excess surfactants are not released into the general environment, should these materials find widespread application in consumer goods. With further refinement of this technique, large noble metal nanoparticles will enable the development of optical waveguiding devices, single molecule sensors, and advanced imaging and spectroscopic techniques.

Chapter III described the use of Bunte salts as a shelf-stable alternative to thiols in the direct synthesis of functionalized nanoparticles. Gold salts can be reduced by sodium borohydride in the presence of a thiol capping agent, imparting functionality and stability to the newly formed particles. Unfortunately, thiols tend to suffer from rapid oxidation to disulfides, reducing their reactivity in ligand exchange processes. Previously, thiols were

often freshly synthesized or stored under stringent inert atmosphere to avoid this shortcoming, yet this solution is inadequate if ligand exchange reactions or direct syntheses are carried out under conditions that promote disulfide formation, including aqueous, biphasic, and basic environments. As an alternative to thiols, Bunte salts are readily synthesized from an organohalide and sodium thiosulfate, yielding an odorless, shelf-stable salt. Bunte salts analogous to the thiols used in the work featured in Chapter II were synthesized, having water-soluble cationic, anionic, and neutral pendant groups. We discovered that Bunte salts can be used in the place of thiols in the direct synthesis of gold nanoparticles. By varying the ratio of reagents, one can simultaneously control both core size and functionality of the products, eliminating the need for ligand exchange and extensive purification. The results of this work provided several clues to the unique kinetics of direct syntheses that substitute Bunte salts for thiols. While thiols bond to gold in a single step, monolayers resulting from the association of Bunte salts have an additional reaction step, where sulfite and excess borohydride are eliminated to yield a thiol. We suspect that this difference in mechanism is responsible for the apparent polydispersity of the nanoparticle products, having the likely consequence of inferior surface passivation. While nucleation events are probably unaffected, exposed surface gold atoms permit the nuclei to grow without the boundaries imposed by a tightly packed ligand shell of thiols. Future investigations could involve simple variations to the reaction conditions, limiting borohydride to equimolar ratios with respect to gold to prevent early surface passivation (since borohydride acts as a complexing agent as well as a reductant), in turn promoting ligand binding. Alternatively, competition with a thiol during

nanoparticle synthesis would provide a clear understanding of the relative affinity for the gold nuclei. Provided the Bunte salt and the thiol have differing pendant groups (for easy spectroscopic analysis) yet similar sterics and solution dynamics, comparison of the products resulting from mixed ligand solutions should offer further insight. Beyond kinetics and mechanistic investigations, the full scope of this reaction has yet to be demonstrated. Future studies should include elucidation of the scope and mechanism of this method, followed by the extension of this reaction to other materials, including noble metal particles and bimetallic materials, as well as the synthesis of new Bunte salts with functional groups specific to a given application.

A route to greener device fabrication was described in Chapter IV, via the assembly of large gold nanoparticles functionalized with ligands having quaternary ammonium groups (TMAT). Since these gold nanoparticles feature optical properties including strong extinction coefficients and facile, yet tightly confined distance-dependent plasmonic coupling abilities, we proposed a simple waveguide structure consisting of nanoparticles assembled through electrostatic interactions upon biomolecular scaffolds. As a scaffold, DNA has been used successfully in similar applications with smaller nanoparticles. Recently, new TEM grids featuring SiO₂ viewing windows were developed, providing superior imaging capability while also providing a readily modifiable substrate for nanomaterials assembly. DNA was stretched over the surface of such a TEM grid, and nanoparticles were allowed to self assemble upon the scaffold in a second step. The resulting arrays were not continuous, composed of clusters rather than individual nanoparticles. This is likely a consequence of the incomplete

functionalization by TMAT described in Chapter II, which leads to cross-linked structures. It is possible that these arrays may possess the optical properties of an array of even larger particles, since clusters often mimic the properties of their single-particle counterparts; further assessment of these arrays is warranted.

The problem of cross-linking during functionalization may be prevented by capping the reactive surface groups of the gold cores prior to functionalization. Alternatively, analogous materials produced by the direct synthesis described in Chapter III may be suitable for creating linear arrays with DNA. Although these particular products tend to have polydisperse size distributions, one could sort the particles using appropriately-sized diafiltration membranes to remove smaller particles.

Many of the challenges described in the previous chapters could be remediated by borrowing a key principle from another, demonstrating that new materials are rarely produced from entirely green methods at inception, yet many of the processes are easily improved. As green chemistry principles are applied to individual aspects of nanosynthesis, whether it is particle synthesis, functionalization, or purification, their combination and use in materials production holds the key to realizing completely green nanodevice processing and applications.

BIBLIOGRAPHY

- (1) Nanostructured Materials, Processing, Properties and Applications; Koch, C. C., Ed.; Noyes Publications: Norwich, New York, 2002.
- (2) Albrecht, M. A.; Evans, C. W.; Raston, C. L. Green chemistry and the health implications of nanoparticles. *Green Chemistry* **2006**, *8*, 417-432.
- (3) McKenzie, L. C.; Hutchison, J. E. Green nanoscience: an integrated approach to greener products, processes, and applications. *Chemistry Today* **2004**, *22*, 30-32.
- (4) Perez-Juste, J.; Pastoriza-Santos, I.; Liz-Marzan, L. M.; Mulvaney, P. Gold nanorods: synthesis, characterization and applications. *Coordination Chemistry Reviews* **2005**, *249*, 1870-1901.
- (5) Warner, M. G.; Hutchison, J. E. Synthesis and assembly of functionalized gold nanoparticles; American Scientific Publishers, 2003.
- (6) Daniel, M.-C.; Astruc, D. Gold nanoparticles: assembly, supramolecular chemistry, quantum-size-related properties, and applications toward biology, catalysis, and nanotechnology. *Chemical Reviews* **2004**, *104*, 293-346.
- (7) Murphy, C. J.; Sau, T. K.; Gole, A. M.; Orendorff, C. J.; Gao, J.; Gou, L.; Hunyadi, S. E.; Li, T. Anisotropic metal nanoparticles: synthesis, assembly, and optical applications. *Journal of Physical Chemistry B* **2005**, *109*, 13857-13870.
- (8) Anastas, P.; Warner, J. Green Chemistry: Theory and Practice; Oxford University Press: New York, 1998.
- (9) "A nanotechnology consumer products inventory," Project on Emerging Nanotechnologies, Woodrow Wilson International Center for Scholars, 2006.
- (10) Kamat, P. V.; Huehn, R.; Nicolaescu, R. A "sense and shoot" approach for photocatalytic degradation of organic contaminants in water. *Journal of Physical Chemistry B* **2002**, *106*, 788-794.
- (11) Hasobe, T.; Imahori, H.; Fukuzumi, S.; Kamat, P. V. Light energy conversion using mixed molecular nanoclusters. Porphyrin and C60 cluster films for efficient photocurrent generation. *Journal of Physical Chemistry B* **2003**, *107*, 12105-12112.

- (12) Venkatasubramanian, R.; Siivola, E.; Colpitts, T.; O'Quinn, B. Thin-film thermoelectric devices with high room-temperature figures of merit. *Nature* **2001**, *413*, 597-602.
- (13) Lloyd, S. M.; Lave, L. B. Life cycle economic and environmental implications of using nanocomposites in automobiles. *Environmental Science and Technology* **2003**, *37*, 3458-3466.
- (14) Hahm, J. i.; Lieber, C. M. Direct ultrasensitive electrical detection of DNA and DNA sequence variations using nanowire nanosensors. *Nano Letters* **2004**, *4*, 51-54.
- (15) Nel, A.; Xia, T.; Maedler, L.; Li, N. Toxic potential of materials at the nanolevel. *Science* **2006**, *311*, 622-627.
- (16) "Approaches to safe nanotechnology: an information exchange with NIOSH," Centers for Disease Control and Prevention, National Institute for Occupational Health and Safety, 2005.
- (17) Chithrani, B. D.; Ghazani, A. A.; Chan, W. C. W. Determining the size and shape dependence of gold nanoparticle uptake into mammalian cells. *Nano Letters* **2006**, *6*, 662-668.
- (18) Magrez, A.; Kasas, S.; Salicio, V.; Pasquier, N.; Seo, J. W.; Celio, M.; Catsicas, S.; Schwaller, B.; Forro, L. Cellular toxicity of carbon-based nanomaterials. *Nano Letters* **2006**, *6*, 1121-1125.
- (19) Colvin, V. L. The potential environmental impact of engineered nanomaterials. *Nature Biotechnology* **2003**, *21*, 1166-1170.
- (20) Science Policy Council, U. S. E. P. A. "U.S. Environmental Protection Agency External Review Draft, Nanotechnology White Paper," 2005.
- (21) Pernodet, N.; Fang, X.; Sun, Y.; Bakhtina, A.; Ramakrishnan, A.; Sokolov, J.; Ulman, A.; Rafailovich, M. Adverse effects of citrate/gold nanoparticles on human dermal fibroblasts. *Small* **2006**, *2*, 766-773.
- (22) Derfus, A. M.; Chan, W. C. W.; Bhatia, S. N. Probing the cytotoxicity of semiconductor quantum dots. *Nano Letters* **2004**, *4*, 11-18.
- (23) Hurt, R. H.; Monthieux, M.; Kane, A. Toxicology of carbon nanomaterials: Status, trends, and perspectives on the special issue. *Carbon* **2006**, *44*, 1028-1033.
- (24) Bekyarova, E.; Ni, Y.; Malarkey, E. B.; Montana, V.; McWilliams, J. L.; Haddon, R. C.; Parpura, V. Applications of carbon nanotubes in biotechnology and biomedicine. *Journal of Biomedical Nanotechnology* **2005**, *1*, 3-17.

- (25) Metals and colloids in urban runoff; Wiesner, M. R.; Characklis, G. W.; Brejchova, D., Eds.; Ann Arbor Press: Chelsea, Mich., 1998.
- (26) Oberdorster, E. Manufactured nanomaterials (fullerenes, C60) induce oxidative stress in the brain of juvenile largemouth bass. *Environmental Health Perspectives* **2004**, *112*, 1058-1062.
- (27) Oberdorster, G.; Oberdorster, E.; Oberdorster, J. Nanotoxicology: an emerging discipline evolving from studies of ultrafine particles. *Environmental Health Perspectives* **2005**, *113*, 823-839.
- (28) Weare, W. W.; Reed, S. M.; Warner, M. G.; Hutchison, J. E. Improved synthesis of small (dCORE ~ 1.5 nm) phosphine-stabilized gold nanoparticles. *Journal of the American Chemical Society* **2000**, *122*, 12890-12891.
- (29) Gardea-Torresdey, J. L.; Parsons, J. G.; Gomez, E.; Peralta-Videa, J.; Troiani, H. E.; Santiago, P.; Yacaman, M. J. Formation and growth of Au nanoparticles inside live alfalfa plants. *Nano Letters* **2002**, *2*, 397-401.
- (30) Mello, J. d.; Mello, A. d. Microscale reactors: nanoscale products. *Lab on a Chip* **2004**, *4*, 11N-15N.
- (31) Turkevich, J.; Stevenson, P. C.; Hillier, J. The nucleation and growth processes in the synthesis of colloidal gold. *Discussions of the Faraday Society* **1951**, No. 11, 55-75.
- (32) Turkevich, J.; Stevenson, P. C.; Hillier, J. The formation of colloidal gold. *Journal of Physical Chemistry* **1953**, *57*, 670-673.
- (33) Glomm, W. R. Functionalized gold nanoparticles for applications in bionanotechnology. *Journal of Dispersion Science and Technology* **2005**, *26*, 389-414.
- (34) Pillai, Z. S.; Kamat, P. V. What factors control the size and shape of silver nanoparticles in the citrate ion reduction method? *Journal of Physical Chemistry B* **2004**, *108*, 945-951.
- (35) Chen, S.; Templeton, A. C.; Murray, R. W. Monolayer-protected cluster growth dynamics. *Langmuir* **2000**, *16*, 3543-3548.
- (36) Donkers, R. L.; Lee, D.; Murray, R. W. Synthesis and isolation of the molecule-like cluster Au₃₈(PhCH₂CH₂S)₂₄. *Langmuir* **2004**, *20*, 1945-1952.
- (37) Jimenez, V. L.; Georganopoulou, D. G.; White, R. J.; Harper, A. S.; Mills, A. J.; Lee, D.; Murray, R. W. Hexanethiolate monolayer protected 38 gold atom cluster. *Langmuir* **2004**, *20*, 6864-6870.

- (38) Kanaras, A. G.; Kamounah, F. S.; Schaumburg, K.; Kiely, C. J.; Brust, M. Thioalkylated tetraethylene glycol: a new ligand for water soluble monolayer protected gold clusters. *Chemical Communications* **2002**, 2294-2295.
- (39) Tshikhudo, T. R.; Wang, Z.; Brust, M. Biocompatible gold nanoparticles. *Materials Science and Technology* **2004**, *20*, 980-984.
- (40) Templeton, A. C.; Cliffler, D. E.; Murray, R. W. Redox and fluorophore functionalization of water-soluble, tiopronin-protected gold clusters. *Journal of the American Chemical Society* **1999**, *121*, 7081-7089.
- (41) Chen, S.; Kimura, K. Synthesis and characterization of carboxylate-modified gold nanoparticle powders dispersible in water. *Langmuir* **1999**, *15*, 1075-1082.
- (42) Pengo, P.; Polizzi, S.; Battagliarin, M.; Pasquato, L.; Scrimin, P. Synthesis, characterization and properties of water-soluble gold nanoparticles with tunable core size. *Journal of Materials Chemistry* **2003**, *13*, 2471-2478.
- (43) Selvakannan, P. R.; Mandal, S.; Phadtare, S.; Pasricha, R.; Sastry, M. Capping of gold nanoparticles by the amino acid lysine renders them water-dispersible. *Langmuir* **2003**, *19*, 3545-3549.
- (44) Fabris, L.; Antonello, S.; Armelao, L.; Donkers, R. L.; Polo, F.; Toniolo, C.; Maran, F. Gold nanoclusters protected by conformationally constrained peptides. *Journal of the American Chemical Society* **2006**, *128*, 326-336.
- (45) Paulini, R.; Frankamp, B. L.; Rotello, V. M. Effects of branched ligands on the structure and stability of monolayers on gold nanoparticles. *Langmuir* **2002**, *18*, 2368-2373.
- (46) Higashi, N.; Kawahara, J.; Niwa, M. Preparation of helical peptide monolayer-coated gold nanoparticles. *Journal of Colloid and Interface Science* **2005**, *288*, 83-87.
- (47) Rowe, M. P.; Plass, K. E.; Kim, K.; Kurdak, C.; Zellers, E. T.; Matzger, A. J. Single-phase synthesis of functionalized gold nanoparticles. *Chemistry of Materials* **2004**, *16*, 3513-3517.
- (48) Latham, A. H.; Williams, M. E. Versatile routes toward functional, water-soluble nanoparticles via trifluoroethyl ester-PEG-thiol ligands. *Langmuir* **2006**, *22*, 4319-4326.
- (49) Yang, J.; Lee, J. Y.; Deivaraj, T. C.; Too, H.-P. An improved procedure for preparing smaller and nearly monodispersed thiol-stabilized platinum nanoparticles. *Langmuir* **2003**, *19*, 10361-10365.

- (50) Eklund, S. E.; Cliffel, D. E. Synthesis and catalytic properties of soluble platinum nanoparticles protected by a thiol monolayer. *Langmuir* **2004**, *20*, 6012-6018.
- (51) Mallikarjuna, N. N.; Varma, R. S. Microwave-assisted shape-controlled bulk synthesis of noble nanocrystals and their catalytic properties. *Crystal Growth and Design* **2007**, *7*, 686-690.
- (52) Jana, N. R.; Peng, X. Single-phase and gram-scale routes toward nearly monodisperse Au and other noble metal nanocrystals. *Journal of the American Chemical Society* **2003**, *125*, 14280-14281.
- (53) Hiramatsu, H.; Osterloh, F. E. A simple large-scale synthesis of nearly monodisperse gold and silver nanoparticles with adjustable sizes and with exchangeable surfactants. *Chemistry of Materials* **2004**, *16*, 2509-2511.
- (54) Aslam, M.; Fu, L.; Su, M.; Vijayamohan, K.; Dravid, V. P. Novel one-step synthesis of amine-stabilized aqueous colloidal gold nanoparticles. *Journal of Materials Chemistry* **2004**, *14*, 1795-1797.
- (55) Schmid, G. Hexachlorododecakis(triphenylphosphine)pentapentacontagold, Au₅₅[P(C₆H₅)₃]₁₂Cl₆. *Inorganic Syntheses* **1990**, *27*, 214-218.
- (56) Schmid, G.; Klein, N.; Korste, L.; Kreibitz, U.; Schoenauer, D. Large transition metal clusters-VI. Ligand exchange reactions on the gold triphenylphosphine chloro cluster, Au₅₅(PPh₃)₁₂Cl₆ - the formation of a water soluble gold (Au₅₅) cluster. *Polyhedron* **1988**, *7*, 605-608.
- (57) Schmid, G.; Pfeil, R.; Boese, R.; Brandermann, F.; Meyer, S.; Calis, G. H. M.; Van der Velden, J. W. A. Au₅₅[P(C₆H₅)₃]₁₂Cl₆ - a gold cluster of unusual size. *Chemische Berichte* **1981**, *114*, 3634-3642.
- (58) Hutchison, J. E.; Foster, E. W.; Warner, M. G.; Reed, S. M.; Weare, W. W.; Buhro, W.; Yu, H. Cluster and polynuclear compounds. Triphenylphosphine-stabilized gold nanoparticles. *Inorganic Syntheses* **2004**, *34*, 228-232.
- (59) Brown, K. R.; Natan, M. J. Hydroxylamine seeding of colloidal Au nanoparticles in solution and on surfaces. *Langmuir* **1998**, *14*, 726-728.
- (60) Brown, K. R.; Walter, D. G.; Natan, M. J. Seeding of colloidal Au nanoparticle solutions. 2. Improved control of particle size and shape. *Chemistry of Materials* **2000**, *12*, 306-313.
- (61) Sau, T. K.; Pal, A.; Jana, N. R.; Wang, Z. L.; Pal, T. Size controlled synthesis of gold nanoparticles using photochemically prepared seed particles. *Journal of Nanoparticle Research* **2001**, *3*, 257-261.

- (62) Sun, Y.; Xia, Y. Gold and silver nanoparticles: a class of chromophores with colors tunable in the range from 400 to 750 nm. *The Analyst* **2003**, *128*, 686-691.
- (63) Mieszawska, A. J.; Zamborini, F. P. Gold nanorods grown directly on surfaces from microscale patterns of gold seeds. *Chemistry of Materials* **2005**, *17*, 3415-3420.
- (64) Mieszawska, A. J.; Jalilian, R.; Sumanasekera, G. U.; Zamborini, F. P. Synthesis of gold nanorod/single-wall carbon nanotube heterojunctions directly on surfaces. *Journal of the American Chemical Society* **2005**, *127*, 10822-10823.
- (65) Perez-Juste, J.; Liz-Marzan, L. M.; Carnie, S.; Chan, D. Y. C.; Mulvaney, P. Electric-field-directed growth of gold nanorods in aqueous surfactant solutions. *Advanced Functional Materials* **2004**, *14*, 571-579.
- (66) Johnson, C. J.; Dujardin, E.; Davis, S. A.; Murphy, C. J.; Mann, S. Growth and form of gold nanorods prepared by seed-mediated, surfactant-directed synthesis. *Journal of Materials Chemistry* **2002**, *12*, 1765-1770.
- (67) Nikoobakht, B.; El-Sayed, M. A. Preparation and growth mechanism of gold nanorods (NRs) using seed-mediated growth method. *Chemistry of Materials* **2003**, *15*, 1957-1962.
- (68) Kuo, C.-H.; Chiang, T.-F.; Chen, L.-J.; Huang, M. H. Synthesis of highly faceted pentagonal- and hexagonal-shaped gold nanoparticles with controlled sizes by sodium dodecyl sulfate. *Langmuir* **2004**, *20*, 7820-7824.
- (69) Jana, N. R. Gram-scale synthesis of soluble, near-monodisperse gold nanorods and other anisotropic nanoparticles. *Small* **2005**, *1*, 875-882.
- (70) Gole, A.; Murphy, C. J. Seed-mediated synthesis of gold nanorods: role of the size and nature of the seed. *Chemistry of Materials* **2004**, *16*, 3633-3640.
- (71) Sau, T. K.; Murphy, C. J. Room temperature, high-yield synthesis of multiple shapes of gold nanoparticles in aqueous solution. *Journal of the American Chemical Society* **2004**, *126*, 8648-8649.
- (72) Millstone, J. E.; Park, S.; Shuford, K. L.; Qin, L.; Schatz, G. C.; Mirkin, C. A. Observation of a quadrupole plasmon mode for a colloidal solution of gold nanoprisms. *Journal of the American Chemical Society* **2005**, *127*, 5312-5313.
- (73) Pei, L.; Mori, K.; Adachi, M. Formation process of two-dimensional networked gold nanowires by citrate reduction of AuCl₄⁻ and the shape stabilization. *Langmuir* **2004**, *20*, 7837-7843.

- (74) Pei, L.; Mori, K.; Adachi, M. Direct chemical synthesis of gold nanowires with 2-D network structure and relationship between the presence of gold ions and shape stability of gold nanowires. *Chemistry Letters* **2004**, *33*, 324-325.
- (75) Hao, E.; Bailey, R. C.; Schatz, G. C.; Hupp, J. T.; Li, S. Synthesis and optical properties of "branched" gold nanocrystals. *Nano Letters* **2004**, *4*, 327-330.
- (76) Chu, H.-C.; Kuo, C.-H.; Huang, M. H. Thermal aqueous solution approach for the synthesis of triangular and hexagonal gold nanoplates with three different size ranges. *Inorganic Chemistry* **2006**, *45*, 808-813.
- (77) Caswell, K. K.; Bender, C. M.; Murphy, C. J. Seedless, surfactantless wet chemical synthesis of silver nanowires. *Nano Letters* **2003**, *3*, 667-669.
- (78) Swami, A.; Kumar, A.; D'Costa, M.; Pasricha, R.; Sastry, M. Variation in morphology of gold nanoparticles synthesized by the spontaneous reduction of aqueous chloroaurate ions by alkylated tyrosine at a liquid-liquid and air-water interface. *Journal of Materials Chemistry* **2004**, *14*, 2696-2702.
- (79) Wiley, B.; Herricks, T.; Sun, Y.; Xia, Y. Polyol synthesis of silver nanoparticles: use of chloride and oxygen to promote the formation of single-crystal, truncated cubes and tetrahedrons. *Nano Letters* **2004**, *4*, 1733-1739.
- (80) Kan, C.; Zhu, X.; Wang, G. Single-crystalline gold microplates: synthesis, characterization, and thermal stability. *Journal of Physical Chemistry B* **2006**, *110*, 4651-4656.
- (81) Brown, L. O.; Hutchison, J. E. Controlled growth of gold nanoparticles during ligand exchange. *Journal of the American Chemical Society* **1999**, *121*, 882-883.
- (82) Teranishi, T.; Hasegawa, S.; Shimizu, T.; Miyake, M. Heat-induced size evolution of gold nanoparticles in the solid state. *Advanced Materials* **2001**, *13*, 1699-1701.
- (83) Shimizu, T.; Teranishi, T.; Hasegawa, S.; Miyake, M. Size evolution of alkanethiol-protected gold nanoparticles by heat treatment in the solid state. *Journal of Physical Chemistry B* **2003**, *107*, 2719-2724.
- (84) Kim, K.-H.; Yamada, M.; Park, D.-W.; Miyake, M. Particle size control of 11-mercaptoundecanoic acid-protected Au nanoparticles by using heat-treatment method. *Chemistry Letters* **2004**, *33*, 344-345.
- (85) Xiong, Y.; Chen, J.; Wiley, B.; Xia, Y.; Yin, Y.; Li, Z.-Y. Size-dependence of surface plasmon resonance and oxidation for Pd nanocubes synthesized via a seed etching process. *Nano Letters* **2005**, *5*, 1237-1242.

- (86) Tsung, C.-K.; Kou, X.; Shi, Q.; Zhang, J.; Yeung, M. H.; Wang, J.; Stucky, G. D. Selective shortening of single-crystalline gold nanorods by mild oxidation. *Journal of the American Chemical Society* **2006**, *128*, 5352-5353.
- (87) Kim, J.-U.; Cha, S.-H.; Shin, K.; Jho, J. Y.; Lee, J.-C. Synthesis of gold nanoparticles from gold(I)-alkanethiolate complexes with supramolecular structures through electron beam irradiation in TEM. *Journal of the American Chemical Society* **2005**, *127*, 9962-9963.
- (88) Yamamoto, M.; Nakamoto, M. New type of monodispersed gold nanoparticles capped by myristate and PPh₃ ligands prepared by controlled thermolysis of [Au(C₁₃H₂₇COO)(PPh₃)]. *Chemistry Letters* **2003**, *32*, 452-453.
- (89) Zhang, L.; Shen, Y.; Xie, A.; Li, S.; Jin, B.; Zhang, Q. One-step synthesis of monodisperse silver nanoparticles beneath vitamin E Langmuir monolayers. *Journal of Physical Chemistry B* **2006**, *110*, 6615-6620.
- (90) Kearns, G. J.; Foster, E. W.; Hutchison, J. E. Substrates for direct imaging of chemically functionalized SiO₂ surfaces by transmission electron microscopy. *Analytical Chemistry* **2006**, *78*, 298-303.
- (91) Schaaff, T. G.; Whetten, R. L. Controlled etching of Au : SR cluster compounds. *Journal of Physical Chemistry B* **1999**, *103*, 9394-9396.
- (92) Sweeney, S. F.; Woehrle, G. H.; Hutchison, J. E. Rapid purification and size separation of gold nanoparticles via diafiltration. *Journal of the American Chemical Society* **2006**, *128*, 3190-3197.
- (93) Murphy, R.; Coleman, J. N.; Cadek, M.; McCarthy, B.; Bent, M.; Drury, A.; Barklie, R. C.; Blau, W. J. High-yield, nondestructive purification and quantification method for multi-walled carbon nanotubes. *Journal of Physical Chemistry B* **2002**, *106*, 3087-3091.
- (94) Erne, B. H.; Van den Pol, E.; Vroege, G. J.; Visser, T.; Wensink, H. H. Size fractionation in a phase-separated colloidal fluid. *Langmuir* **2005**, *21*, 1802-1805.
- (95) Rodriguez-Fernandez, J.; Perez-Juste, J.; Garcia de Abajo, F. J.; Liz-Marzan, L. M. Seeded growth of submicron Au colloids with quadrupole plasmon resonance modes. *Langmuir* **2006**, *22*, 7007-7010.
- (96) An, K. H.; Park, J. S.; Yang, C.-M.; Jeong, S. Y.; Lim, S. C.; Kang, C.; Son, J.-H.; Jeong, M. S.; Lee, Y. H. A diameter-selective attack of metallic carbon nanotubes by nitronium ions. *Journal of the American Chemical Society* **2005**, *127*, 5196-5203.

- (97) Shi, J.; Verweij, H. Synthesis and purification of oxide nanoparticle dispersions by modified emulsion precipitation. *Langmuir* **2005**, *21*, 5570-5575.
- (98) Woehrle, G. H.; Hutchison, J. E. Thiol-functionalized undecagold clusters by ligand exchange: synthesis, mechanism, and properties. *Inorganic Chemistry* **2005**, *44*, 6149-6158.
- (99) Park, T.-J.; Banerjee, S.; Hemraj-Benny, T.; Wong, S. S. Purification strategies and purity visualization techniques for single-walled carbon nanotubes. *Journal of Materials Chemistry* **2006**, *16*, 141-154.
- (100) Al-Somali, A. M.; Krueger, K. M.; Falkner, J. C.; Colvin, V. L. Recycling size exclusion chromatography for the analysis and separation of nanocrystalline gold. *Analytical Chemistry* **2004**, *76*, 5903-5910.
- (101) Sperling, R. A.; Pellegrino, T.; Li, J. K.; Chang, W. H.; Parak, W. J. Electrophoretic separation of nanoparticles with a discrete number of functional groups. *Advanced Functional Materials* **2006**, *16*, 943-948.
- (102) Dalwadi, G.; Benson, H. A. E.; Chen, Y. Comparison of diafiltration and tangential flow filtration for purification of nanoparticle suspensions. *Pharmaceutical Research* **2005**, *22*, 2152-2162.
- (103) Kim, Y.; Luzzi, D. E. Purification of pulsed laser synthesized single wall carbon nanotubes by magnetic filtration. *Journal of Physical Chemistry B* **2005**, *109*, 16636-16643.
- (104) Peng, X. Green chemical approaches toward high-quality semiconductor nanocrystals. *Chemistry- A European Journal* **2002**, *8*, 334-339.
- (105) Zhang, Q.; Gupta, S.; Emrick, T.; Russell, T. P. Surface-functionalized CdSe nanorods for assembly in diblock copolymer templates. *Journal of the American Chemical Society* **2006**, *128*, 3898-3899.
- (106) Ludolph, B.; Malik, M. A. Novel single molecule precursor routes for the direct synthesis of highly monodispersed quantum dots of cadmium or zinc sulfide or selenide. *Chemical Communications* **1998**, 1849-1850.
- (107) Mekis, I.; Talapin, D. V.; Kornowski, A.; Haase, M.; Weller, H. One-pot synthesis of highly luminescent CdSe/CdS core-shell nanocrystals via organometallic and "greener" chemical approaches. *Journal of Physical Chemistry B* **2003**, *107*, 7454-7462.

- (108) Bao, C.; Jin, M.; Lu, R.; Xue, P.; Zhang, Q.; Wang, D.; Zhao, Y. Surfactant-ligand co-assisted solvothermal technique for the synthesis of different-shaped CdS nanorod-based materials. *Journal of Solid State Chemistry* **2003**, *175*, 322-327.
- (109) Querner, C.; Reiss, P.; Bleuse, J.; Pron, A. Chelating ligands for nanocrystals' surface functionalization. *Journal of the American Chemical Society* **2004**, *126*, 11574-11582.
- (110) Asokan, S.; Krueger, K. M.; Alkhawaldeh, A.; Carreon, A. R.; Mu, Z.; Colvin, V. L.; Mantzaris, N. V.; Wong, M. S. The use of heat transfer fluids in the synthesis of high-quality CdSe quantum dots, core/shell quantum dots, and quantum rods. *Nanotechnology* **2005**, *16*, 2000-2011.
- (111) Li, L. S.; Pradhan, N.; Wang, Y.; Peng, X. High quality ZnSe and ZnS nanocrystals formed by activating zinc carboxylate precursors. *Nano Letters* **2004**, *4*, 2261-2264.
- (112) Deng, Z.; Cao, L.; Tang, F.; Zou, B. A new route to zinc-blende CdSe nanocrystals: mechanism and synthesis. *Journal of Physical Chemistry B* **2005**, *109*, 16671-16675.
- (113) Hirai, T.; Watanabe, T.; Komasaawa, I. Preparation of semiconductor nanoparticle-polymer composites by direct reverse micelle polymerization using polymerizable surfactants. *Journal of Physical Chemistry B* **2000**, *104*, 8962-8966.
- (114) Li, Q.; Kumar, V.; Li, Y.; Zhang, H.; Marks, T. J.; Chang, R. P. H. Fabrication of ZnO nanorods and nanotubes in aqueous solutions. *Chemistry of Materials* **2005**, *17*, 1001-1006.
- (115) Zhang, D.-F.; Sun, L.-D.; Yin, J.-L.; Yan, C.-H.; Wang, R.-M. Attachment-driven morphology evolution of rectangular ZnO nanowires. *Journal of Physical Chemistry B* **2005**, *109*, 8786-8790.
- (116) Zhao, Y.; Kwon, Y.-U. Templateless hydrothermal synthesis of aligned ZnO nanorods. *Chemistry Letters* **2004**, *33*, 1578-1579.
- (117) Kar, S.; Pal, B. N.; Chaudhuri, S.; Chakravorty, D. One-dimensional ZnO nanostructure arrays: synthesis and characterization. *Journal of Physical Chemistry B* **2006**, *110*, 4605-4611.
- (118) Ngomsik, A. F. B., A.; Draye, M.; Cote, G.; Cabuil, V. Magnetic nano- and microparticles for metal removal and environmental applications: a review. *Comptes Rendus Chimie* **2005**, *8*, 963-970.

- (119) Lin, C.-R.; Chu, Y.-M.; Wang, S.-C. Magnetic properties of magnetite nanoparticles prepared by mechanochemical reaction. *Materials Letters* **2006**, *60*, 447-450.
- (120) Yaacob, I. I.; Nunes, A. C.; Bose, A. Magnetic nanoparticles produced in spontaneous cationic-anionic vesicles: room temperature synthesis and characterization. *Journal of Colloid and Interface Science* **1995**, *171*, 73-84.
- (121) Li, Y.; Cai, W.; Duan, G.; Sun, F.; Cao, B.; Lu, F. 2D nanoparticle arrays by partial dissolution of ordered pore films. *Materials Letters* **2004**, *59*, 276-279.
- (122) Yu, S.; Chow, G. M. Carboxyl group (-CO₂H) functionalized ferrimagnetic iron oxide nanoparticles for potential bioapplications. *Journal of Materials Chemistry* **2004**, *14*, 2781-2786.
- (123) Lyon, J. L.; Fleming, D. A.; Stone, M. B.; Schiffer, P.; Williams, M. E. Synthesis of Fe oxide core/Au shell nanoparticles by iterative hydroxylamine seeding. *Nano Letters* **2004**, *4*, 719-723.
- (124) Frankamp, B. L.; Fischer, N. O.; Hong, R.; Srivastava, S.; Rotello, V. M. Surface modification using cubic silsesquioxane ligands. Facile synthesis of water-soluble metal oxide nanoparticles. *Chemistry of Materials* **2006**, *18*, 956-959.
- (125) Wang, L.; Yang, Z.; Gao, J.; Xu, K.; Gu, H.; Zhang, B.; Zhang, X.; Xu, B. A biocompatible method of decorporation: bisphosphonate-modified magnetite nanoparticles to remove uranyl ions from blood. *Journal of the American Chemical Society* **2006**, *128*, 13358-13359.
- (126) Esumi, K.; Sarashina, S.; Yoshimura, T. Synthesis of gold nanoparticles from an organometallic compound in supercritical carbon dioxide. *Langmuir* **2004**, *20*, 5189-5191.
- (127) Shah, P. S.; Hanrath, T.; Johnston, K. P.; Korgel, B. A. Nanocrystal and nanowire synthesis and dispersibility in supercritical fluids. *Journal of Physical Chemistry B* **2004**, *108*, 9574-9587.
- (128) Stallings, W. E.; Lamb, H. H. Synthesis of nanostructured titania powders via hydrolysis of titanium isopropoxide in supercritical carbon dioxide. *Langmuir* **2003**, *19*, 2989-2994.
- (129) Ziegler, K. J.; Doty, R. C.; Johnston, K. P.; Korgel, B. A. Synthesis of organic monolayer-stabilized copper nanocrystals in supercritical water. *Journal of the American Chemical Society* **2001**, *123*, 7797-7803.

- (130) Wang, J.; Zhang, C.; Liu, Z.; Ding, K.; Yang, Z. A simple and efficient route to prepare inorganic compound/polymer composites in supercritical fluids. *Macromolecular Rapid Communications* **2006**, *27*, 787-792.
- (131) Ohde, H.; Hunt, F.; Wai, C. M. Synthesis of silver and copper nanoparticles in a water-in-supercritical-carbon dioxide microemulsion. *Chemistry of Materials* **2001**, *13*, 4130-4135.
- (132) Liu, J.; Anand, M.; Roberts, C. B. Synthesis and extraction of b-D-glucose-stabilized Au nanoparticles processed into low-defect, wide-area thin films and ordered arrays using CO₂-expanded liquids. *Langmuir* **2006**, *22*, 3964-3971.
- (133) Pessey, V.; Garriga, R.; Weill, F.; Chevalier, B.; Etourneau, J.; Cansell, F. Control of particle growth by chemical transformation in supercritical CO₂/ethanol mixtures. *Journal of Materials Chemistry* **2002**, *12*, 958-965.
- (134) Johnson, C. A.; Sharma, S.; Subramaniam, B.; Borovik, A. S. Nanoparticulate metal complexes prepared with compressed carbon dioxide: correlation of particle morphology with precursor structure. *Journal of the American Chemical Society* **2005**, *127*, 9698-9699.
- (135) Strauss, S. H. The search for larger and more weakly coordinating anions. *Chemical Reviews* **1993**, *93*, 927-942.
- (136) Kim, K.-S.; Demberelnyamba, D.; Lee, H. Size-selective synthesis of gold and platinum nanoparticles using novel thiol-functionalized ionic liquids. *Langmuir* **2004**, *20*, 556-560.
- (137) Tatumi, R.; Fujihara, H. Remarkably stable gold nanoparticles functionalized with a zwitterionic liquid based on imidazolium sulfonate in a high concentration of aqueous electrolyte and ionic liquid. *Chemical Communications* **2005**, 83-85.
- (138) Itoh, H.; Naka, K.; Chujo, Y. Synthesis of gold nanoparticles modified with ionic liquid based on the imidazolium cation. *Journal of the American Chemical Society* **2004**, *126*, 3026-3027.
- (139) Li, Z.; Liu, Z.; Zhang, J.; Han, B.; Du, J.; Gao, Y.; Jiang, T. Synthesis of single-crystal gold nanosheets of large size in ionic liquids. *Journal of Physical Chemistry B* **2005**, *109*, 14445-14448.
- (140) Kim, K.-S.; Choi, S.; Cha, J.-H.; Yeon, S.-H.; Lee, H. Facile one-pot synthesis of gold nanoparticles using alcohol ionic liquids. *Journal of Materials Chemistry* **2006**, *16*, 1315-1317.

- (141) Wang, Y.; Yang, H. Oleic acid as the capping agent in the synthesis of noble metal nanoparticles in imidazolium-based ionic liquids. *Chemical Communications* **2006**, 2545-2547.
- (142) Scheeren, C. W.; Machado, G.; Teixeira, S. R.; Morais, J.; Domingos, J. B.; Dupont, J. Synthesis and characterization of Pt(0) nanoparticles in imidazolium ionic liquids. *Journal of Physical Chemistry B* **2006**, *110*, 13011-13020.
- (143) Scheeren, C. W.; Machado, G.; Dupont, J.; Fichtner, P. F. P.; Teixeira, S. R. Nanoscale Pt(0) particles prepared in imidazolium room temperature ionic liquids: synthesis from an organometallic precursor, characterization, and catalytic properties in hydrogenation reactions. *Inorganic Chemistry* **2003**, *42*, 4738-4742.
- (144) Zhao, Z. W.; Guo, Z. P.; Ding, J.; Wexler, D.; Ma, Z. F.; Zhang, D. Y.; Liu, H. K. Novel ionic liquid supported synthesis of platinum-based electrocatalysts on multiwalled carbon nanotubes. *Electrochemistry Communications* **2006**, *8*, 245-250.
- (145) Antonietti, M.; Kuang, D.; Smarsly, B.; Zhou, Y. Ionic liquids for the convenient synthesis of functional nanoparticles and other inorganic nanostructures. *Angewandte Chemie, International Edition* **2004**, *43*, 4988-4992.
- (146) Nakashima, T.; Kimizuka, N. Interfacial synthesis of hollow TiO₂ microspheres in ionic liquids. *Journal of the American Chemical Society* **2003**, *125*, 6386-6387.
- (147) Yoo, K.; Choi, H.; Dionysiou, D. D. Ionic liquid assisted preparation of nanostructured TiO₂ particles. *Chemical Communications* **2004**, 2000-2001.
- (148) Zhou, X.; Xie, Z.-X.; Jiang, Z.-Y.; Kuang, Q.; Zhang, S.-H.; Xu, T.; Huang, R.-B.; Zheng, L.-S. Formation of ZnO hexagonal micro-pyramids: a successful control of the exposed polar surfaces with the assistance of an ionic liquid. *Chemical Communications* **2005**, 5572-5574.
- (149) Chen, L. J.; Zhang, S. M.; Wu, Z. S.; Zhang, Z. J.; Dang, H. X. Preparation of PbS-type PbO nanocrystals in a room-temperature ionic liquid. *Materials Letters* **2005**, *59*, 3119-3121.
- (150) Yang, L.-X.; Zhu, Y.-J.; Wang, W.-W.; Tong, H.; Ruan, M.-L. Synthesis and formation mechanism of nanoneedles and nanorods of manganese oxide octahedral molecular sieve using an ionic liquid. *Journal of Physical Chemistry B* **2006**, *110*, 6609-6614.
- (151) Wang, Y.; Yang, H. Synthesis of CoPt nanorods in ionic liquids. *Journal of the American Chemical Society* **2005**, *127*, 5316-5317.

- (152) Jiang, J.; Yu, S.-H.; Yao, W.-T.; Ge, H.; Zhang, G.-Z. Morphogenesis and crystallization of Bi₂S₃ nanostructures by an ionic liquid-assisted templating route: synthesis, formation mechanism, and properties. *Chemistry of Materials* **2005**, *17*, 6094-6100.
- (153) Jacob, D. S.; Bitton, L.; Grinblat, J.; Felner, I.; Koltypin, Y.; Gedanken, A. Are ionic liquids really a boon for the synthesis of inorganic materials? A general method for the fabrication of nanosized metal fluorides. *Chemistry of Materials* **2006**, *18*, 3162-3168.
- (154) Nuss, S.; Bottcher, H.; Wurm, H.; Hallensleben, M. L. Gold nanoparticles with covalently attached polymer chains. *Angewandte Chemie, International Edition* **2001**, *40*, 4016-4018.
- (155) Kamata, K.; Lu, Y.; Xia, Y. Synthesis and characterization of monodispersed core-shell spherical colloids with movable cores. *Journal of the American Chemical Society* **2003**, *125*, 2384-2385.
- (156) Li, D.; Jones, G. L.; Dunlap, J. R.; Hua, F.; Zhao, B. Thermosensitive hairy hybrid nanoparticles synthesized by surface-initiated atom transfer radical polymerization. *Langmuir* **2006**, *22*, 3344-3351.
- (157) Mangeney, C.; Ferrage, F.; Aujard, I.; Marchi-Artzner, V.; Jullien, L.; Ouari, O.; Rekaie, E. D.; Laschewsky, A.; Vikholm, I.; Sadowski, J. W. Synthesis and properties of water-soluble gold colloids covalently derivatized with neutral polymer monolayers. *Journal of the American Chemical Society* **2002**, *124*, 5811-5821.
- (158) Liu, S.; Han, M. Synthesis, functionalization, and bioconjugation of monodisperse, silica-coated gold nanoparticles: Robust bioprobes. *Advanced Functional Materials* **2005**, *15*, 961-967.
- (159) Prasad, B. L. V.; Arumugam, S. K.; Bala, T.; Sastry, M. Solvent-adaptable silver nanoparticles. *Langmuir* **2005**, *21*, 822-826.
- (160) Huang, J.; He, C.; Liu, X.; Xiao, Y.; Mya, K. Y.; Chai, J. Formation and characterization of water-soluble platinum nanoparticles using a unique approach based on the hydrosilylation reaction. *Langmuir* **2004**, *20*, 5145-5148.
- (161) Templeton, A. C.; Hostetler, M. J.; Kraft, C. T.; Murray, R. W. Reactivity of monolayer-protected gold cluster molecules: steric effects. *Journal of the American Chemical Society* **1998**, *120*, 1906-1911.

- (162) Templeton, A. C.; Hostetler, M. J.; Warmoth, E. K.; Chen, S.; Hartshorn, C. M.; Krishnamurthy, V. M.; Forbes, M. D. E.; Murray, R. W. Gateway reactions to diverse, polyfunctional monolayer-protected gold clusters. *Journal of the American Chemical Society* **1998**, *120*, 4845-4849.
- (163) Dai, Q.; Worden James, G.; Trullinger, J.; Huo, Q. A "nanonecklace" synthesized from monofunctionalized gold nanoparticles. *Journal of the American Chemical Society* **2005**, *127*, 8008-8009.
- (164) Kell, A. J.; Donkers, R. L.; Workentin, M. S. Core size effects on the reactivity of organic substrates as monolayers on gold nanoparticles. *Langmuir* **2005**, *21*, 735-742.
- (165) Hua, F.; Swihart, M. T.; Ruckenstein, E. Efficient surface grafting of luminescent silicon quantum dots by photoinitiated hydrosilylation. *Langmuir* **2005**, *21*, 6054-6062.
- (166) Woehrle, G. H.; Warner, M. G.; Hutchison, J. E. Molecular-level control of feature separation in one-dimensional nanostructure assemblies formed by biomolecular nanolithography. *Langmuir* **2004**, *20*, 5982-5988.
- (167) Warner, M. G.; Hutchison, J. E. Linear assemblies of nanoparticles electrostatically organized on DNA scaffolds. *Nature Materials* **2003**, *2*, 272-277.
- (168) Woehrle, G. H.; Brown, L. O.; Hutchison, J. E. Thiol-functionalized, 1.5-nm gold nanoparticles through ligand exchange reactions: scope and mechanism of ligand exchange. *Journal of the American Chemical Society* **2005**, *127*, 2172-2183.
- (169) Balasubramanian, R.; Guo, R.; Mills, A. J.; Murray, R. W. Reaction of Au₅₅(PPh₃)₁₂Cl₆ with thiols yields thiolate monolayer protected Au₇₅ clusters. *Journal of the American Chemical Society* **2005**, *127*, 8126-8132.
- (170) Ionita, P.; Caragheorgheopol, A.; Gilbert, B. C.; Chechik, V. Mechanistic study of a place-exchange reaction of Au nanoparticles with spin-labeled disulfides. *Langmuir* **2004**, *20*, 11536-11544.
- (171) Warner, M. G.; Reed, S. M.; Hutchison, J. E. Small, water-soluble, ligand-stabilized gold nanoparticles synthesized by interfacial ligand exchange reactions. *Chemistry of Materials* **2000**, *12*, 3316-3320.
- (172) Jahn, W. Review: chemical aspects of the use of gold clusters in structural biology. *Journal of Structural Biology* **1999**, *127*, 106-112.
- (173) Schmid, G.; Baumle, M.; Beyer, N. Ordered two-dimensional monolayers of Au₅₅ clusters. *Angewandte Chemie, International Edition* **2000**, *39*, 181-183.

- (174) Petroski, J.; Chou, M. H.; Creutz, C. Rapid phosphine exchange on 1.5-nm gold nanoparticles. *Inorganic Chemistry* **2004**, *43*, 1597-1599.
- (175) Ingram, R. S.; Hostetler, M. J.; Murray, R. W. Poly-hetero-w-functionalized alkanethiolate-stabilized gold cluster compounds. *Journal of the American Chemical Society* **1997**, *119*, 9175-9178.
- (176) Hostetler, M. J.; Green, S. J.; Stokes, J. J.; Murray, R. W. Monolayers in three dimensions: synthesis and electrochemistry of w-functionalized alkanethiolate-stabilized gold cluster compounds. *Journal of the American Chemical Society* **1996**, *118*, 4212-4213.
- (177) Foos, E. E.; Snow, A. W.; Twigg, M. E. Synthesis and characterization of water soluble gold nanoclusters of varied core size. *Journal of Cluster Science* **2002**, *13*, 543-552.
- (178) Foos, E. E.; Snow, A. W.; Twigg, M. E.; Ancona, M. G. Thiol-terminated di-, tri-, and tetraethylene oxide functionalized gold nanoparticles: a water-soluble, charge-neutral cluster. *Chemistry of Materials* **2002**, *14*, 2401-2408.
- (179) Hong, R.; Fernandez, J. M.; Nakade, H.; Arvizo, R.; Emrick, T.; Rotello, V. M. In situ observation of place exchange reactions of gold nanoparticles. Correlation of monolayer structure and stability. *Chemical Communications* **2006**, 2347-2349.
- (180) Hostetler, M. J.; Templeton, A. C.; Murray, R. W. Dynamics of place-exchange reactions on monolayer-protected gold cluster molecules. *Langmuir* **1999**, *15*, 3782-3789.
- (181) Song, Y.; Murray, R. W. Dynamics and extent of ligand exchange depend on electronic charge of metal nanoparticles. *Journal of the American Chemical Society* **2002**, *124*, 7096-7102.
- (182) Guo, R.; Song, Y.; Wang, G.; Murray, R. W. Does core size matter in the kinetics of ligand exchanges of monolayer-protected Au clusters? *Journal of the American Chemical Society* **2005**, *127*, 2752-2757.
- (183) Worden, J. G.; Dai, Q.; Shaffer, A. W.; Huo, Q. Monofunctional group-modified gold nanoparticles from solid phase synthesis approach: solid support and experimental condition effect. *Chemistry of Materials* **2004**, *16*, 3746-3755.
- (184) Brown, L. O.; Hutchison, J. E. Formation and electron diffraction studies of ordered 2-D and 3-D superlattices of amine-stabilized gold nanocrystals. *Journal of Physical Chemistry B* **2001**, *105*, 8911-8916.

- (185) Berven, C. A.; Clark, L.; Mooster, J. L.; Wybourne, M. N.; Hutchison, J. E. Defect-tolerant single-electron charging at room temperature in metal nanoparticle decorated biopolymers. *Advanced Materials* **2001**, *13*, 109-113.
- (186) Brown, L. O.; Hutchison, J. E. Convenient preparation of stable, narrow-dispersity, gold nanocrystals by ligand exchange reactions. *Journal of the American Chemical Society* **1997**, *119*, 12384-12385.
- (187) Woehrle Gerd, H.; Brown Leif, O.; Hutchison James, E. Thiol-functionalized, 1.5-nm gold nanoparticles through ligand exchange reactions: scope and mechanism of ligand exchange. *Journal of the American Chemical Society* **2005**, *127*, 2172-2183.
- (188) Woehrle, G. H.; Warner, M. G.; Hutchison, J. E. Ligand exchange reactions yield subnanometer, thiol-stabilized gold particles with defined optical transitions. *Journal of Physical Chemistry B* **2002**, *106*, 9979-9981.
- (189) Finke, R. G.; Oezkar, S. Molecular insights for how preferred oxoanions bind to and stabilize transition-metal nanoclusters: a tridentate, C₃ symmetry, lattice size-matching binding model. *Coordination Chemistry Reviews* **2004**, *248*, 135-146.
- (190) Nichols, R. J.; Burgess, I.; Young, K. L.; Zamlynny, V.; Lipkowski, J. A quantitative evaluation of the adsorption of citrate on Au(111) using SNIFTIRS. *Journal of Electroanalytical Chemistry* **2004**, *563*, 33-39.
- (191) Wanner, M.; Gerthsen, D.; Jester, S.-S.; Sarkar, B.; Schwederski, B. Treatment of citrate-capped Au colloids with NaCl, NaBr and Na₂SO₄: a TEM, EAS and EPR study of the accompanying changes. *Colloid and Polymer Science* **2005**, *283*, 783-792.
- (192) Niemeyer, C. M.; Ceyhan, B.; Gao, S.; Chi, L.; Peschel, S.; Simon, U. Site-selective immobilization of gold nanoparticles functionalized with DNA oligomers. *Colloid and Polymer Science* **2001**, *279*, 68-72.
- (193) Xie, H.; Tkachenko, A. G.; Glomm, W. R.; Ryan, J. A.; Brennaman, M. K.; Papanikolas, J. M.; Franzen, S.; Feldheim, D. L. Critical flocculation concentrations, binding isotherms, and ligand exchange properties of peptide-modified gold nanoparticles studied by UV-visible, fluorescence, and time-correlated single photon counting spectroscopies. *Analytical Chemistry* **2003**, *75*, 5797-5805.
- (194) Levy, R.; Thanh Nguyen, T. K.; Doty, R. C.; Hussain, I.; Nichols Richard, J.; Schiffrin David, J.; Brust, M.; Fernig David, G. Rational and combinatorial design of peptide capping ligands for gold nanoparticles. *Journal of the American Chemical Society* **2004**, *126*, 10076-10084.

- (195) Zhu, T.; Vasilev, K.; Kreiter, M.; Mittler, S.; Knoll, W. Surface modification of citrate-reduced colloidal gold nanoparticles with 2-mercaptosuccinic acid. *Langmuir* **2003**, *19*, 9518-9525.
- (196) Lin, S.-Y.; Tsai, Y.-T.; Chen, C.-C.; Lin, C.-M.; Chen, C.-h. Two-step functionalization of neutral and positively charged thiols onto citrate-stabilized Au nanoparticles. *Journal of Physical Chemistry B* **2004**, *108*, 2134-2139.
- (197) Weisbecker, C. S.; Merritt, M. V.; Whitesides, G. M. Molecular self-assembly of aliphatic thiols on gold colloids. *Langmuir* **1996**, *12*, 3763-3772.
- (198) Gandubert, V. J.; Lennox, R. B. Assessment of 4-(dimethylamino)pyridine as a capping agent for gold nanoparticles. *Langmuir* **2005**, *21*, 6532-6539.
- (199) Constable, D. J. C.; Curzons, A. D.; Cunningham, V. L. Metrics to 'green chemistry' - which are the best? *Green Chemistry* **2002**, *4*, 521-527.
- (200) Maier, S. A.; Kik, P. G.; Atwater, H. A. Observation of coupled plasmon-polariton modes in Au nanoparticle chain waveguides of different lengths: estimation of waveguide loss. *Applied Physics Letters* **2002**, *81*, 1714-1716.
- (201) Maier, S. A.; Kik, P. G.; Atwater, H. A. Optical pulse propagation in metal nanoparticle chain waveguides. *Physical Review B: Condensed Matter and Materials Physics* **2003**, *67*, 205402-205405.
- (202) Maier, S. A.; Brongersma, M. L.; Kik, P. G.; Meltzer, S.; Requicha, A. A. G.; Atwater, H. A. Plasmonics - a route to nanoscale optical devices. *Advanced Materials* **2001**, *13*, 1501-1505.
- (203) Berven, C. A.; Wybourne, M. N.; Clarke, L.; Longstreth, L.; Hutchison, J. E.; Mooster, J. L. Background charge fluctuations and the transport properties of biopolymer-gold nanoparticle complexes. *Journal of Applied Physics* **2002**, *92*, 4513-4517.
- (204) Shih, S.-M.; Su, W.-F.; Lin, Y.-J.; Wu, C.-S.; Chen, C.-D. Two-dimensional arrays of self-assembled gold and sulfur-containing fullerene nanoparticles. *Langmuir* **2002**, *18*, 3332-3335.
- (205) Lin, S.; Li, M.; Dujardin, E.; Girard, C.; Mann, S. One-dimensional plasmon coupling by facile self-assembly of gold nanoparticles into branched chain networks. *Advanced Materials* **2005**, *17*, 2553-2559.
- (206) Bergkvist, M.; Mark, S. S.; Yang, X.; Angert, E. R.; Batt, C. A. Bionanofabrication of ordered nanoparticle arrays: Effect of particle properties and adsorption conditions. *Journal of Physical Chemistry B* **2004**, *108*, 8241-8248.

- (207) Warner, M. G.; Hutchison, J. E. Linear assemblies of nanoparticles electrostatically organized on DNA scaffolds. *Nature Materials* **2003**, *2*, 272-277.
- (208) Reinhard, B. M.; Siu, M.; Agarwal, H.; Alivisatos, A. P.; Liphardt, J. Calibration of dynamic molecular rulers based on plasmon coupling between gold nanoparticles. *Nano Letters* **2005**, *5*, 2246-2252.
- (209) Deng, Z.; Tian, Y.; Lee, S.-H.; Ribbe, A. E.; Mao, C. DNA-encoded self-assembly of gold nanoparticles into one-dimensional arrays. *Angewandte Chemie, International Edition* **2005**, *44*, 3582-3585.
- (210) Hutter, E.; Fendler, J. H. Exploitation of localized surface plasmon resonance. *Advanced Materials* **2004**, *16*, 1685-1706.
- (211) Brust, M.; Walker, M.; Bethell, D.; Schiffrin, D. J.; Whyman, R. Synthesis of thiol-derivatized gold nanoparticles in a two-phase liquid-liquid system. *Chemical Communications* **1994**, *15*, 801-802.
- (212) Brust, M.; Fink, J.; Bethell, D.; Schiffrin, D. J.; Kiely, C. Synthesis and reactions of functionalized gold nanoparticles. *Chemical Communications* **1995**, *16*, 1655-1656.
- (213) Simonian, A. L.; Good, T. A.; Wang, S. S.; Wild, J. R. Nanoparticle-based optical biosensors for the direct detection of organophosphate chemical warfare agents and pesticides. *Analytica Chimica Acta* **2005**, *534*, 69-77.
- (214) Aili, D.; Enander, K.; Rydberg, J.; Lundstroem, I.; Baltzer, L.; Liedberg, B. Aggregation-induced folding of a de novo designed polypeptide immobilized on gold nanoparticles. *Journal of the American Chemical Society* **2006**, *128*, 2194-2195.
- (215) Huang, C.-C.; Chang, H.-T. Selective gold-nanoparticle-based "turn-on" fluorescent sensors for detection of mercury(II) in aqueous solution. *Analytical Chemistry* **2006**, *78*, 8332-8338.
- (216) Farokhzad, O. C.; Khademhosseini, A.; Jon, S.; Hermmann, A.; Cheng, J.; Chin, C.; Kiselyuk, A.; Teply, B.; Eng, G.; Langer, R. Microfluidic system for studying the interaction of nanoparticles and microparticles with cells. *Analytical Chemistry* **2005**, *77*, 5453-5459.
- (217) Zhong, Z.; Male, K. B.; Luong, J. H. T. More recent progress in the preparation of Au nanostructures, properties, and applications. *Analytical Letters* **2003**, *36*, 3097-3118.
- (218) Citrin, D. S. Plasmon polaritons in finite-length metal-nanoparticle chains: the role of chain length unravelled. *Nano Letters* **2005**, *5*, 985-989.

- (219) Yatsui, T.; Nomura, W.; Ohtsu, M. Self-assembly of size- and position-controlled ultralong nanodot chains using near-field optical desorption. *Nano Letters* **2005**, *5*, 2548-2551.
- (220) Lal, S.; Westcott, S. L.; Taylor, R. N.; Jackson, J. B.; Nordlander, P.; Halas, N. J. Light interaction between gold nanoshells plasmon resonance and planar optical waveguides. *Journal of Physical Chemistry B* **2002**, *106*, 5609-5612.
- (221) Yonezawa, T.; Sutoh, M.; Kunitake, T. Practical preparation of size-controlled gold nanoparticles in water. *Chemistry Letters* **1997**, 619-620.
- (222) Jana, N. R.; Gearheart, L.; Murphy, C. J. Seeding growth for size control of 5-40 nm diameter gold nanoparticles. *Langmuir* **2001**, *17*, 6782-6786.
- (223) Qi, Z.-M.; Zhou, H.-S.; Matsuda, N.; Honma, I.; Shimada, K.; Takatsu, A.; Kato, K. Characterization of gold nanoparticles synthesized using sucrose by seeding formation in the solid phase and seeding growth in aqueous solution. *Journal of Physical Chemistry B* **2004**, *108*, 7006-7011.
- (224) Wilcoxon, J. P.; Provencio, P. P. Heterogeneous growth of metal clusters from solutions of seed nanoparticles. *Journal of the American Chemical Society* **2004**, *126*, 6402-6408.
- (225) Kim, T.; Lee, K.; Gong, M.-S.; Joo, S.-W. Control of gold nanoparticle aggregates by manipulation of interparticle interaction. *Langmuir* **2005**, *21*, 9524-9528.
- (226) Gittins, D. I.; Caruso, F. Tailoring the polyelectrolyte coating of metal nanoparticles. *Journal of Physical Chemistry B* **2001**, *105*, 6846-6852.
- (227) Li, D.; He, Q.; Cui, Y.; Duan, L.; Li, J. Immobilization of glucose oxidase onto gold nanoparticles with enhanced thermostability. *Biochemical and Biophysical Research Communications* **2007**, *355*, 488-493.
- (228) Yonezawa, T.; Kunitake, T. Practical preparation of anionic mercapto ligand-stabilized gold nanoparticles and their immobilization. *Colloids and Surfaces, A: Physicochemical and Engineering Aspects* **1999**, *149*, 193-199.
- (229) Li, G.; Fuhrhop, J.-H. Anticorrosive lipid monolayers with rigid walls around porphyrin-based 2 nm gaps on 20 nm gold particles. *Langmuir* **2002**, *18*, 7740-7747.
- (230) Gitis, V.; Haught, R. C.; Clark, R. M.; Gun, J.; Lev, O. Nanoscale probes for the evaluation of the integrity of ultrafiltration membranes. *Journal of Membrane Science* **2006**, *276*, 199-207.

- (231) McMahon, J. M.; Emory, S. R. Phase transfer of large gold nanoparticles to organic solvents with increased stability. *Langmuir* **2007**, *23*, 1414-1418.
- (232) Yockell-Lelievre, H.; Desbiens, J.; Ritcey, A. Two-dimensional self-organization of polystyrene-capped gold nanoparticles. *Langmuir* **2007**, *23*, 2843-2850.
- (233) Liu, Y.; Shipton, M. K.; Ryan, J.; Kaufman, E. D.; Franzen, S.; Feldheim, D. L. Synthesis, stability, and cellular internalization of gold nanoparticles containing mixed peptide-poly(ethylene glycol) monolayers. *Analytical Chemistry* **2007**, *79*, 2221-2229.
- (234) Pan, B.; Gao, F.; Ao, L.; Tian, H.; He, R.; Cui, D. Controlled self-assembly of thiol-terminated poly(amidoamine) dendrimer and gold nanoparticles. *Colloids and Surfaces, A: Physicochemical and Engineering Aspects* **2005**, *259*, 89-94.
- (235) Hu, M.; Yamaguchi, Y.; Okubo, T. Self-assembly of water-dispersed gold nanoparticles stabilized by a thiolated glycol derivative. *Journal of Nanoparticle Research* **2005**, *7*, 187-193.
- (236) Reynolds, A. J.; Haines, A. H.; Russell, D. A. Gold glyconanoparticles for mimics and measurement of metal ion-mediated carbohydrate-carbohydrate interactions. *Langmuir* **2006**, *22*, 1156-1163.
- (237) Wang, Z.; Levy, R.; Fernig David, G.; Brust, M. The peptide route to multifunctional gold nanoparticles. *Bioconjugate Chemistry* **2005**, *16*, 497-500.
- (238) Sakura, T.; Takahashi, T.; Kataoka, K.; Nagasaki, Y. One-pot preparation of mono-dispersed and physiologically stabilized gold colloid. *Colloid and Polymer Science* **2005**, *284*, 97-101.
- (239) Reinhard, B. M.; Sheikholeslami, S.; Mastroianni, A.; Alivisatos, A. P.; Liphardt, J. Use of plasmon coupling to reveal the dynamics of DNA bending and cleavage by single EcoRV restriction enzymes. *Proceedings of the National Academy of Sciences of the United States of America* **2007**, *104*, 2667-2672.
- (240) Lim, I. I. S.; Ip, W.; Crew, E.; Njoki, P. N.; Mott, D.; Zhong, C.-J.; Pan, Y.; Zhou, S. Homocysteine-mediated reactivity and assembly of gold nanoparticles. *Langmuir* **2007**, *23*, 826-833.
- (241) Li, G.; Lauer, M.; Schulz, A.; Boettcher, C.; Li, F.; Fuhrhop, J.-H. Spherical and planar gold(0) nanoparticles with a rigid gold(I)-anion or a fluid gold(0)-acetone surface. *Langmuir* **2003**, *19*, 6483-6491.
- (242) Chechik, V. Reduced reactivity of aged Au nanoparticles in ligand exchange reactions. *Journal of the American Chemical Society* **2004**, *126*, 7780-7781.

- (243) Murray, C. B.; Kagan, C. R.; Bawendi, M. G. Self-organization of CdSe nanocrystallites into three-dimensional quantum dot superlattices. *Science* **1995**, *270*, 1335-1338.
- (244) Cushing, B. L.; Kolesnichenko, V. L.; O'Connor, C. J. Recent advances in the liquid-phase syntheses of inorganic nanoparticles. *Chemical Reviews* **2004**, *104*, 3893-3946.
- (245) El-Sayed, M. A. Some interesting properties of metals confined in time and nanometer space of different shapes. *Accounts of Chemical Research* **2001**, *34*, 257-264.
- (246) Roduner, E. Size matters: why nanomaterials are different. *Chemical Society Reviews* **2006**, *35*, 583-592.
- (247) Kim, J.; Lema, K.; Ukaigwe, M.; Lee, D. Facile preparative route to alkanethiolate-coated Au₃₈ nanoparticles: postsynthesis core size evolution. *Langmuir* **2007**, *23*, 7853-7858.
- (248) Demirci, S.; Enustun, B. V.; Turkevich, J. Stability of colloidal gold and determination of the Hamaker constant. *Journal of Physical Chemistry* **1978**, *82*, 2710-2711.
- (249) Enustun, B. V.; Turkevich, J. Coagulation of colloidal gold. *Journal of the American Chemical Society* **1963**, *85*, 3317-3328.
- (250) Hostetler, M. J.; Wingate, J. E.; Zhong, C. J.; Harris, J. E.; Vachet, R. W.; Clark, M. R.; Londono, J. D.; Green, S. J.; Stokes, J. J.; Wignall, G. D.; Glish, G. L.; Porter, M. D.; Evans, N. D.; Murray, R. W. Alkanethiolate gold cluster molecules with core diameters from 1.5 to 5.2 nm: core and monolayer properties as a function of core size. *Langmuir* **1998**, *14*, 17-30.
- (251) Jorgensen, J. M.; Erlacher, K.; Pedersen, J. S.; Gothelf, K. V. Preparation temperature dependence of size and polydispersity of alkylthiol monolayer protected gold clusters. *Langmuir* **2005**, *21*, 10320-10323.
- (252) Hussain, I.; Graham, S.; Wang, Z.; Tan, B.; Sherrington, D. C.; Rannard, S. P.; Cooper, A. I.; Brust, M. Size-controlled synthesis of near-monodisperse gold nanoparticles in the 1-4 nm range using polymeric stabilizers. *Journal of the American Chemical Society* **2005**, *127*, 16398-16399.
- (253) Brust, M.; Kiely, C. J. Some recent advances in nanostructure preparation from gold and silver particles: a short topical review. *Colloids and Surfaces, A: Physicochemical and Engineering Aspects* **2002**, *202*, 175-186.

- (254) Lee, S.; Perez-Luna, V. H. Dextran-gold nanoparticle hybrid material for biomolecule immobilization and detection. *Analytical Chemistry* **2005**, *77*, 7204-7211.
- (255) Dahl, J. A.; Jespersen, M. L.; Hutchison, J. E. Functionalization of citrate stabilized gold nanoparticles with water-soluble thiols. *manuscript in preparation* **2007**.
- (256) Yu, H.; Gibbons, P. C.; Kelton, K. F.; Buhro, W. E. Heterogeneous seeded growth. A potentially general synthesis of monodisperse metallic nanoparticles. *Journal of the American Chemical Society* **2001**, *123*, 9198-9199.
- (257) Shon, Y. S.; Cutler, E. Aqueous synthesis of alkanethiolate-protected Ag nanoparticles using Bunte salts. *Langmuir* **2004**, *20*, 6626-6630.
- (258) Shon, Y. S.; Wuelfing, W. P.; Murray, R. W. Water-soluble, sulfonic acid-functionalized, monolayer-protected nanoparticles and an ionically conductive molten salt containing them. *Langmuir* **2001**, *17*, 1255-1261.
- (259) Shon, Y. S.; Gross, S. M.; Dawson, B.; Porter, M.; Murray, R. W. Alkanethiolate-protected gold clusters generated from sodium S-dodecylthiosulfate (Bunte salts). *Langmuir* **2000**, *16*, 6555-6561.
- (260) Yon, J.-N.; Bricklebank, N.; Allen, D. W.; Gardiner, P. H. E.; Light, M. E.; Hursthouse, M. B. Phosphonioalkylthiosulfate zwitterions-new masked thiol ligands for the formation of cationic functionalised gold nanoparticles. *Organic & Biomolecular Chemistry* **2006**, *4*, 4345-4351.
- (261) Lukkari, J.; Meretoja, M.; Kartio, I.; Laajalehto, K.; Rajamaki, M.; Lindstrom, M.; Kankare, J. Organic thiosulfates (Bunte salts): novel surface-active sulfur compounds for the preparation of self-assembled monolayers on gold. *Langmuir* **1999**, *15*, 3529-3537.
- (262) Lusk, A. T.; Jennings, G. K. Characterization of self-assembled monolayers formed from sodium S-alkyl thiosulfates on copper. *Langmuir* **2001**, *17*, 7830-7836.
- (263) Maier, S. A.; Kik, P. G.; Brongersma, M. L.; Atwater, H. A. Electromagnetic energy transport below the diffraction limit in periodic metal nanostructures. *Proceedings of SPIE-The International Society for Optical Engineering* **2001**, *4456*, 22-30.
- (264) Maier, S. A.; Kik, P. G.; Atwater, H. A.; Meltzer, S.; Harel, E.; Koel, B. E.; Requicha, A. A. G. Local detection of electromagnetic energy transport below the diffraction limit in metal nanoparticle plasmon waveguides. *Nature Materials* **2003**, *2*, 229-232.

- (265) Kim, J. Y.; Osterloh, F. E. Planar gold nanoparticle clusters as microscale mirrors. *Journal of the American Chemical Society* **2006**, *128*, 3868-3869.
- (266) Brouwer, E. A. M.; Kooij, E. S.; Hakbijl, M.; Wormeester, H.; Poelsema, B. Deposition kinetics of nanocolloidal gold particles. *Colloids and Surfaces, A: Physicochemical and Engineering Aspects* **2005**, *267*, 133-138.
- (267) Mewe, A. A.; Kooij, E. S.; Poelsema, B. Seeded-growth approach to selective metallization of microcontact-printed patterns. *Langmuir* **2006**, *22*, 5584-5587.
- (268) Ma, D.; Guan, J.; Normandin, F.; Denomme, S.; Enright, G.; Veres, T.; Simard, B. Multifunctional nano-architecture for biomedical applications. *Chemistry of Materials* **2006**, *18*, 1920-1927.
- (269) Bourlinos, A. B.; Chowdhury, S. R.; Herrera, R.; Jiang, D. D.; Zhang, Q.; Archer, L. A.; Giannelis, E. P. Functionalized nanostructures with liquid-like behavior: Expanding the gallery of available nanostructures. *Advanced Functional Materials* **2005**, *15*, 1285-1290.
- (270) Fu, A.; Micheel, C. M.; Cha, J.; Chang, H.; Yang, H.; Alivisatos, A. P. Discrete nanostructures of quantum dots/Au with DNA. *Journal of the American Chemical Society* **2004**, *126*, 10832-10833.
- (271) Park, S.-J.; Lazarides, A. A.; Storhoff, J. J.; Pesce, L.; Alivisatos, A. P. The structural characterization of oligonucleotide-modified gold nanoparticle networks formed by DNA hybridization. *Journal of Physical Chemistry B* **2004**, *108*, 12375-12380.
- (272) Jin, R.; Wu, G.; Li, Z.; Mirkin, C. A.; Schatz, G. C. What controls the melting properties of DNA-linked gold nanoparticle assemblies? *Journal of the American Chemical Society* **2003**, *125*, 1643-1654.
- (273) Zhao, W.; Gao, Y.; Kandadai, S. A.; Brook, M. A.; Li, Y. DNA polymerization on gold nanoparticles through rolling circle amplification: towards novel scaffolds for three-dimensional periodic nanoassemblies. *Angewandte Chemie, International Edition* **2006**, *45*, 2409-2413.
- (274) Bayer, J.; Raedler, J. O.; Blossey, R. Chains, dimers, and sandwiches: melting behavior of DNA nanoassemblies. *Nano Letters* **2005**, *5*, 497-501.
- (275) Ongaro, A.; Griffin, F.; Beecher, P.; Nagle, L.; Iacopino, D.; Quinn, A.; Redmond, G.; Fitzmaurice, D. DNA-templated assembly of conducting gold nanowires between gold electrodes on a silicon oxide substrate. *Chemistry of Materials* **2005**, *17*, 1959-1964.

- (276) Nasalean, L.; Baudrey, S.; Leontis, N. B.; Jaeger, L. Controlling RNA self-assembly to form filaments. *Nucleic Acids Research* **2006**, *34*, 1381-1392.
- (277) Koyfman, A. Y.; Braun, G.; Magonov, S.; Chworos, A.; Reich, N. O.; Jaeger, L. Controlled spacing of cationic gold nanoparticles by nanocrown RNA. *Journal of the American Chemical Society* **2005**, *127*, 11886-11887.
- (278) Khaled, A.; Guo, S.; Li, F.; Guo, P. Controllable self-assembly of nanoparticles for specific delivery of multiple therapeutic molecules to cancer cells using RNA nanotechnology. *Nano Letters* **2005**, *5*, 1797-1808.
- (279) Nam, K. T.; Kim, D. W.; Yoo, P. J.; Chiang, C. Y.; Meethong, N.; Hammond, P. T.; Chiang, Y. M.; Belcher, A. M. Virus-enabled synthesis and assembly of nanowires for lithium ion battery electrodes. *Science* **2006**, *312*, 885-888.
- (280) Huang, Y.; Chiang, C.-Y.; Lee, S. K.; Gao, Y.; Hu, E. L.; De Yoreo, J.; Belcher, A. M. Programmable assembly of nanoarchitectures using genetically engineered viruses. *Nano Letters* **2005**, *5*, 1429-1434.
- (281) Slocik, J. M.; Naik, R. R.; Stone, M. O.; Wright, D. W. Viral templates for gold nanoparticle synthesis. *Journal of Materials Chemistry* **2005**, *15*, 749-753.
- (282) Falkner, J. C.; Turner, M. E.; Bosworth, J. K.; Trentler, T. J.; Johnson, J. E.; Lin, T.; Colvin, V. L. Virus crystals as nanocomposite scaffolds. *Journal of the American Chemical Society* **2005**, *127*, 5274-5275.
- (283) Portney, N. G.; Singh, K.; Chaudhary, S.; Destito, G.; Schneemann, A.; Manchester, M.; Ozkan, M. Organic and inorganic nanoparticle hybrids. *Langmuir* **2005**, *21*, 2098-2103.
- (284) Lee, S.-W.; Lee, S. K.; Belcher, A. M. Virus-based alignment of inorganic, organic, and biological nanosized materials. *Advanced Materials* **2003**, *15*, 689-692.
- (285) Li, Z.; Chung, S.-W.; Nam, J.-M.; Ginger, D. S.; Mirkin, C. A. Living templates for the hierarchical assembly of gold nanoparticles. *Angewandte Chemie, International Edition* **2003**, *42*, 2306-2309.
- (286) Park, S.-J.; Lazarides, A. A.; Mirkin, C. A.; Letsinger, R. L. Directed assembly of periodic materials from protein and oligonucleotide-modified nanoparticle building blocks. *Angewandte Chemie, International Edition* **2001**, *40*, 2909-2912.
- (287) Bhattacharya, R.; Patra, C. R.; Wang, S.; Lu, L.; Yaszemski, M. J.; Mukhopadhyay, D.; Mukherjee, P. Assembly of gold nanoparticles in a rod-like fashion using proteins as templates. *Advanced Functional Materials* **2006**, *16*, 395-400.

- (288) Yu, A.; Gentle, I.; Lu, G.; Caruso, F. Nanoassembly of biocompatible microcapsules for urease encapsulation and their use as biomimetic reactors. *Chemical Communications* **2006**, 2150-2152.
- (289) McMillan, R. A.; Howard, J.; Zaluzec, N. J.; Kagawa, H. K.; Mogul, R.; Li, Y.-F.; Paavola, C. D.; Trent, J. D. A self-assembling protein template for constrained synthesis and patterning of nanoparticle arrays. *Journal of the American Chemical Society* **2005**, *127*, 2800-2801.
- (290) Mark, S. S.; Bergkvist, M.; Yang, X.; Teixeira, L. M.; Bhatnagar, P.; Angert, E. R.; Batt, C. A. Bionanofabrication of metallic and semiconductor nanoparticle arrays using S-layer protein lattices with different lateral spacings and geometries. *Langmuir* **2006**, *22*, 3763-3774.
- (291) Murthy, V. S.; Cha, J. N.; Stucky, G. D.; Wong, M. S. Charge-driven flocculation of poly(L-lysine)-gold nanoparticle assemblies leading to hollow microspheres. *Journal of the American Chemical Society* **2004**, *126*, 5292-5299.
- (292) Fu, X.; Wang, Y.; Huang, L.; Sha, Y.; Gui, L.; Lai, L.; Tang, Y. Assemblies of metal nanoparticles and self-assembled peptide fibrils-formation of double helical and single-chain arrays of metal nanoparticles. *Advanced Materials* **2003**, *15*, 902-906.
- (293) Liu Xiang, Y.; Sawant Prashant, D.; Tan Wee, B.; Noor, I. B. M.; Pramesti, C.; Chen, B. H. Creating new supramolecular materials by architecture of three-dimensional nanocrystal fiber networks. *Journal of the American Chemical Society* **2002**, *124*, 15055-15063.
- (294) Shenton, W.; Davis, S. A.; Mann, S. Directed self-assembly of nanoparticles into macroscopic materials using antibody-antigen recognition. *Advanced Materials* **1999**, *11*, 449-452.
- (295) Dessinges, M. N.; Maier, B.; Zhang, Y.; Peliti, M.; Bensimon, D.; Croquette, V. Stretching single stranded DNA, a model polyelectrolyte. *Physical Review Letters* **2002**, *89*, 248101-248104.